

On factors controlling the mobility of organic compounds in water-rock interactions

vorgelegt von
M. Sc. Geologin
Yaling Zhu

Von der Fakultät VI - Planen Bauen Umwelt
der Technischen Universität Berlin
zur Erlangung des akademischen Grades

Doktor der Naturwissenschaften
Dr. rer. nat.

genehmigte Dissertation

Promotionsausschuss:

Vorsitzender: Prof. Dr. Wilhelm Dominik

Gutachter: Prof. Dr. Brian Horsfield

Gutachter: Prof. Dr. Heinz Wilkes

Tag der wissenschaftlichen Aussprache: 19. März 2019

Berlin 2019

Dedication

This document is dedicated to my family!

ACKNOWLEDGEMENTS

First of all I would like to express my gratitude to my supervisor Dr. Andrea Vieth-Hillebrand for uncountable inspiring discussions and excellent supervision throughout my Ph.D. study. Without her dedication, the present work would not have been possible. I gratefully acknowledge Prof. Dr. Brian Horsfield for providing me the opportunity to join his group and leading me to the organic geochemistry world. I would also like to thank him for his motivation and valuable advices.

Franziska Wilke is thanked for supervising me in inorganic geochemistry aspect at the beginning of the project. I would like to thank Alex Vetter and Andreas Hübner for sharing literature and reports related to shale gas and hydraulic fracturing when they were in charge of SHIP (shale gas information platform). Special thanks go out to the technical staff at the organic geochemistry group at GFZ, namely Kristin Günther, Wilma Mierke, Cornelia Karger, Anke Kaminsky, Mirco Rahn and Ferdinand Perssen. Without their assistances and supports, it's impossible to carry out this work.

Further thanks are directed to my colleagues at GFZ. Kai Mangelsdorf, Stefanie Pötz, Mareike Noah, Nick Mahlstedt, Karsten Adler, Ilya Ostanin, Gabriela Marcano and Volker Ziegs are thanked for their useful advices and suggestions. My sincere gratitude goes to Claudia Engelhardt for helping me handle numerous obstacles. I would like to thank Frauke Stobbe from the Welcome Center of Potsdam, for all her kind help that solves a lot of difficult troubles for us and makes our life much easier in Germany. I also want to thank the Chinese colleagues Jingqiang Tan, Shengyu Yang, Nana Mu, Huiwen Yue and Yufu Han for sharing the ups and downs of my life in Germany.

Chinese Scholarship Council and the European Union's Horizon 2020 research and innovation program are greatly acknowledged for sponsoring my Ph.D. study.

My heartfelt gratitude goes to my great parents for their unconditional love and encouragement. I also extend my sincere word of thanks to my parents-in-law for their understanding and support during the special period. Words cannot express my appreciation and love to my husband Changpeng Yu and my son Yichong Yu. I am glad that you are in my life.

LIST OF PUBLICATIONS

Articles in peer-reviewed journals

- (1) Zhu, Y., Vieth-Hillebrand, A., Wilke, F.D.H., Horsfield, B., 2015. Characterization of water-soluble organic compounds released from black shales and coals. *International Journal of Coal Geology* 150–151, 265-275 (postprint), <https://doi.org/10.1016/j.coal.2015.09.009>.
- (2) Zhu, Y., Vieth-Hillebrand, A., Noah, M., Poetz, S., 2019. Molecular characterization of extracted dissolved organic matter from New Zealand coals identified by ultrahigh resolution mass spectrometry. *International Journal of Coal Geology* 203, 74-86 (postprint), <https://doi.org/10.1016/j.coal.2019.01.007>.
- (3) Zhu, Y., Vieth-Hillebrand, A., Noah, M., Poetz, S., 2019. Molecular characterization of the water-soluble organic compounds from Posidonia shales using ultra-high resolution mass spectrometry, (final draft ready for submission).

This cumulative thesis includes three manuscripts. Chapter 2 and Chapter 3 were already published as the article (1) and article (2), respectively. Chapter 4 contains the manuscript (3) that is close to submission.

Presentations at international symposia

- (1) Zhu, Y., Vieth-Hillebrand, A., Wilke, F.D.H., Horsfield, B., 2014, Mobilization of organic compounds from shales during shale gas extraction: GeoShale, Poland. Poster.
- (2) Zhu, Y., Vieth-Hillebrand, A., Horsfield, B., 2015, Characterizing the main controls on the water-soluble organic compounds released from black shales and coals: IMOG, Czech Republic. Oral Presentation.
- (3) Zhu, Y., Vieth-Hillebrand, A., Noah, M., Poetz, S., 2017, Molecular characterization of DOM extracted from coals identified by FT-ICR-MS: IMOG, Florence. Poster.
- (4) Zhu, Y., Vieth-Hillebrand, A., Wilke, F.D.H., Horsfield, B., 2017, Investigation of water-soluble organic matter extracted from shales during leaching experiments: EGU, Vienna. Poster.

ABSTRACT

The chemistry of organic compounds is based on carbon, the fifteenth most abundant element in the crust. Deriving from mainly biological systems, organic compounds can be incorporated into sedimentary rocks, and remain within the lithosphere for extended geological time periods, undergoing lengthy exposure to elevated temperatures and pressures which results in chemical transformations and physical redistributions. Ultimately these compounds are returned to the Earth's surface and atmosphere where they are oxidized back to CO₂. This is the carbon cycle. While dissolved organic matter (DOM) has been studied extensively in the early parts of that cycle, very little is known about the occurrence and composition of DOM in organic-rich sedimentary rocks such as black shales and coals. The aim of this thesis was to quantitatively and molecularly characterize DOM of black shales and coals in order to examine factors controlling its liberation and composition. Simulated water extraction experiments have been performed using four Type II marine shales namely the Posidonia, Duvernay, Bakken, and Alum shales and Type III New Zealand coals. Different chromatographic and mass spectrometric methods, namely liquid chromatography-organic carbon detection (LC-OCD), ion chromatography (IC), gas chromatography-mass spectrometry (GC-MS) and Fourier transform ion cyclotron resonance mass spectrometry (FT-ICR-MS) were employed in unravelling the composition and concentration of the extracted DOM in the water extracts. Furthermore, Rock-Eval pyrolysis, pyrolysis - gas chromatography (Py-GC) were also carried out to examine the organic matter properties of the original samples.

Using LC-OCD, the DOC yields of all the samples have been found to decrease steeply with increasing diagenesis and remain low throughout catagenesis. When normalized to TOC, the concentrations of DOC are comparable for the coal and shale samples with the same maturity. Using size exclusion chromatography (SEC), the extracted DOM was divided into four different fractions: Macro-2, Macro-3, Acids and Neutrals. Relatively high amounts of Macro-2 and Macro-3 fractions can be observed in the extracted DOM of the immature samples while the extracted DOM of the mature and overmature samples are featured by high amount of Neutrals. The Macro-2 and Macro-3 fractions in the extracted DOM of coals tend to contain more aromatic compounds and the molecular masses of most constituents within these two fractions are higher than for the shale extracts. With the analysis of IC, formate and

acetate have been identified as the two main low molecular weight organic acids (LMWOAs) in the extracted DOM. The concentrations of formate and acetate decrease with increasing maturation of most shale samples and remain low after reaching the oil window except for the three overmature Posidonia shales from the Haddessen well. High acetate concentrations observed in the overmature samples are speculated to be caused by the hydrothermal brines. The brines might provide water and heat source to enhance the generation of acetate.

To get further insights into the molecular composition of the extracted DOM, FT-ICR-MS has been applied to the solid-phase extractable DOM of New Zealand coals and Posidonia shales. In the extracted DOM of the coals, O_x class is the prominent elemental class with more than 80% TMIA. The distributions of the O_x class and the DBE of each oxygen class are quite similar for the extracted DOM of the two lignites, and show big differences to those of the three bituminous coals. The variations of average DBE of the oxygen classes have been calculated to infer the oxygen-containing functional groups. More hydroxyl and ether groups are involved in the O_{1-5} classes and more carboxyl and carbonyl functional groups are involved in O_{9-16} classes. The low abundance of O_{9-16} in the extracts of the bituminous coals compared to the extracts of lignites is likely due to the loss of oxygen via eliminations of carboxyl and carbonyl groups during the zone of organic diagenesis ($< 0.5\% R_o$). The oxygen-containing compounds in the extracted DOM of the bituminous coal are more aromatic than that of the lignites as evaluated by a newly developed aromaticity index (AI_{coal}).

Different from the coal extracts, the extracted DOM of the Posidonia shales is dominated by the S_zO_x elemental class followed by the O_x class. The relative intensities of S_1O_x classes show a Gaussian distribution with the highest intensity in S_1O_5 or S_1O_6 class, while the distribution of relative intensities of O_x classes varies for the shale samples with different maturity. Based on the DBE distributions and the carbon number distributions of O_x and S_1O_x classes, the molecular core structure of most compounds in the mature shale extracts are speculated to contain an additional benzene ring compared to the immature shale extracts. Sulfonic acid function has been deduced to be the common functional group in $S_1O_{\geq 3}$ classes. The general composition of DOM in the water extracts is compared with that of the solvent extracts of the same samples, and the enormous differences indicate that the extracted DOM composition is strongly determined by the polarity of the organic compounds.

KURZFASSUNG

Die Chemie organischer Verbindungen ist geprägt durch das Element Kohlenstoff, das in der Häufigkeitsverteilung der Elemente in der Erdkruste an 15. Stelle steht. Aus biologischen Systemen stammend werden organische Verbindungen in Sedimentgesteine eingebaut und verbleiben über geologische Zeiträume in der Lithosphäre und durchlaufen dabei chemische Prozesse und physikalische Umverteilungen in Abhängigkeit von erhöhten Temperaturen und Drücken. Letztendlich gelangen organische Verbindungen wieder an die Erdoberfläche und in die Atmosphäre, wo sie zu CO₂ oxidiert werden. Dies ist der Kohlenstoffkreislauf. Während gelöstes organisches Material (dissolved organic matter – DOM) in den frühen Phasen dieses Kreislaufes bereits intensiv untersucht wurden, ist wenig bekannt über das Vorkommen und die Zusammensetzung des DOM in Sedimentgesteinen mit hohem Anteil an organischen Verbindungen wie Schwarzschiefer und Kohlen. Das Ziel der vorliegenden Arbeit war es das DOM aus Schiefer und Kohlen quantitativ und in seiner molekularen Zusammensetzung zu charakterisieren um die wichtigsten Einflussfaktoren für die Freisetzung und Zusammensetzung bestimmen zu können. Im Labor wurden Extraktionsexperimente durchgeführt mit Proben von vier verschiedenen Schiefergesteinen mariner Herkunft (Kerogentyp II – Posidonienschiefer, Duvernay, Bakken und Alum) und Kohleproben aus Neuseeland (Kerogentyp III). Mit verschiedenen chromatographischen und massenspektrometrischen Methoden – namentlich Flüssigkeitschromatographie-Kohlenstoffdetektion (LC-OCD), Ionenchromatographie (IC), Gaschromatographie-Massenspektrometrie (GC-MS) und Fouriertransformation-Ionenzyklotronresonanz-Massenspektrometrie (FT-ICR-MS) – wurden die Zusammensetzung und die Konzentrationen organischer Verbindungen in den wässrigen Extrakten aufgeklärt. Zusätzlich wurden die Eigenschaften des natürlichen organischen Materials in den Sedimentgesteinen mittels Rock-Eval-Pyrolyse und Pyrolyse-Gaschromatographie (Py-GC) untersucht.

Mittels LC-OCD konnte festgestellt werden, dass die Gehalte an gelöstem organischem Kohlenstoff (DOC) in den Wasserextrakten mit der Diagenese des Sedimentgesteins stark zurückgehen und während der Katagenese auf geringem Niveau bleiben. Wenn die DOC-Konzentrationen auf den Gehalt an organischem Kohlenstoff im Sedimentgestein normiert wurden, ergaben sich übereinstimmende Werte für Schiefergestein und Kohlen in Abhängigkeit von der thermischen Reife des organischen Materials. Mit der

Molekülgrößenausschlusschromatographie (size exclusion chromatography – SEC) konnte das extrahierte DOM in vier verschiedene Fraktionen unterteilt werden: Makro-2, Makro-3, Säuren und Neutralstoffe. In dem extrahierten DOM der unreifen Sedimentgesteine konnten relativ hohe Gehalte der Fraktionen Makro-2 und Makro-3 nachgewiesen werden, wohingegen das extrahierbare DOM aus reifen bzw. sehr reifen Proben durch hohe Anteile an Neutralstoffen charakterisiert war. In den Wasserextrakten der Kohleproben gab es in den Makro-2 und Makro-3 Fraktionen mehr aromatische Verbindungen und höhere Molekülmassen als in den Wasserextrakten der Schiefergesteine. Mit der IC wurden Formiat und Acetat als die Hauptvertreter der niedermolekularen organischen Säuren im extrahierten DOM nachgewiesen. Für die meisten Schiefergesteine zeigte sich ein Rückgang der Konzentrationen von Formiat und Acetat im extrahierten DOM in Abhängigkeit von der zunehmenden Reife des organischen Materials und sehr geringe Konzentrationen innerhalb des Ölfensters. Nur die Proben des Posidonienschiefers aus der Haddessen-Bohrung zeigten einen Anstieg der Acetat-Konzentrationen im extrahierten DOM der überreifen Gesteine, welcher mit dem Einfluss hydrothermalen Wässers im Zusammenhang stehen kann. Die hydrothermalen Wässer können als Wasser- und Energiequelle zur Bildung von Acetat beigetragen haben.

Um einen tieferen Einblick in die molekulare Zusammensetzung des extrahierten DOM zu erhalten wurden die Extrakte des Posidonienschiefers und der Kohlen mit FT-ICR-MS untersucht. Der extrahierte DOM der Kohlen wird zu mehr als 80% dominiert von sauerstoffhaltigen organischen Verbindungen (Ox-Verbindungen). Die Verteilung der Ox-Verbindungen und der Doppelbindungsäquivalente (DBÄ) für jede Ox-Klasse ist ähnlich für das extrahierte DOM aus den beiden Braunkohlen jedoch deutlich verschieden für das extrahierte DOM der bituminösen Kohlen. Das berechnete durchschnittliche DBÄ (DBEaverage) der Ox-Verbindungen wurde genutzt um Annahmen über die möglichen sauerstoffhaltigen funktionellen Gruppen abzuleiten. Bei den O1-5 Verbindungen liegen vermutlich mehr Hydroxyl- und Etherfunktionalitäten vor, wohingegen die O9-16 Verbindungen eher durch Carboxyl- und Carbonylfunktionalitäten geprägt sein werden. Die geringe Häufigkeit von O9-16 Verbindungen in den wässrigen Extrakten der bituminösen Kohlen kann die Abspaltung von Carboxyl- und Carbonylfunktionalitäten während der Diagenese ($<0,5\%$ Ro) verdeutlichen. Mit Hilfe des neu modifizierten Aromatizitätsindex (AI_{coal}) konnte gezeigt werden dass die Ox-Verbindungen im extrahierten DOM der bituminösen Kohlen stärker aromatisch sind als die Ox-Verbindungen im extrahierten DOM der Braunkohlen.

Im Gegensatz zu den Kohleextrakten ist das extrahierte DOM der Posidonienschiefer dominiert durch SzOx-Verbindungen, gefolgt von den Ox-Verbindungen. Die relativen Intensitäten der S1Ox-Verbindungen zeigte eine Gaußsche Verteilung mit dem Maximum bei den S1O5 bzw. den S1O6 Verbindungen, wohingegen die relativen Intensitäten der Ox-Verbindungen in ihrer Verteilung deutlich reifeabhängig sind. Anhand der Verteilungen der DBÄ und der Kohlenstoffanzahl wurden für die Ox-Verbindungen und die S1Ox-Verbindungen Rückschlüsse auf mögliche Strukturen bzw. Bestandteile der Strukturen gezogen. Das extrahierte DOM der reifen Posidonienschiefer scheint sich durch einen zusätzlichen Benzolring vom extrahierten DOM der unreifen Posidonienschiefer zu unterscheiden. Bei den S1O>3-Verbindungen scheint die Sulfonsäure eine vorherrschende Struktur darzustellen. Die molekulare Zusammensetzung des extrahierten DOM unterscheidet sich vor allem durch die Polarität der organischen Verbindungen von der Zusammensetzung der Lösungsmittel-Extrakte der gleichen Posidonienschiefer.

CONTENTS

Acknowledgements.....	I
List of Publications	III
Abstract.....	V
Kurzfassung	VII
Contents	XI
List of Figures	XV
List of Tables	XIX
List of Abbreviations	XXI
1. Introduction.....	1
1.1 Dissolved organic matter.....	1
1.2 DOM released from black shales and coals	4
1.3 Analytical approaches for DOM characterization.....	6
1.3.1 DOM isolation and purification.....	6
1.3.2 DOM characterization	7
1.4 Sedimentary macromolecular organic matter	8
1.4.1 Type of kerogen.....	8
1.4.2 Evolution of kerogen organic matter	11
1.4.3 Macromolecular organic matter in black shales	13
1.4.4 Macromolecular organic matter in coals	14
1.5 Research objectives	15
1.6 Structure of the dissertation	17
2. Characterization of water-soluble organic compounds released from black shales and coals.....	19
2.1 Abstract	19
2.2 Introduction	20

2.3 Materials.....	21
2.3.1 Posidonia shale	22
2.3.2 Bakken shale.....	22
2.3.3 Duvernay shale	23
2.3.4 Alum shale.....	23
2.3.5 New Zealand coal	23
2.4 Methods.....	25
2.4.1 Sample extraction	25
2.4.2 Analytical methods.....	26
2.5 Results	28
2.5.1 Extraction of DOC.....	28
2.5.2 Composition of DOC.....	29
2.5.3 Occurrence of individual organic acids in the extracts	33
2.6 Discussion	35
2.6.1 Effect of shale and coal organic matter composition on water extracts	35
2.6.2 Effect of burial processes on composition of water extracts	37
2.7 Summary and Conclusions.....	41
2.8 Acknowledgments.....	42
3. Molecular characterization of extracted dissolved organic matter from New Zealand coals identified by ultrahigh resolution mass spectrometry	43
3.1 Abstract	43
3.2 Introduction	44
3.3 Samples and methods	46
3.3.1 Sample set.....	46
3.3.2 Methods	47
3.4 Results and discussion.....	51
3.4.1 General characterization of coal organic matter.....	51
3.4.2 Composition of the extracted DOM	53

3.4.3 Detailed characterization of the oxygen containing compounds.....	62
3.5 Summary and Conclusions.....	68
3.6 Acknowledgements	69
3.7 Supplementary material.....	70
4. Molecular characterization of the water-soluble organic compounds from Posidonia shales using ultra-high resolution mass spectrometry	75
4.1 Abstract	75
4.2 Introduction	76
4.3 Materials and methods	78
4.3.1 Geological setting and samples	78
4.3.2 Sample preparation for FT-ICR-MS analysis.....	79
4.3.3 FT-ICR-MS analysis	79
4.3.4 Mass Calibration and Data Analysis	79
4.4 Results and discussion.....	80
4.4.1 General composition of DOM in aqueous shale extracts	80
4.4.2 Elemental Class Distribution.....	83
4.4.3 Compound class distribution	85
4.4.4 Detailed characterization of selected compound classes.....	87
4.5 Summary and Conclusion	95
4.6 Acknowledgements	96
4.7 Supplementary material	97
5. Summary and Outlook	100
5.1 Summary	100
5.2 Outlook.....	104
References.....	106

LIST OF FIGURES

Figure 1.1. Van Krevelen diagram indicating the different diagenetic, catagenetic and metagenetic evolution pathways of the three kerogen types concerning the H/C and O/C atomic ratios (Vandenbroucke and Largeau, 2007).	9
Figure 2.1. Bulk properties of the sediment pyrolysates concerning alkyl chain length distribution and petroleum type organofacies using the ternary diagram of Horsfield (1989).	25
Figure 2.2. Ternary diagram showing the relative contents of clays, quartz and carbonate minerals for the studied shale samples	25
Figure 2.3. DOC concentrations of shale and coal extracts plotted over Tmax in mg/g rock (a) and in mg/g TOC (b).	29
Figure 2.4. SEC chromatograms giving intensity of (a) IR-signal and (b) UV-signal over run time of the analytical separation of shale extracts.....	30
Figure 2.5. SEC chromatograms giving intensity of (a) IR-signal and (b) UV-signal over run time of the analytical separation of coal extracts.	31
Figure 2.6. The relative percentages of the different DOC fractions extracted from shales and coals, (a) Posidonia shales; (b) Bakken shales; (c) Duvernay shales; (d) Alum shales; (e) New Zealand coals.	32
Figure 2.7. The concentrations of formate (a) and acetate (b) extracted from shales and coals of different maturities.	34
Figure 2.8. Comparison of formate and acetate concentrations in the water extracts. The linear regression excludes the extracts of P7, P8 and P9 and New Zealand coals.	37
Figure 2.9. Concentrations of formate (a) and acetate (b) in the extracts are plotted over the oxygen index (OI) values of the shales and coals.	39
Figure 2.10. The concentrations of inorganic anions in Posidonia extracts. The concentrations of fluoride, sulfate and nitrate are in the same order of magnitude for most Posidonia samples, only extracts of P8 and P9 show extremely high concentrations of chloride....	40
Figure 2.11. The variation of acetate concentrations in Posidonia extracts (left Y axis) and porosities of the shales (right Y axis) with increasing maturity.....	41

Figure 3.1. Ternary diagram showing petroleum type organofacies assessment according to Horsfield (1989) based on molecular compositions from open-system pyrolysis GC-FID analysis.	51
Figure 3.2. The amounts of n-alkanes in the solvent extracts of the five New Zealand coals.	52
Figure 3.3. Van Krevelen diagrams for the extracted DOM of lignite G004541 (a) and of bituminous coal G001997 (b) as well as DOM from shelf (c) as detected by negative ion mode ESI FT-ICR-MS analysis. The compounds are divided into four groups according to the O/C and H/C values (I: $H/C > 1$ and $O/C < 0.5$ including lipids, proteins and part of the lignins, II: $H/C > 1$ and $O/C > 0.5$ including amino sugars, carbohydrates and part of the tannins, III: $H/C < 1$ and $O/C < 0.5$ including condensed hydrocarbons and part of the lignins and IV: $H/C < 1$ and $O/C > 0.5$ including partly condensed hydrocarbons and tannins). The differences between extracted DOM of the lignite and the bituminous coal are indicated by light green rectangles. Figure (c) is adapted from (Schmidt et al., 2009).	55
Figure 3.4. ESI negative FT-ICR mass spectra of the extracted DOM from the five coal samples. Prominent peaks are numbered and represent these formulas: 1 - $C_9H_5O_6$; 2- $C_9H_5O_7$; 3 - $C_9H_5O_8$; 4 - $C_{10}H_5O_8$; 5 - $C_{10}H_5O_9$; 6- $C_{12}H_7O_9$; 7- $C_{13}H_7O_{10}$	57
Figure 3.5. Extracted ion chromatograms (m/z 221 + 251 + 279 + 281 + 309) from GC-MS analysis of the methyl esters of BPCAs and hydroxyl-substituted BPCAs in the extracted DOM of coal sample (G004541): methyl esters of benzene tricarboxylic acids (1, 2, 3; m/z 221), hydroxybenzene tricarboxylic acids (4, 5; m/z 251), benzene tetracarboxylic acids (6, 7, 9; m/z 279), dihydroxybenzene tricarboxylic acids (8; m/z 281), hydroxybenzene tetracarboxylic acids (10; m/z 309).	60
Figure 3.6. The relative abundance of BPCA groups in the extracted DOM of the five coal samples as calculated from GC-MS results.	61
Figure 3.7. Bar chart displaying the percentage of individual elemental classes in the extracted DOM of the five coals as detected in negative ion ESI spectra.	62
Figure 3.8. Relative intensities of the different Ox classes in the extracted DOM of the coal samples.	63
Figure 3.9. DBE class distributions found in the O3 (a), O6 (b), O8 (c), and O11 (d) classes.	64

Figure 3.10. Average DBE of each O1-16 class is plotted over the respective oxygen number. The plots can be divided into three groups, O1-5, O6-8 and O9-16 as indicated by the elliptical frames.	66
Figure 3.11. Van Krevelen diagrams show the molecular formulae in O1-5 (left), O9-16 (right) classes of the sample G004541. Aliphatic, aromatic and condensed aromatic structures can be identified with threshold criteria of the $AI_{coal} \leq 0.5$, $0.5 \leq AI_{coal} < 0.67$ and $AI_{coal} \geq 0.67$, respectively.	68
Figure 3.12. Relative intensities of the oxygen compounds classified as condensed aromatic, aromatic and aliphatic fractions based on the calculation of AI_{coal} for the extracted DOM of five coals.	68
Figure S3.1. Extracted ion chromatograms of BPCAs (m/z 105 + 163 + 221 + 279 + 337 + 395), OH-BPCAs (m/z 135 + 193 + 251 + 309) and 2OH-BPCAs (m/z 165 + 223 + 281 + 339) in the extracted DOM of lignite G004541.	71
Figure S3.2. DBE distribution of the Ox classes in the extracted DOM of the coal samples. .	73
Figure S3.3. Variation of average DBE of each oxygen class. The plots are divided into three groups, O1-5, O6-8 and O9-16 as indicated by different symbols.	74
Figure 4.1. Broadband negative ion ESI FT-ICR mass spectra of water extracts DOM of the six Posidonia shale samples with increasing maturity (as indicated by the R_o values). The pie charts display the elemental class distribution. Symbols refer to different elemental classes. OxSz compounds are depicted with triangles, Ox compounds with squares. LAS compounds are indicated by open circles.	81
Figure 4.2. Van Krevelen diagrams comparison for (a) all formulae observed in DOM of water extracts from black shale WI, $R_o = 0.53\%$, (b) formulae observed in DOM of water extracts from a New Zealand coal sample, $R_o = 0.52\%$, (c) formulae observed in DOM of solvent extracts from the same black shale WI. Ellipses indicate elemental ratios consistent with compound classes listed (Sleighter and Hatcher, 2007; Hockaday et al., 2009). The compounds are divided into four groups according to the O/C and H/C values (I: $H/C > 1$ and $O/C < 0.5$ including lipids, proteins and part of the lignins, II: $H/C > 1$ and $O/C > 0.5$ including amino sugars, carbohydrates and part of the tannins, III: $H/C < 1$ and $O/C < 0.5$ including condensed aromatics and part of the lignins and IV: $H/C < 1$ and $O/C > 0.5$ including partly condensed aromatics and tannins).	83

Figure 4.3. Relative intensities of the different Ox classes in DOM of the Posidonia shale extracts.	86
Figure 4.4. Relative intensities of the different SIOx classes in DOM of Posidonia shale extracts.	87
Figure 4.5. DBE distribution of the O1-6 classes in the DOM of Posidonia shale extracts. ...	88
Figure 4.6. Carbon number distribution of O1 class with 7 and 10 DBEs.....	91
Figure 4.7. Carbon number distribution of O2 class with different DBEs.....	91
Figure 4.8. Carbon number distribution of O3 class with different DBEs.....	92
Figure 4.9. Carbon number distribution of O4 class with different DBEs.....	92
Figure 4.10. DBE distribution of the SIO3-8 classes in the DOM of Posidonia shale extracts.	93
Figure 4.11. Carbon number distribution of SIO3 class with 5 DBEs.	94
Figure S4.1. The linear correlation between the relative intensity of LAS and the volume of water extracts used for SPE.....	97
Figure S4.2. Van Krevelen diagrams based on extracted DOM of the Posidonia shales from negative ion mode ESI FT-ICR-MS analysis. Ellipses indicate elemental ratios consistent with compound classes listed (Sleighter and Hatcher, 2007; Hockaday et al., 2009). The compounds are divided into four groups according to the O/C and H/C values (I: H/C>1 and O/C <0.5 including lipids, proteins and part of the lignins, II: H/C>1 and O/C >0.5 including amino sugars, carbohydrates and part of the tannins, III: H/C<1 and O/C <0.5 including condensed hydrocarbons and part of the lignins and IV: H/C<1 and O/C >0.5 including partly condensed hydrocarbons and tannins).	98
Figure S4.3. Compound class distribution of the OxS1 and OxS2 classes in the water extracts of the six Posidonia shale samples.	99
Figure S4.4. The possible core structures of compounds with 10 DBE in O2 class.....	99

LIST OF TABLES

Table 2.1. Sample origin and Rock-Eval pyrolysis characteristics. Hydrogen Index (HI) and Oxygen Index (OI) are measured in mg hydrocarbons/g organic carbon and mg CO ₂ /g organic carbon, respectively. TOC and Rock-Eval data of Duvernay shales and New Zealand coals were taken from (Dieckmann, 1999) and Glombitza (2011), respectively. Posidonia, Bakken and Alum shale samples were analyzed in this study. Ro values of Posidonia, Bakken, Alum and New Zealand samples were taken from Rullkötter et al. (1988), Dembicki and Pirkle (1985), Buchardt and Lewan (1990), and Glombitza (2011) respectively. Ro of Duvernay shales was calculated using the empirical formula %Ro = 0.018 * Tmax - 7.16 (%) (Jarvie et al., 2007).	23
Table 2.2. Description of LC-OCD fractions. Modified from Huber et al. (2011) and Penru et al. (2013).	28
Table 3.1. General information of the coal samples. Hydrogen Index (HI) and Oxygen Index (OI) are measured in mg hydrocarbon/g organic carbon and mg CO ₂ /g organic carbon, respectively (Zhu et al., 2015).	47
Table 3.2. Concentrations of solvent extractable organic matter and n-alkanes, carbon preference index (CPI) and pristane/phytane (Pr/Ph) ratios as well as the extracted DOM in terms of mg C/l and mg C/g TOC of the five coal samples.	56
Table 3.3. Total numbers of assigned peaks and their distribution in the main elemental classes, total mass range as well as average values of DBE, elemental numbers (carbon, hydrogen, oxygen) and molecular weight.	56
Table 3.4. General information of the seven elevated peaks.	59
Table 3.5. Equations and R ² values of the linear regressions when plotting average DBE vs oxygen number for O1-5, O6-8 and O9-16 classes. The x values are equal to the number of oxygen atoms in the molecular formula. The y values are equal to the average DBE values in each oxygen class.	67
Table 4.1. Bulk source rock characterization of the Posidonia Shale samples from six boreholes in the Hils Syncline, Northern Germany.	78
Table 4.2. General characterization of the ESI FT-ICR mass spectra for extracted DOM of Posidonia shale samples.	84

LIST OF ABBREVIATIONS

2OH-B3CA	Dihydroxybenzene tricarboxylic acids
AIcoal	Modified aromaticity index
B3CA	Benzene tricarboxylic acid
B4CA	Benzene tetracarboxylic acid
BB	Building blocks
BP	Biopolymers
BPCAs	Benzenepolycarboxylic acids
BSR	Bacterial sulfate reduction
BTEX	Benzene, toluene, ethylbenzene and xylene
CBM	Coalbed methane
CPI	Carbon Preference Index
Da	Daltons
DBE	Double bond equivalents
DI	Dielmissen
DO	Dohnsen
DOC	Dissolved organic carbon
DOM	Dissolved organic matter
DOS	Dissolved organic sulfur
ESI	Electrospray ionization
FID	Flame ionization detector
FT-ICR MS	Fourier transform ion cyclotron resonance mass spectrometry
GC-MS	Gas chromatography-mass spectrometry
HAD	Haddessen

HAR	Harderode
HI	Hydrogen Index
HS	Humic substances
IC	Ion chromatography
IHSS	International Humic Substances Society
LAS	Linear alkylbenzene sulfonic acids
LC-MS	Liquid chromatography-mass spectrometry
LC-OCD	Liquid chromatography-organic carbon detection
LMW-A	Low molecular weight acids
LMW-N	Low molecular weight neutrals
LMWOAs	Low molecular weight organic acids
MPLC	Medium Pressure Liquid Chromatography
NaOH	Sodium hydroxide
NMR	Nuclear magnetic resonance
NPCAs	Naphthalenepolycarboxylic acids
OH-B3CA	Hydroxybenzene tricarboxylic acid
OH-B4CA	Hydroxybenzene tetracarboxylic acids
OI	Oxygen Index
PAHs	Polycyclic aromatic hydrocarbons
Ph	Phytane
Pr	Pristane
Py-GC	Open-system pyrolysis gas chromatography
SEC	Size exclusion chromatography
SEOM	Solvent extractable organic matter
SPE	Solid phase extraction

TMIA	Total monoisotopic ion abundance
WE	Wenzen
WI	Wickensen
XPS	X-ray absorption spectroscopy
XRD	X-ray Diffraction

1. INTRODUCTION

1.1 Dissolved organic matter

Dissolved organic matter (DOM) is often operationally defined as organic compounds that pass through a 0.45µm filter (Herbert and Bertsch, 1995). It is a ubiquitous and highly complex mixture of organic molecules comprising mostly of carbon, oxygen, hydrogen and other heteroatoms like sulfur, nitrogen and phosphorus. As one of the largest reservoirs of organic carbon in surface and shallow environments (Bushaw et al., 1996; Hansell et al., 2009), DOM plays an important role in the global carbon cycle (Mopper and Kieber, 2002; Carlson and Hansell, 2015). It controls a number of physical, chemical and biological processes in both terrestrial and aquatic environments (Thurman, 1985). DOM in the subsurface also serves as carbon and energy sources for the deep biosphere (Parkes et al., 2000; Horsfield et al., 2006; Vu et al., 2013) and plays an important role in biogeochemical element and nutrient cycles due to its quantity and reactivity (D'Hondt et al., 2002). Furthermore, DOM is involved in processes as binding and transport of heavy metals and toxic organic compounds (Helz et al., 1996; Dórea et al., 2007; Beesley et al., 2010).

The concentration of DOM is generally very low in aquifers. As carbon comprises around half of the total DOM, quantitative measurements of DOM are based on the content of dissolved organic carbon (DOC). The average concentrations of DOC differ substantially for different types of aquatic environments. The DOC concentrations range between 2 to 60mg/L in surface water and 0.1 to 17mg/L in ground water (Aiken, 1985; Thurman, 1985; Bourbonniere, 1989; Artinger et al., 2000). Highest concentrations of DOC are often found in the waters originating from swamps, marshes and bogs, where large amounts of organic debris can be found (Chin et al., 1998). Lowest concentrations are found in groundwater, where DOM is often depleted within the first few meters of the subsurface (Marmonier et al., 1995). Lakes and rivers are intermediates with the DOC concentrations in range of 2 to 10 mg/L (Thurman, 1985).

DOM is a complex mixture of thousands of organic compounds with varying structures and weights. Due to the great heterogeneity of DOM, the low concentration of individual compounds molecular, analysis of DOM is a great challenge. Additionally, the DOM concentrations and composition are highly variable among different environments, which

increase the difficulty of DOM analysis. The molecular structure of only a minor fraction of DOM (5%) is known (Dittmar and Stubbins, 2014). The chemical compositions of DOM range from largely aliphatic to highly unsaturated aromatic compounds on the one hand side and from hydrophobic to hydrophilic compounds on the other hand side (Matilainen et al., 2011). The molecules of DOC carry all kinds of functional groups with amide, ketone, carboxyl and hydroxyl groups as the prominent functional groups (Leenheer and Croué, 2003). The hydrophilic DOM fraction is rich in aromatic carbon, phenolic structures and conjugated double bonds, while hydrophobic DOM contains a higher proportion of aliphatic carbon and nitrogenous compounds, such as carbohydrates, proteins, sugars and amino compounds (Perdue and Ritchie, 2003; Matilainen et al., 2011).

The molecular weights of DOM can range from a few hundreds to 100,000 Daltons (Da). Based on the molecular weights, organic components of hydrophilic DOM are divided into five fractions: biopolymers (BP), humic substances (HS), building blocks (BB), low molecular weight neutrals (LMW-N), and acids (LMW-A) (Huber et al., 2011). Although this grouping is arbitrarily defined, physio-chemical characteristics assigned to each fraction are comparable with other studies (Zhou et al., 2000; Lankes et al., 2009). The BP fraction is characterized as consisting of the largest molecular weight compounds with 10 kDa or higher. They are known to comprise polysaccharides and some nitrogen-containing materials such as proteins or amino sugars, which are considered to be labile compounds (Huber et al., 2011). BP may appear as a product of microbial production rather than from physical leaching of large molecules. Thus, the original leachates normally do not contain high concentration of BP. It has been found that the majority of DOM from surface environments is comprised of HS and BB (Aiken, 1985; Wassenaar et al., 1990). The HS in DOM normally have a molecular size of 800-1000Da (Penru et al., 2013) and consist of a heterogeneous mixture of complex molecules, which can be subdivided into humic and fulvic acids. Humic and fulvic acids are operationally defined by the solubility in aqueous solution, both fractions can be dissolved in alkaline solution but humic acids precipitate in acid solution (Stevenson, 1994). Humic acids are similar to allochthonous humics formed from pedogenic environments while fulvic acids are more autochthonous, microbial-derived humics (Huber et al., 2011). BB is essentially degraded HS with humic-like characterization but lower molecular weight (350-500Da). In contrast to HS, BB cannot be removed by flocculation. The final two fractions are LMW acid and neutral fractions, which contain monoprotic acids, amino sugars, ketones and aldehydes (Kennedy et al., 2005; Huber et al., 2011).

Low molecular weight organic acids (LMWOAs) generally refer to carboxylic organic compounds that are ubiquitous in DOM. These acids have relatively high solubility and are widely distributed in various environments. In the subsurface, they are involved in numerous and diverse biogeochemical processes. The production and consumption of LMWOAs are mainly controlled by microbial activity. LMWOAs are primary products of decomposition and fermentation of macromolecular organic matter and act as electron donors for microbial respiration and methanogenesis (Sørensen et al., 1981; Kleerebezem et al., 1999; Finke et al., 2007). Thus, LMWOAs are important carriers of materials and energy in the subsurface biosphere. LMWOAs have also been observed in formation waters of oil and petroleum reservoirs (Carothers and Kharaka, 1978; Barth, 1991). The generation of carboxylic organic acids in sedimentary basins has been attributed to the cleavage of carboxylate functional groups involved in kerogen during the early thermal maturation stage (Surdam and Crossey, 1985; Cooles et al., 1987; Kawamura and Kaplan, 1987). The release of carboxylic organic acids from different source rock types has been reported in simulated maturation experiments in the lab (Kawamura et al., 1986; Lundegard and Senftle, 1987; Barth et al., 1988). It has also been demonstrated that organic acids have been involved as major alteration product of aqueous *n*-alkane oxidation (Seewald, 2001c). Additionally, mineral oxidation of sedimentary organic matter may produce organic acids during thermal maturation as well (Eglinton et al., 1987; Borgund and Barth, 1994).

Many compounds within the DOM mixture contain sulfur, the so-called dissolved organic sulfur (DOS). Although DOS makes up the largest reservoir of organic sulfur in the ocean and plays a significant role in global biogeochemical cycles, knowledge on the DOS molecular composition, sources and turnover rate is scarce (Levine, 2016; Dittmar et al., 2017). The quantification of DOS is analytically hampered by the high background concentration of sulfate, which exceeds the concentration of DOS by five orders of magnitude (Ksionzek et al., 2016). Organic sulfur compounds can be formed by both biotic and abiotic reactions (Amrani, 2014). The most prominent biotic process involved in sulfur cycle is sulfate reduction. The dissimilatory sulfate reduction is a respiratory process used by some bacteria and archaea to generate energy under anaerobic conditions. This process is called bacterial sulfate reduction (BSR) (Amrani, 2014). The assimilatory sulfate reduction is carried out by many organisms such as plants and chemosynthetic sulfur bacteria. This process enables the production of precursors for other sulfur organic metabolites (Schiff and Fankhauser, 1981). Inorganic sulfur can also be incorporated abiotically into DOM to form sulfur-containing organic compounds like sulfonates, the so-called sulfurization (Sinninghe

Damsté et al., 1989; Schmidt et al., 2009). It is reported that at least 75-90% of sedimentary organic sulfur is resulting from early diagenetic sulfurization processes (Anderson and Pratt, 1995). Abiotic sulfurization plays an important role in the preservation and stabilization of organic matter in sediments (Sinninghe Damste and De Leeuw, 1990; Amrani, 2014). Sulfidic environments represent a source of potentially labile and reduced DOS. Natural DOM may be sulfurized in sulfidic systems; this has been evident by the distinctly higher concentrations of DOS in the sulfidic environments than in oxidizing ones (Sleighter et al., 2014; Gomez-Saez et al., 2016). Molecular structure characterization of DOS indicated that the sulfonic acid group is fully oxidized and most stable functional group of DOS and ubiquitously existing in the oxic water column (Pohlabein and Dittmar, 2015).

1.2 DOM released from black shales and coals

During geological maturation, coals and black shales undergo several biotic and abiotic alteration processes, with cleavage of chemical structures in the organic matrix and production of water-soluble organic compounds. Coals and black shales of low maturity contain a high abundance of easily cleaved bridge structures. Thus, more dissolved organic compounds can be detected in the groundwater associated with coals and black shales of lower maturity (Fisher and Santamaria, 2002). DOM derived from coals and black shales has been extensively investigated as a potential substrate for the deep biosphere (Horsfield et al., 2006; Vieth et al., 2008; Glombitza et al., 2009).

In sedimentary organic matter, significant amounts of heteroatoms incorporated in various functional groups can be released and produce oxygen-, nitrogen- and sulfur-bearing DOM. Loss of oxygen-containing functional groups during maturation of coals and black shales is well known and can be detected by the decrease of atomic O/C ratios and the decrease of infrared -OH, -COOH, C=O adsorption intensities (Robin and Rouxhet, 1978; Kelemen et al., 2002; Bernard et al., 2012; Vu et al., 2013). Laboratory experiments conducted by Lewan and Fisher (1994) demonstrate that carboxylic acids can be released from shales by interaction with water. They suggested that these organic acids were bound to kerogen macromolecules in the shales by weak hydrogen bonds, thus preserving them during diagenesis, but allowing the acids to be easily released from the kerogen with water. Saturated aliphatic carboxylic acids with two to five carbon atoms are the most commonly observed organic acids in subsurface water with the general concentration order of acetate >> propionate > butyrate > valerate (Fisher, 1987; Means and Hubbard, 1987). A number of

studies aimed to simulate groundwater leaching of organic compounds from lignites with distilled water in laboratories (Orem et al., 1999; Maharaj et al., 2014; Doskočil et al., 2015; Kosateva et al., 2017). In all these aqueous leachates, aromatic and aliphatic moieties with high degree of oxygen-containing functionalities have been reported. High concentrations of hydroxyl-, methoxy- phenols and hydroxyl-, methoxy- benzenes occur in the extracts of lignite (Maharaj et al., 2014). Carboxyl groups involved in benzene carboxylic acids and their derivatives, short-chain aliphatic fatty acids and polyols has been detected in leachates from Bulgarian lignites (Kosateva et al., 2017). Oxygen-containing functional groups such as carboxyl group, alcohols, ethers and esters attached to slightly large molecules have been reported to be the predominant compounds in the Moravian lignite extracts (Doskočil et al., 2015). Other DOM such as condensed aromatic compounds and their derivatives, lignin, carbohydrates and N-containing compounds have also been detected in the leachates of lignite (Peuravuori et al., 2006).

Nowadays, extensive investigation of DOM has been conducted with the development of gas extraction from unconventional shale gas and coalbed methane (CBM) reservoirs (Maguire-Boyle and Barron, 2014; Maharaj et al., 2014; Orem et al., 2014; Butkovskyi et al., 2017). The applications of hydraulic fracturing and horizontal drilling have greatly improved the natural gas extraction efficiency. During shale gas and CBM exploitation, a mixture of the injected fracturing fluid and formation brines entrapped in the target formations flows back to the surface within several days after hydraulic fracking, which is called flowback water (Gregory et al., 2011; Barbot et al., 2013). Water produced during the life time of oil and gas production, is commonly called produced water (Gregory et al., 2011). The large volume of the flowback and produced water during the gas exploitation is a significant challenge for proper handling and treatment (Fakhru'l-Razi et al., 2009). One aspect of the wastewater quality that has been addressed is the composition of DOM (Orem et al., 2007a; Maguire-Boyle and Barron, 2014; Orem et al., 2014). The chemical compositions of DOM in the flowback and produced water are variable, which depend on the composition of organic matter in the fractured formation, the local formation water and the chemical additives added during the natural gas production (Tellez et al., 2005; Luck and Gonsior, 2017).

In the flowback and produced water of shale gas exploitation, more than a thousand geogenic organic compounds have been identified (Wolford, 2011; Strong et al., 2013; Cluff et al., 2014; Orem et al., 2014; Lester et al., 2015; Thacker et al., 2015). Benzene, toluene, ethylbenzene and xylene (BTEX) compounds are the most frequently detected organic

compounds with the concentrations above detection limits (Akob et al., 2015; Lester et al., 2015; Ziemkiewicz and Thomas He, 2015; Khan et al., 2016). Other aromatic compounds including polycyclic aromatic hydrocarbons (PCA), phenol, methyl phenol, dimethyl phenol, methylnaphthalene, phenanthrene and pyrene have been quantified in flowback and produced water samples (Hayes, 2009; Lester et al., 2015). Aliphatic hydrocarbons with carbon number up to 32, alcohols and heterocyclic compounds have also been reported in the produced water (Orem et al., 2014). Fatty acids such as acetate and formate have been regarded as biodegradation products of polymers used in fracturing fluid (Lester et al., 2015). However, these LMWOAs have also been detected in the water extracts of coal samples (Vieth et al., 2008). In the produced water of CBM, detected extractable hydrocarbons include PAHs, heterocyclic compounds, other aromatics (e.g. substituted biphenyls and alkyl benzenes), phenols and substituted phenols, long chain fatty acids and alkanes with carbon number up to 25 (Orem et al., 2007c; Orem et al., 2014). Organic substances in flowback and produced water from hydraulic fracturing of black shale have a similar range of compound classes as CBM produced water, but with lower levels of aromatic compounds and higher levels of aliphatic ones (Orem et al., 2014). This may reflect the organic matter differences within black shales and coals that the algal-derived shales show more aliphatic nature and vascular plant-derived coals show more aromatic character.

1.3 Analytical approaches for DOM characterization

It is a major analytical challenge to have a comprehensive understanding of the composition and general chemical structures of DOM. One reason is that DOM compounds are often present in extremely low concentrations while the inorganic salts exceed this value by several orders of magnitude, which can adversely affect the chemical analysis. Another reason is the heterogeneity and complexity of DOM that complicates the separation and detection. Chromatographic techniques can divide the DOM into fractions according to the polarity and molecular size, which are still too complex for unequivocal molecular and structural identification with conventional spectroscopic detections or fragmentation experiments (Reemtsma, 2001; Mopper et al., 2007).

1.3.1 DOM isolation and purification

Different methods have been applied to increase the DOM concentration and to remove salts. The commonly used isolation and purification methods include ultrafiltration (UF),

reverse osmosis (RO), reverse osmosis combined with electro dialysis (RO/ED) and solid phase extraction (SPE) (Leenheer and Croué, 2003; Mopper et al., 2007; Nebbioso and Piccolo, 2013; Minor et al., 2014).

SPE is the most commonly used isolation method now, which has been chosen in this work. SPE with commercially prepacked cartridges is an easy to handle method that does not require major instrumentation and can even be performed in the field (Simjouw et al., 2005). A large number of samples can be processed in parallel. The general principle of SPE is that when the samples pass through a cartridge, DOM can be retained on the solid phase in the cartridge and then be eluted from the solid phase by organic solvents such as methanol. The cartridge filled with a styrene divinyl benzene polymer sorbent (Varian PPL) has been proved to be one of the most efficient sorbents for DOM extraction with extraction efficiencies ranging from 40% to above 60%, depending on DOM type (Dittmar et al., 2008). The PPL resin is able to retain highly polar to nonpolar substances of DOM in large volumes of water (Dittmar et al., 2008). Samples have to be acidified to pH 2 before the isolation to increase the extraction efficiency. As a large amount of DOM is lost during the isolation and concentration processes, all the results obtained from mass spectrometric analyses of the SPE-treated samples refer only to this SPE-amenable part of the DOM in this thesis.

1.3.2 DOM characterization

The molecular structure of DOM was characterized by numerous techniques, such as pyrolysis gas chromatography DOM - mass spectrometry (GC-MS), chemical degradation GC-MS, liquid chromatography - mass spectrometry (LC-MS), nuclear magnetic resonance (NMR), X-ray absorption spectroscopy (XPS) as well as optical methods in previous studies (Olivella et al., 2002; Kim et al., 2003e; Derenne and Nguyen Tu, 2014). However, most of these methods are biased and/or fail to resolve the complex DOM mixture (Hatcher et al., 2001; Leenheer and Croué, 2003). The low resolution GC-MS and LC-MS can examine only a small portion of overall DOM. Furthermore, pyrolysis and chemolysis are invasive techniques that can destruct most constituents in DOM and form new products. NMR and XPS can deliver useful information about functional groups of the bulk DOM, but fail to give molecular-level details. The UV-visible absorption and fluorescence analyses are commonly used to determine the composition and concentration of DOM in aqueous systems (Murphy et al., 2008; Spencer et al., 2009). However, these two approaches can only provide information on the chromophoric DOM and fluorescent DOM fractions of the DOM pool.

In the last decade, Fourier transform ion cyclotron resonance mass spectrometry (FT-ICR-MS) has emerged as an important tool for the molecular-level characterization of the complex DOM mixture. FT-ICR-MS is one of most powerful techniques that are able to distinguish tens of thousands of ions with different concentrations simultaneously and without chromatographic sample preparation. Combined with electrospray ionization (ESI), a soft ionization method, it is particularly promising for the characterization of polar molecules. It exhibits a very high mass accuracy with mass defect below 1ppm for the assigned molecular formulae (Stenson et al., 2003; Koch et al., 2005). As FT-ICR-MS is the only method that can reach the resolution and mass accuracy requirement for unique and unambiguous molecular formulas assignment currently, it has rapidly become one of the first choices in DOM studies (Kim et al., 2003e).

The fundamentals behind FT-ICR-MS are easily illustrated. After ionization of the molecules, ions are focused by funnel system of the ion optics and a quadrupole. The ions enter the collision cell and accumulate there. The collision cell is an additional quadrupole mass analyzer, which enables a selective ion filtration. The ions enter the ICR cell and circulate at their cyclotron frequencies in orbital trajectory. The ICR cell is a penning trap with strong permanent superconducting magnet field. The cyclotron frequency of their orbit depends inversely on the mass-to-charge ratio of the ions. Because the frequencies can be measured more accurately than any other physical property, FT-ICR-MS provides the highest mass measurement accuracy currently available.

1.4 Sedimentary macromolecular organic matter

One possible source of DOM in natural environments is the organic matter (OM) present in sediments. After the death of organisms, the OM is subjected to decomposition and preservation. Main part of the OM is degraded and recycled as energy source for other organisms; part of the OM survives this biological cycle and directly incorporates into sediments and undergoes various alterations during burial, which is the primary source of sedimentary OM. Both the marine and terrestrial OM contains dispersed macromolecular organic matter, namely kerogen, can act as the source rock for the petroleum formation.

1.4.1 Type of kerogen

Kerogen, defined as the fraction of sedimentary OM insoluble in common organic solvents (Forsman and Hunt, 1958; Durand, 1980) is in contrast to the soluble part of OM that

is termed bitumen. The bitumen usually represents only 1-10% of the total OM while the kerogen typically comprises more than 90% (Rullkötter et al., 1992; Summons, 2013). According to the origin of the source material and depositional conditions, kerogen can be divided into three distinct types: Type I, II and III (Fig. 1.1). The three different kerogen types can also be recognized by elemental analysis (Van Krevelen, 1950; Durand and Espitalié, 1973) and Rock-Eval pyrolysis (Espitalie et al., 1977).

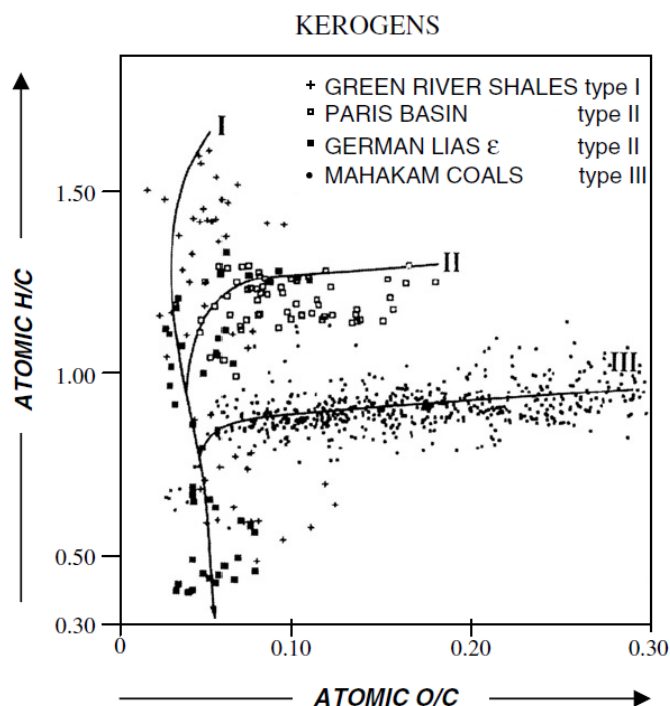


Figure 1.1. Van Krevelen diagram indicating the different diagenetic, catagenetic and metagenetic evolution pathways of the three kerogen types concerning the H/C and O/C atomic ratios (Vandenbroucke and Largeau, 2007).

Type I kerogen is characterized by a high initial H/C atomic ratio above 1.5 and low initial O/C ratio generally below 0.1. These values indicate that the type I kerogen of immature samples is highly aliphatic and the content of aromatic bonds is generally low compared to other types of organic matter. The small amount of oxygen is mainly bound in ether groups (Fester and Robinson, 1966). The formation of type I kerogen has been attributed to result from intense accumulation of algal material or strong biodegradation of lipids and waxes (Tissot and Welte, 1984). Algal material as the source biomass suggests a lacustrine depositional environmental or deposition being closely related to the shorelines (e.g. lagoons). Most common macerals are liptinites, in particular alginite. Organic solvent extracts as well as the generated oil and the pyrolysis products of this kerogen are rich in long chain *n*-alkanes

with chain length up to more than 40 carbon numbers. The hydrogen index (HI) which reflects the hydrocarbon generation potential is much higher for type I kerogen (>600 mg HC/g TOC) compared to other kerogen types. Despite the high oil generation potential of type I kerogen, their rare occurrence accounts for only 2.7% of the world's petroleum and gas reserves (Klemme and Ulmishek, 1991). One example of type I kerogen is the Green River shale that resulted from a combination of both algal and microbial lipids (Tissot and Welte, 1984).

Contrary to type I kerogen, type II kerogen frequently exists in many petroleum source rocks and oil shales, e.g. the lower Toarcian Posidonia shale in Northwestern Germany, the Devonian-Mississippian Bakken shale in North Dakota (USA), the upper Devonian Duvernay shale in the Western Canada Sedimentary Basin and the middle Cambrian to lower Ordovician Alum shale in Denmark. For the immature type II kerogen, the H/C and O/C atomic ratios are about 1.3 and 0.15, respectively. The OM contains more polyaromatic units and naphthenic rings than the type I kerogen. Beside the large amount of aromatics, the aliphatic rings can become aromatized with progressive maturation (Vandenbroucke and Largeau, 2007). The chain length of the *n*-alkane is restricted to carbon number range less than 25 in both solvent extracts and pyrolysates (Vandenbroucke and Largeau, 2007). Type II kerogen is commonly related to marine sediments where the primary source of biomass is of planktonic origin, also allochthonous terrestrial organic debris can be found. With HI values between 200 and 600 mg HC/g TOC, the type II kerogen shows a generally lower oil generation potential than type I kerogen. As the sea-water sulfate can penetrate into sediment, sulfur is always associated with type II kerogen. The sulfur rich kerogens are grouped to type II-S, which is a subgroup of type II kerogen containing 8-14% (by weight) organic sulfur (Orr, 1986).

Type III kerogen is featured with a relatively low initial H/C ratio less than 1.0 and a high initial O/C atomic ratio up to 0.3 at low maturity stage. The hydrogen content is low due to the relatively high abundance of condensed aromatic and oxygen-containing structures (Tissot and Welte, 1984). The depositional environments of this kerogen type are often deltaic systems and continental margin areas. Only the highly resistant chemical constituents of the terrestrial organic matter can be incorporated in the sediment. Fast burial with high subsidence rates prevents the bacterial degradation of the organic matter. Type III kerogen contains a huge amount of aromatic structures with short aliphatic chains (<C18) originated from ligneous debris and minor amount of long chain aliphatic structures derived from higher

plants. As the ligneous debris mainly generates gas and aliphatic protective coating generates oil (Killops et al., 1998), the variable gas vs. oil generation potential of type III kerogen cannot be estimated only by the H/C atomic ratio or the Rock-Eval HI value (Isaksen et al., 1998) but depends on the proportion of the two main constituents within the kerogen structure.

1.4.2 Evolution of kerogen organic matter

As organic matter is buried in sediments, the molecular structure is no longer in equilibrium with the depositional environment due to various microbial, geochemical and geothermal alteration processes. Rearrangements and degradation of the macromolecular organic matter take place to reach a new thermodynamic equilibrium with the new surroundings, which is the so called maturation process. Using vitrinite reflectance microscopy, the maturation processes of organic matter can be divided into three stages: diagenesis ($R_o < 0.5\%$), catagenesis ($0.5\% < R_o < 2\%$) and metagenesis ($R_o > 2\%$) (Tissot and Welte, 1984).

After deposition of the sediment in a restricted environment, the early diagenesis starts. The sediment contains plenty of water, minerals, organic matter and microorganisms. The living organisms can participate in the biodegradation and decomposition of organic matter. Previous biogenic polymers (proteins, carbohydrates) are destroyed by microbial activity during the sedimentation. The most notable change during early diagenesis is loss of nitrogen. The degradation of nitrogen-containing compounds is mainly related to elimination of amino acids and ammonia via hydrolysis reaction (Schnitzer, 1985). The end of the early diagenesis is featured by the process when nitrogen-containing compounds are no longer hydrolysable. On the contrary, sulfur can be incorporated in marine sediments during early diagenesis to form sulfur rich kerogen (Type II-S). Sulfur can be introduced into the sediments abiotically in form of pyrite microcrystals or framboids and biotically by sulfate reducing bacteria (SRB) (Berner, 1984).

The stage of diagenesis is featured by an important decrease of oxygen and a relative increase of carbon with ongoing subsidence and maturation. When referring to the Van Krevelen diagram (Fig. 1.1), a marked decrease of the O/C ratio and a slight decrease of H/C can be observed at this stage. The main degradation and alteration processes during diagenesis are biotic. The loss of oxygen is mainly by emission of water and carbon dioxide through dehydroxylation and decarboxylation reactions of the organic matter. It has been discovered that the C=O groups involved in acids and ketones are more easily eliminated than esters

(Robin and Rouxhet, 1978). With ongoing burial, the moisture of organic matter decreases while temperature and pressure increase with depth. The temperature can reach up to 100°C during diagenesis (Killops and Killops, 2013).

Although loss of oxygen continues at the early stage of catagenesis, the main feature of catagenesis is the loss of hydrogen and the decrease of H/C atomic ratio due to the generation and expulsion of hydrocarbons. The beginning of catagenesis is defined as the so-called oil window, which starts at temperatures around 100°C and shows its maximum at temperatures of about 150°C (Killops and Killops, 2013). Organic matter has experienced two main changes: liquid petroleum is firstly produced during the progressive evolution; wet gas and condensate are generated later. The maturation process leads to progressive elimination of aliphatic bonds as well as ongoing aromatization and more condensed solid residue of the kerogen (Robin and Rouxhet, 1978; Lis et al., 2005; Werner-Zwanziger et al., 2005; Kelemen et al., 2007; Petersen et al., 2008). During this stage, the molecular weight of the generated hydrocarbon becomes lower and lower, significant amount of methane is produced simultaneously. At thermal maturity with vitrinite reflectance higher than 1.5%, the generation of gas (methane) through secondary cracking of hydrocarbons can be observed (Dieckmann et al., 1998). The end of catagenesis is defined by H/C atomic ratio of 0.5 or a vitrinite reflectance of 2% (Tissot and Welte, 1984). At this maturation stage, the three types of kerogen plot in the same region of the Van Krevelen diagram and can no longer be distinguished.

The beginning of metagenesis corresponds to a vitrinite reflectance of 2%. During this stage, aliphatic and C=O bonds are vanished and the main bond is aromatic. The structure reorganization and ring condensation reactions of the kerogen occur and the aromaticity of the organic matter continues to increase accordingly. The thermal cracking and elimination of aromatic methyl groups leads to the generation of methane simultaneously. Part of the released methane may be derived from secondary cracking of already generated higher hydrocarbons. Also, some heterocompounds are generated in form of CO₂, H₂S and N₂ (Behar et al., 2000). The stage of metagenesis is totally situated in the dry gas zone. Although the three kerogen types are plotted in the same zone in the Van Krevelen diagram, the size of the aromatic clusters in the macromolecules varies depending on the kerogen type, they increase from type I to type III.

1.4.3 Macromolecular organic matter in black shales

Black shales are dark colored, extremely fine-grained sediments that normally occur in thin layers under anaerobic conditions in many areas (Swanson and Swanson, 1961). The most important characteristic that differentiates black shale from other mudstone is the high content of organic matter, which is the main cause for the dark color of black shales. The organic carbon content of black shales is mostly in the range of 2-10%, a few shales even contain more than 20% organic carbon (Tourtelot, 1979). The organic matter in black shales can originate from both terrestrial and marine sources. But the pre-Silurian organic matter mainly comes from marine sources as no (or only few) land plants existed before Silurian or Devonian time (Engel and Macko, 2013). The black shales from different areas investigated in this thesis are all originated from marine organic matter. As the marine organic matter can be easily metabolized by microorganisms, oxygen can be consumed and sulfide can be produced, the anoxic environment again favors the accumulation of organic matter (Engel and Macko, 2013). Black shales are important from both the geological and economic points of view as source rocks of petroleum and natural gas. It has been estimated that more than 90% of the recoverable oil and gas reserves have been generated from black shales worldwide (Klemme and Ulmishek, 1991).

Significant chemical and structural evolution happened to the macromolecules in black shales with increasing thermal maturation. In artificial maturation experiments, it has been shown that kerogen may decompose into heavy NSO compounds that can rapidly undergo secondary cracking to generate hydrocarbons and new NSO compounds (Lewan et al., 1985; Lewan, 1997; Behar et al., 2008a; Behar et al., 2008b; Behar et al., 2010). Asphaltenes and polar NSO compounds do not appear to act as simple intermediate products between kerogen and hydrocarbon during oil and gas generation. They are also involved in the chemical variation during maturation via second order reactions (Michels et al., 1996; Vu et al., 2008). Normally, with increasing maturation the net loss of carbon is indicated by the decrease in TOC content (Rullkötter et al., 1988). The immature black shale is featured by plenty of aliphatic components and high concentrations of oxygen and sulfur-containing functional groups with only a few isolated aromatic structures while the overmature black shales are dominated by poorly condensed aromatic structures and fewer aliphatic chains (Schenk et al., 1986; Behar and Vandenbroucke, 1987; Horsfield and Dueppenbecker, 1991; Patience et al., 1992; Requejo et al., 1992; Putschew et al., 1998; Lis et al., 2005; Smernik et al., 2006). With increasing maturation, the alkyl carbon types are progressively lost from kerogen and

concentrate the bulk of the aromatics in the residual kerogen; new aromatics are formed by aromatization/condensation reactions at the same time, which together increase the aromaticity of the kerogen (Barwise et al., 1984; Patience et al., 1992). During the aromatization, the distribution of aromatic carbon types changes substantially. The relative abundances of bridgehead (ring junction) and protonated aromatic carbons increase, whereas phenolic and alkylated aromatic carbon declines or remains roughly constant, respectively (Patience et al., 1992). Meanwhile, the percentage of heteroatom-bonded carbon (to O or S) also declines consistently.

1.4.4 Macromolecular organic matter in coals

A notable amount of sedimentary organic matter is concentrated in form of coals. Coals have been defined as “readily combustible rock containing more than 50% by weight and 70% by volume of carbonaceous material” (Schopf, 1956). Beside the minor amount of inorganic minerals, the major part of the coals consists of organic constituents originating mainly from terrestrial plant material. After deposition in sedimentary basin, the organic matter was protected by water and mud from intense aerobic degradation. As the burial depth increases, the organic material might undergo a sequence of physical, chemical and biochemical changes (diagenesis and catagenesis) that result in the loss of oxygen and hydrogen as well as carbon condensation.

The organic matter of coals can be grouped into three maceral groups: liptinite, vitrinite and inertinite (Stach et al., 1982). Liptinites are derived mostly from algae or spores, pollens, cuticles and resins of the original plant material. The organic materials are rich in hydrogen content and thus have a huge petroleum generation potential. Vitrinites are derived from wood, bark and roots that contain less hydrogen than the liptinite. Inertinites are mainly the degradation products of other macerals that contain the least amount of hydrogen within the three macerals, which are consequently rich in carbon (Stach et al., 1982; Hunt, 1991; Boreham and Powell, 1993; Taylor et al., 1998). Coals normally contain different proportions of the three maceral groups and show different capacities to generate oil and gas (Saxby and Shibaoka, 1986; Mukhopadhyay et al., 1991).

According to the coal-forming plants, coals can be classified as sapropelic coal and humic coal. Sapropelic coals are less common than humic coals. They are mainly derived from microscopic plants and comprise large amounts of autochthonous algae. Humic coals are mainly derived from high plants and the major organic components are lignins and celluloses.

The main maceral group of humic coals is vitrinite. Humic coals can be classified into peat, lignite, sub-bituminous coal, volatile bituminous coal and anthracite according to their thermal maturity rank. To evaluate the rank of coal, various parameters like moisture content, calorific value, vitrinite reflectance and volatile matter content can be used (Tissot and Welte, 1984).

Less than 10% of the woody debris is accumulated as peat; other part of the organic material is lost during peat formation by microbial consumption or remineralization (Given and Dickinson, 1975). Nevertheless, the efficiency of peat formation is higher than organic matter accumulation in marine sediments. Peat generally has a water content of up to 95%. In general, there are two stages during peat formation. The first stage starts immediately below the surface and is characterized by strong oxidation. The second stage is under reducing conditions, progressive loss of moisture (dehydration) through both physical compaction and chemical transformation are occurring to the buried peat, and anaerobic bacteria are believed to take an active role in the catalyzation. The formation of lignite is featured by microbial alteration of lignin (Hatcher, 1990) and loss of oxygen-containing groups. The condensation reaction, cleavage of ether bonds as well as formation of phenols are also happening during this stage. Ongoing maturation leads to significant structural changes to lignite. The lignite contains no undecomposed dead plant and start to form layers geologically. The vitrinite macerals become more homogeneous under the microscope. Dehydroxylation reactions force the conversion of lignites into sub-bituminous coals (Hatcher and Clifford, 1997). During this process, dihydroxy phenols as the main compound units in lignite are transformed to phenols in sub-bituminous coals (Hatcher, 1990; Hatcher and Clifford, 1997). The start of catagenesis in humic coals is related to the generation of high volatile bituminous coals at a vitrinite reflectance of $R_o = 0.5\%$. Depletion of oxygen continues and gas can be generated. The main reactions are condensation and aromatization. Thus, the aromaticity of the organic matter increases at this rank of maturation. The decrease of O/C atomic ratio is terminated at this maturation stage (Fig. 1.1). The increasing temperature and pressure lead to ongoing condensation and polymerization of aromatic compounds. Anthracite representing the most mature rank of coalification process starts at a vitrinite reflectance of $R_o = 2\%$.

1.5 Research objectives

Representing the major sites at which sedimentary organic carbon is preserved, black shales and coals could release quantitatively significant masses of organic compounds to the

surrounding environment when they are exposed to water during production operations. This applies to shale gas and coalbed methane exploitation, CO₂ storage, and geothermal energy production. The DOM released from black shales and coals during hydraulic fracking operations has been highlighted as a potential hazard especially during the storage, transport and disposal of wastewater. It is therefore important to characterize the DOM, and that means establishing links between DOM composition and that of the in-situ organic matter. In that regard, the organic matter of both black shales and coals is subject to thermal degradation and structural rearrangements related to changing physical and chemical environments during the burial process (Tissot and Welte, 1984). These changes along the maturation processes are probably reflected in the molecular composition of the extracted DOM. Besides thermal maturation, other aspects such as the kerogen type and organofacies variations of the organic matter and the polarity of the DOM also have to be taken into account.

Different aliphatic and aromatic compounds in the flowback and produced water of shale gas and CBM exploitation have been reported before (Maguire-Boyle and Barron, 2014; Orem et al., 2014; Ferrer and Thurman, 2015). However, they did not provide a holistic perspective on the DOM composition and the factors that shape the DOM liberation. Non-targeted techniques with extremely high resolution like FT-ICR-MS can highlight the diversity of organic compounds within different samples and fill the gap. To understand the molecular composition and mobilization of the DOM released from black shales and coals, the main questions addressed within the scope of this thesis are:

- 1) What is the composition of the extracted DOM of black shales and coals? Is the extracted DOM comparable to DOM in natural waters?
- 2) What differences can be observed in the extracted DOM related to kerogen type and organofacies of the sedimentary organic matter?
- 3) Which effect does the thermal maturity of the sedimentary organic matter have on the molecular composition of the extracted DOM?
- 4) What are other controlling factors of the composition and amount of individual compounds in the extracted DOM?

To answer the research questions, black shales and coals were extracted with water to investigate the water soluble organic compounds. In order to cover a wide variety of geological settings, thirty-five samples from the Posidonia Shale, Bakken Shale, Duvernay Formation, Alum Shale and New Zealand coals were investigated in this study. Coals were selected to differentiate mobility of organic compounds from different natural organic matter

types. The five New Zealand coals represent two different organofacies according to the alkyl chain length distribution of their pyrolysate and their palynofloras differences. The shale samples cover a broad range of organic matter and mineral compositions. The shales from the Posidonia and Duvernay are rich in carbonate while those from the Bakken and Alum are characterized by high amounts of quartz and clay, respectively. The Posidonia shale samples collected from six shallow boreholes are quite uniform with respect to their depositional environment and organofacies, and cover a perfect maturation range from immature to overmature. Therefore, they have been considered to be the ideal sample set to investigate the effect of maturity on the mobilization of DOM. The DOM in the water extracts were analyzed by different analytical techniques and evaluated as follows:

1) This dissertation not only quantifies the extracted DOM but also different DOM fractions that have been divided according to the molecular weights by LC-OCD. Particular emphasis is laid on LMWOAs as they are ubiquitous. The general information on factors that influence the mobility of different water-soluble organic compounds is provided.

2) In addition, water extracts from the Posidonia Shale and New Zealand coals are investigated with FT-ICR-MS, which can provide molecular insight into individual organic compounds after SPE. The possible molecular structures and important groups or functional moieties of organic matter in the extracted DOM of black shales and coals are inferred based on molecular formulas. As the coal samples represent two different organofacies, the influence of organofacies on the DOM composition can also be illustrated. Apart from the coal samples that consist of terrestrial organic matter, shale samples were derived from marine organic matter. The differences in the extracted DOM of black shale and coal samples are compared. As the Posidonia shale samples represent a complete maturation series with similar organofacies, the influence of thermal maturity on the overall composition of extracted DOM can be clarified.

1.6 Structure of the dissertation

This cumulative thesis addresses the above mentioned research questions in three manuscripts. Chapter 2 and Chapter 3 were already published; Chapter 4 contains a manuscript close to submission.

Chapter 2 reveals how maturation and organofacies of samples affect the bulk yields and compositions of the extracted DOM, different DOM fractions and individual LMWOAs of different coals and black shales during water extraction.

Chapter 3 introduces the molecular composition of the extracted DOM of New Zealand coals and describes the influence of organofacies on the composition of O-containing compounds. The molecular structure and source of the prominent compounds in extracted DOM have been clarified. The O-containing functional groups in different O_x classes have been illustrated.

Chapter 4 introduces the molecular composition of the extracted DOM of Posidonia shale samples and illustrates the effects of thermal maturity on the extracted DOM composition. The DOM of the water extracts and the solvent extracts of the same sample has been compared. The extracted DOM of samples with different kerogen types has been compared as well.

Chapter 5 summarizes the results of the preceding chapters and provides answers to the research questions and an outlook for future work.

2. CHARACTERIZATION OF WATER-SOLUBLE ORGANIC COMPOUNDS RELEASED FROM BLACK SHALES AND COALS¹

2.1 Abstract

Knowledge of the composition of dissolved organic compounds as well as the main controls on their mobilization from natural organic matter is prerequisite for a comprehensive understanding of the fluid-rock interactions taking place in shale environments and coal seams over both geological and human timescales. In this study, black shales and coals from five different geological settings and covering the maturity range $R_o = 0.3\text{--}2.6\%$ were extracted with deionized water. The dissolved organic carbon (DOC) yields were found to decrease rapidly with increasing diagenesis and remain low throughout catagenesis. Four different fractions of DOC have been qualitatively and quantitatively characterized in the study using size exclusion chromatography (SEC). Acetate is the dominant low molecular weight organic acid (LMWOA) in all extracts of shales and coals of bituminous rank. The concentrations of individual LMWOA also decrease with increasing maturity of the samples except for acetate extracted from the overmature Posidonia shale from the Haddessen well, which was influenced by hydrothermal brines. The positive correlation between the Oxygen Index (OI) and respective LMWOA yield indicates that OI is a significant factor influencing the extraction of organic acids from shales. The yields of both DOC and individual organic acids normalized to TOC are in the same order of magnitude for coals and shales with the same maturity. However, the extracts of coals tend to contain more aromatic compounds and the molecular masses of most constituents included in macromolecular fractions are higher than for shale extracts. These results suggested that different kerogen types show comparable

¹ This chapter has been published as: Zhu, Y., Vieth-Hillebrand, A., Wilke, F.D.H., Horsfield, B., 2015. Characterization of water-soluble organic compounds released from black shales and coals: *International Journal of Coal Geology* 150–151, 265–275 (postprint), <https://doi.org/10.1016/j.coal.2015.09.009>.

amounts of DOC being extracted, but different DOC composition. Thus, both the origin of organic matter and thermal maturation progress during deposition has significant influence on water extract composition.

2.2 Introduction

Dissolved organic carbon (DOC) is defined as the fraction of organic matter in water that passes through a filter with pore size $0.45\mu\text{m}$ (Herbert and Bertsch, 1995). DOC in near-surface groundwater and natural formation waters like oil field brines has been studied for years (Leenheer and Croué, 2003; Lepane et al., 2004; Schmidt et al., 2009) and the first insights into the molecular composition have been provided. Special attention has been paid to the abundance and origin of low molecular weight organic acids (LMWOAs) in subsurface brines (Means and Hubbard, 1987). LMWOAs have been proposed as tracers or proximity indicators of hydrocarbons (Zinger and Kravchik, 1973), and Kharaka et al. (1983) argued that acid anions are important precursors of natural gas via thermal cracking. LMWOAs are assumed to create secondary porosity in the subsurface by increasing the dissolution of aluminosilicates and carbonates (Surdam et al., 1984). Additionally, LMWOAs can act as feedstock for the deep terrestrial biosphere (Horsfield et al., 2006; Vieth et al., 2008). As far as oil and gas production is concerned, it has been reported that LMWOAs make up a dominant fraction of DOC in waters utilized during oil shale retorting (Leenheer et al., 1982; Dobson et al., 1985). High concentrations of formate and acetate in flowback waters were previously reported in fracturing flowback (Olsson et al., 2013; Lester et al., 2015). The amount and composition of other organic compounds in flowback and produced waters from hydraulic fracturing of shales have been reported in recent years (Maguire-Boyle and Barron, 2014; Orem et al., 2014). Although the occurrence of DOC and LMWOAs in different types of natural waters is well documented, only little work has been done to elucidate the relation between their quantitative and qualitative occurrence in water and the properties of the rock they have been in contact with.

Black shales and coals usually contain high concentrations of organic matter. During progressive burial over geological times, reactive functional groups within the organic material are thermally degraded. It is well known that during diagenesis, with vitrinite reflectance (R_o) below 0.5%, biopolymers such as polysaccharides, proteins and amino sugars are initially degraded by microorganisms in the water column and in young sediments, after which a loss of hydrolysable moieties takes place during continuing subsidence (Tissot and

Welte, 1984). Catagenesis ($R_o = 0.5 - 2.0\%$) is characterized by the progressive cracking of carbon-carbon and carbon-oxygen bonds accompanied by aromatization and condensation of the kerogen (Robin and Rouxhet, 1978; Lis et al., 2005; Werner-Zwanziger et al., 2005; Kelemen et al., 2007; Petersen et al., 2008). The generation of LMWOAs in sedimentary basins has been attributed to the cleavage of kerogen fragments containing carboxylic functional groups during the early stage of thermal maturation (Cooles et al., 1987). Decreasing yields of ester-bound LMWOA generated with increasing maturity of coals has been reported (Glombitza et al., 2009). In addition, oxidation reactions involving mineral oxidants may also produce organic acids during thermal maturation (Surdam et al., 1993; Borgund and Barth, 1994; Seewald, 2001a, c).

Knowing the composition, molecular size and structure of the DOC as well as the main controls on the release of DOC are prerequisites for a better understanding of the fluid-rock interactions taking place in shale environments over both geological and human timescales. Soxhlet extraction of marine sediments accesses a larger and more complex pool of organic matter than that contained in interstitial pore water (Schmidt et al., 2014). Hot water extraction of organic matter has also been previously applied to soils to examine the labile organic fractions (Ghani et al., 2003; Gregorich et al., 2003; Bu et al., 2010; Sarkhot et al., 2011). Thus, water extraction is an appropriate tool for studying the soluble organic matter released during the interaction between water and rock. As far as we are aware, leaching experiments have only rarely been applied to black shales and coals (Bou-Raad et al., 2000; Vieth et al., 2008) and little attention has been paid to how DOC composition varies as a function of organofacies, organic matter type and maturity. In the present contribution, we report the composition of DOC in water extracts from shales and coals not only of different geological ages and depositional settings, thereby covering different kerogen types, but also different thermal maturation levels, enabling the controls of progressive thermal maturation on composition of water extracts to be documented.

2.3 Materials

Thirty-two organic-rich black shales and coals from around the world, representing a wide range of depositional settings and ages (Paleozoic through Cenozoic age) were selected for this study (Table 2.1). The samples cover a maturity range from immature ($R_o = 0.29$; $T_{max} = 409^\circ\text{C}$) to overmature ($R_o = 2.6$; $T_{max} = 602^\circ\text{C}$) with TOC contents of shales and coals extending up to 15% and 67%, respectively. The chain length distribution of *n*-alkyl moieties

(C₁₋₅ total, *n*-C₆₋₁₄, *n*-C₁₅₊) in pyrolysates of the original samples is illustrated in the ternary diagram of Horsfield (1989) (Fig. 2.1). The pyrolysate compositions of shale samples indicate Paraffinic-Naphthenic-Aromatic Low Wax Oil petroleum type as well as Gas and Condensate petroleum type organofacies. The chain length distributions of the macromolecular organic matter in shale samples are closely similar despite their diverse origins. The three bituminous coals (C3, C4 and C5) fall in the High Wax, Paraffinic-Naphthenic-Aromatic Oil petroleum type and the two lignites C1 and C2 fall in Paraffinic Oil High Wax organofacies. Relative percentages of the three main minerals of the shale samples are shown in Figure 2.2. The Posidonia and Duvernay shales are dominated by carbonate, whereas the Bakken and Alum shales are characterized by higher contents of quartz and clays, respectively.

2.3.1 Posidonia shale

The Lower Toarcian Posidonia shale samples are from three shallow boreholes (Wickensen, Harderode, Haddessen) located in the Hils Syncline of Northwest Germany and cover a large maturity range from immature to overmature (Rullkötter et al., 1988). The shale was deposited in a restricted epicontinental sea with prevailing anoxic conditions, and the organic matter originates mostly from marine phytoplankton with minor terrigenous input (Littke et al., 1991). Comprehensive studies on the Posidonia shales have been presented by several authors, on nanoscale structure (Bernard et al., 2010; Bernard et al., 2012), petrophysical characteristics (Mann and Müller, 1988) and biogeochemistry (Wilkes et al., 1998). The depositional conditions and the preservation of organic matter are considered to be uniform for the three sampling sites (Littke et al., 1988; Rullkötter et al., 1988; Littke et al., 1991).

2.3.2 Bakken shale

The Devonian-Mississippian Bakken shale samples from six wells located in the Williston Basin in North Dakota, USA and covering the immature to mature range, were supplied by the North Dakota Geological Survey. The Bakken shale was deposited in an epicontinental setting (Jiang et al., 2001) under anoxic and uniformly quiet conditions, judging by the widespread occurrence of planar and thin laminations (Webster, 1984). Amorphous organic matter derived from marine algae dominates, and terrestrial contributions are minor (Smith and Bustin, 1998). The detailed petroleum system has been investigated in previous studies (Leenheer, 1984; Muscio et al., 1994; Jiang and Li, 2002; Kuhn et al., 2010; Kuhn et al., 2012).

2.3.3 Duvernay shale

Six samples were taken from the Upper Devonian Duvernay Formation in the Western Canada Sedimentary Basin, and supplied by the Geological Survey of Canada. They follow a progressive trend in maturity from northeast to southwest. Two principal interbedded lithofacies are present: the nodular to nodular-banded lime mudstones exhibit varying degrees of bioturbation and indicate relatively oxygenated conditions; the dark bituminous laminated lime mudstones were deposited in deep water under oxygen-starved conditions (Creaney and Allan, 1990; Chow et al., 1995; Li et al., 1997; Dieckmann et al., 2004). The organic matter is mainly of marine planktonic origin as indicated by, for example, the biomarker value of pristane/*n*-C₁₇ versus phytane/*n*-C₁₈ (Li et al., 1997) and petrographic composition (Dieckmann, 1999).

2.3.4 Alum shale

The Alum shale samples were collected from a shallow well located in the south of the island of Bornholm, Denmark, which covers stratigraphic ages from Middle Cambrian to Lower Ordovician (Schovsbo et al., 2011). The shale formation is considered to have been deposited in a predominantly anoxic marine environment as the TOC content of the Alum shale is very high (Buchardt et al., 1986; Buchardt and Lewan, 1990). The Alum shale comprises homogeneous fine-grained mudstone and a low proportion of limestone occurring as beds and nodules, which indicate a uniform depositional environment (Buchardt et al., 1986). All the Alum shale samples, having evolved from an alginate-rich Type II kerogen (Horsfield et al., 1992), have a very high thermal maturity with the reflectance of “vitrinite-like” particles being about 2.3% (Buchardt and Lewan, 1990).

2.3.5 New Zealand coal

The Cenozoic coal samples were gathered from one drilled core and two coal mines in New Zealand. Three samples were taken from the DEBITS-1 well located in the Waikato Coalfield, two of which were lignites from above an unconformity and one of sub-bituminous rank from below the unconformity (Kallmeyer et al., 2006). The sample from Rotowaro Mine in Waikato Basin represents sub-bituminous coal and the one from Welcome Mine in West Coast Basin is a coal of High Volatile Bituminous rank (Vu et al., 2009).

Table 2.1. Sample origin and Rock-Eval pyrolysis characteristics. Hydrogen Index (HI) and Oxygen Index (OI) are measured in mg hydrocarbons/g organic carbon and mg CO₂/g organic carbon,

respectively. TOC and Rock-Eval data of Duvernay shales and New Zealand coals were taken from (Dieckmann, 1999) and Glombitza (2011), respectively. Posidonia, Bakken and Alum shale samples were analyzed in this study. Ro values of Posidonia, Bakken, Alum and New Zealand samples were taken from Rullkötter et al. (1988), Dembicki and Pirkle (1985), Buchardt and Lewan (1990), and Glombitza (2011) respectively. R_o of Duvernay shales was calculated using the empirical formula $\%R_o = 0.018 * T_{max} - 7.16$ (%) (Jarvie et al., 2007).

G number	ID	Well	Depth (m)	TOC (%)	Tmax (°C)	OI	HI	Ro (%)
<i>(A) Black shale, Posidonia Formation, Germany, Lower Jurassic, Type II</i>								
G007156	P1	Wickensen	58.2	9.9	430	14	664	0.53
G007141*	P2	Wickensen	42.2	9.0	432	16	658	0.53
G007129	P3	Wickensen	30.2	11.4	433	14	634	0.53
G007107	P4	Harderode	77.3	4.8	447	7	340	0.88
G007036*	P5	Harderode	42.5	7.2	449	7	384	0.88
G007049	P6	Harderode	55.7	11.0	449	5	282	0.88
G007085	P7	Haddessen	36.6	9.2	466	9	87	1.45
G007104*	P8	Haddessen	51.0	5.0	466	16	79	1.45
G007119	P9	Haddessen	60.6	7.7	469	8	66	1.45
<i>(B) Black shale, Bakken Formation, USA, Mississippian, Type II</i>								
G0012465*	B1	Daniel Anderson 1	1012.1	9.4	409	28	360	0.35
G0012466	B2	Dobrinski 18-44	2631.7	14.9	423	12	420	0.45
G0012469	B3	Nordstog 14-23-161-98H	2651.6	12.1	440	3	462	0.7
G0012470	B4	Loucks 44-30	2350.8	15.0	440	2	460	0.75
G0012467*	B5	Titan E-Gierke 20-1-H	3351.6	11.9	452	3	118	0.86
G0012468	B6	BR 12-29	3253.7	8.4	452	4	93	1.1
<i>(C) Black shale, Duvernay formation, Canada, Late Devonian, Type II</i>								
G000609*	D1	Sarcee et al Pibroc	1395.9	6.4	418	19	619	0.36
G000586	D2	Imperial Kingman	1404.2	2.4	427	32	412	0.53
G000632	D3	Bangg Imperial	1677.9	5.5	431	6	621	0.6
G000552	D4	Tomahawk	2337.5	4.8	435	7	620	0.67
G000607*	D5	Imperial Cynthia	2976.1	1.9	447	12	92	0.89
G000624*	D5	Banff Aguit Ram River	4623.9	2.0	542	17	4	2.6
<i>(D) Black shale, Alum Formation, Denmark, Lower Ordovician to Middle Cambrian, Type II</i>								
G008528	A1	Skelbro-2	39.6	6.3	564	2	3	2.3
G008505*	A2	Skelbro-2	27.0	10.1	591	8	4	2.3
G008527	A3	Skelbro-2	38.7	8.1	591	2	3	2.3
G008480	A4	Skelbro-2	15.0	11.2	599	1	7	2.3
G008473	A5	Skelbro-2	11.8	7.7	600	4	3	2.3
G008495	A6	Skelbro-2	21.1	11.4	602	34	10	2.3

Table 2.1 Sample origin and Rock-Eval pyrolysis characteristics. -continued

G number	ID	Well	Depth (m)	TOC (%)	Tmax (°C)	OI	HI	Ro (%)
----------	----	------	-----------	---------	-----------	----	----	--------

(E) Coal, New Zealand, Cenozoic, Type III

G004541*	C1	DEBITS-1	18.9	45.1	414	95	192	0.29
G004543*	C2	DEBITS-1	62.5	35.9	414	80	366	0.29
G004547*	C3	DEBITS-1	140.5	58.2	419	26	172	0.39
G001981*	C4	Rotowaro Mine	Outcrop	61.2	422	32	154	0.45
G001997*	C5	Welcome Mine	Outcrop	67.4	424	15	209	0.52

*: Samples selected for display in Figures 2.4 and 2.5 are covering the whole range of maturity from each location.

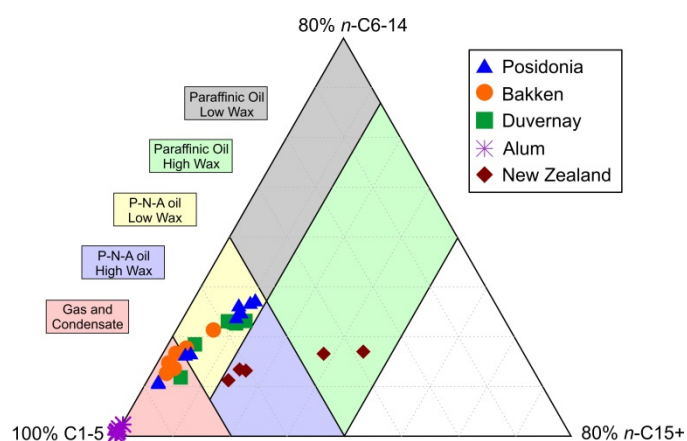


Figure 2.1. Bulk properties of the sediment pyrolysates concerning alkyl chain length distribution and petroleum type organofacies using the ternary diagram of Horsfield (1989).

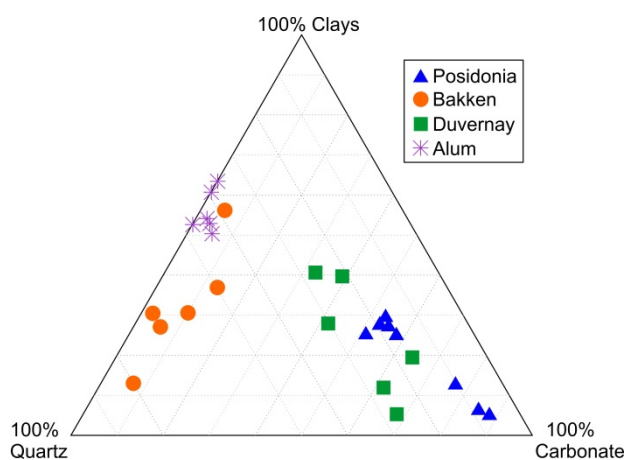


Figure 2.2. Ternary diagram showing the relative contents of clays, quartz and carbonate minerals for the studied shale samples

2.4 Methods

2.4.1 Sample extraction

The experimental set up consisted of reaction vessels, equipped with a reflux condenser, in which the samples (10g; previously freeze-dried and ground) were extracted with deionized water (125ml) by heating to 100°C for 48 hours. The water had been treated via UV-

photooxidation (Simplicity 185, Millipore) to remove organic compounds prior to the experiments. The extracts were vacuum filtered using 0.45 µm polypropylene filters. The samples were stored at 4°C in the refrigerator and later analyzed by different chromatographic methods. The reproducibility of the extraction was evaluated by running 6 parallel extractions. The standard deviation of the concentration of individual organic acids from the six extracts is below 10% (data not shown).

2.4.2 Analytical methods

2.4.2.1 Determination of total organic carbon (TOC) and Rock-Eval Pyrolysis

Determination of the total carbon content (TOC) was achieved by measuring the carbon dioxide formed by combustion at 1350°C using a Leco SC-632 IR-detector. Finely crushed rock samples were treated with diluted HCl at 60°C to remove inorganic carbon. The Rock-Eval analyses were performed using a Rock-Eval 6 instrument and following the procedure described in NIGOGA 4th edition (Weiss et al., 2000).

2.4.2.2 Open-system pyrolysis gas chromatography (Py-GC)

Open-system Py-GC was applied to all the shale and coal samples. Depending on TOC, up to 35 mg of each crushed sample was placed into a small glass tube, which was sealed and inserted into a Quantum MSSV-2 Thermal Analyzer (Horsfield et al., 1989; Horsfield et al., 2015). The sample was heated in a flow of helium at 300°C for 5 min to get rid of volatile constituents and pollutants. Afterwards, the sample was pyrolyzed at the rate of 50°C min⁻¹ from 300°C to 600°C. Pyrolysis products were collected in a cryogenic trap from which they were later liberated and directly transferred into an Agilent GC 6890A gas chromatograph. Boiling ranges (C₁₋₅, *n*-C₆₋₁₄ and *n*-C₁₅₊) and individual compounds were quantified by external standardization using *n*-butane.

2.4.2.3 X-ray Diffraction (XRD)

The mineral composition of the shale samples was determined by X-ray diffraction (XRD) followed by Rietveld refinement for a quantitative evaluation. XRD analyses were performed using a PANalytical Empyrean. The software EVA (Bruker) was used to identify the minerals and the program AutoQuant for Rietveld calculations was used to determine the amount of the identified minerals (detection limit ~1 wt %).

2.4.2.4 Ion chromatography (IC)

Extracts were analyzed in replicate by ion chromatography (IC) using conductivity detection (ICS 3000, Dionex) to determine the content of organic acids (formate, acetate, propionate, butyrate, valerate and oxalate) and different anions (F^- , PO_4^{3-} , NO_3^- , Cl^- and SO_4^{2-}); the detection limit was about 0.1 mg L^{-1} . The equipment used an ASRS Ultra II 2 mm suppressor and a Dionex conductivity detector. For chromatographic separation of the anions the analytical column AS 11 HC (Dionex Corp.) was used at a constant temperature of 35°C . Samples were eluted using KOH solution of varying concentrations over time. The initial KOH concentration was 0.5 mmol L^{-1} and held for 8 min. After 10 min, a concentration of 15 mmol L^{-1} KOH was reached and kept constant for 10 min. After 30 min analysis time, a concentration of 60 mmol L^{-1} KOH was reached, followed by a rapid increase to 100 mmol L^{-1} reached after 30.2 min analysis time. At 32 min, the KOH concentration was again at the initial level of 0.5 mmol L^{-1} and kept there for an additional 15 min to equilibrate the system. For quantification of organic acids, standards containing all investigated compounds were measured in different concentrations every day. The standard deviation of sample and standard quantification is below 10% (determined by at least two measurements).

2.4.2.5 Liquid chromatography- organic carbon detection (LC-OCD)

The characterization and quantification of the dissolved organic carbon (DOC) and its fractions were conducted by size-exclusion-chromatography (SEC) with subsequent UV ($\lambda=254 \text{ nm}$) and IR detection by LC-OCD (Huber and Frimmel, 1996). Phosphate buffer (pH 6.85; $2.7 \text{ g L}^{-1} \text{ KH}_2\text{PO}_4$, $1.6 \text{ g L}^{-1} \text{ Na}_2\text{HPO}_4$) was used as mobile phase set to a flow of 1.1 mL min^{-1} (Huber et al., 2011). The chromatographic column was packed with Toyopearl HW-50S resin and had a size of $250 \times 20 \text{ mm}$. The solid phase separates the components according to their molecular mass, where increasing retention time indicates decreasing molecular mass (Pelekani et al., 1999). With LC-OCD the organic matter can be separated into five different fractions referred to as Macro-1 ($>10000 \text{ Da}$), Macro-2 ($\sim 1000 \text{ Da}$), Macro-3 ($350\text{-}500 \text{ Da}$), Acids ($<350 \text{ Da}$) and Neutrals ($<350 \text{ Da}$) (Huber et al., 2011) (Table 2.2). Constituents of Macro-3 fraction are assumed to reflect breakdown products of constituents of Macro-2 fraction and are described alternatively as material similar to humic substances but with lower molecular masses (Huber et al., 2011). The properties and origins of each fraction are shown in Table 2.2. The amount of DOC was quantified by IR-detection of released CO_2 after UV-oxidation ($\lambda=185 \text{ nm}$) in a Gräntzel thin-film reactor. For molecular mass calibration, humic

and fulvic acid standards of the Suwannee River, provided by the International Humic Substances Society (IHSS), were used.

Table 2.2. Description of LC-OCD fractions. Modified from Huber et al. (2011) and Penru et al. (2013).

Fraction (This study)	Fraction (Huber et al., 2011)	Molecular mass range	Properties	Description
Macro-1	Biopolymers	>10000 Da	Not UV-absorbable, hydrophilic	Polysaccharides and proteins
Macro-2	Humic substances	~1000 Da	Highly UV-absorbable, hydrophobic	Calibration based on Suwannee River standard from IHSS
Macro-3	Building blocks	350-500 Da	UV-absorbable	Breakdown products of humic substances
Acids	Low molecular weight acids	<350 Da	Negatively charged	Low molecular weight aliphatic acids
Neutrals	Low molecular weight neutrals	<350 Da	Weakly or uncharged hydrophilic, amphiphilic	Alcohols, aldehydes, ketones, amino acids

2.5 Results

2.5.1 Extraction of DOC

The concentrations of DOC versus maturity (T_{\max}) for the five series under study are shown in Figure 2.3. In general, the concentrations of DOC decreased steeply with progressive maturation and then remained at low values for samples with T_{\max} higher than 435°C. The DOC concentrations ranged from 0.01 to 2.1 mg/g rock (Fig. 2.3a) or 0.03 to 15.1 mg/g TOC (Fig. 2.3b), respectively. The amounts of DOC were comparable in the extracts of Posidonia, Bakken, and Duvernay shales, while the Alum extracts had the lowest concentrations of DOC and the New Zealand coal extracts showed the highest DOC concentrations. When the DOC concentration was normalized to TOC of the extracted shales and coals, the Alum extracts still showed the lowest DOC concentrations but the DOC concentrations of the New Zealand coal extracts were no longer outstanding (Fig. 2.3b).

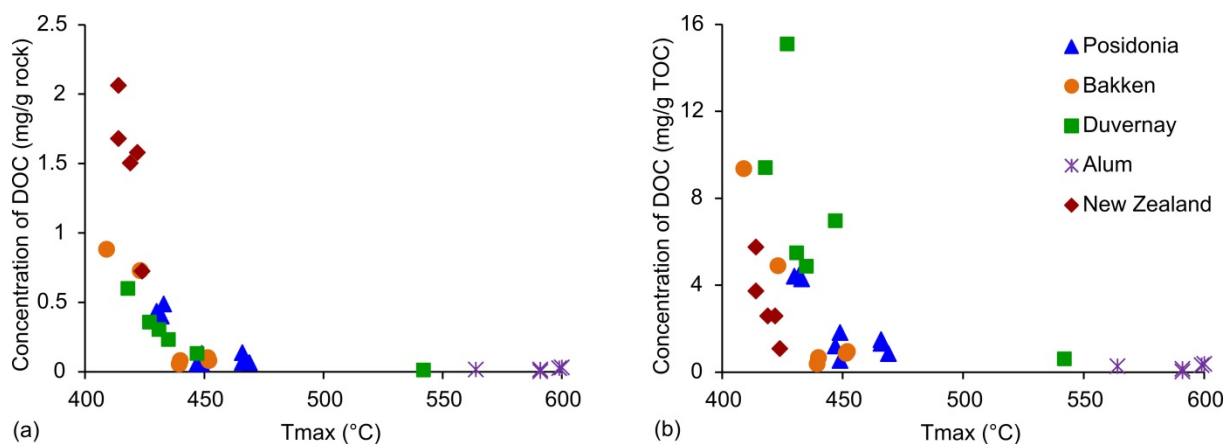


Figure 2.3. DOC concentrations of shale and coal extracts plotted over T_{\max} in mg/g rock (a) and in mg/g TOC (b).

2.5.2 Composition of DOC

Using size-exclusion chromatography (SEC), DOC can be separated into different fractions according to their molecular masses. The chromatograms of selected shale extracts are shown in Fig. 2.4. These shales have been selected as they represent the whole range of maturity occurring at the different locations. The DOC of the shale extracts was characterized by one prominent peak (peak 1) at an elution time of 47.2 min in the IR-chromatogram. This peak was considered to represent the Acid fraction based on the elution order of authentic standards. Peak 2 was characteristic of the Macro-3 fraction and appeared at a retention time of 42.5 min, except for the extracts of immature samples B1 and D1 where it appeared a little later at 43.1 min. A small peak 3 appearing at 39.8 min represented the Macro-2 fraction, which is of higher molecular mass than the Macro-3 fraction. The compounds eluting at a later retention time than 50 min correspond to the Neutral fraction. We identified some peaks belonging to the Neutral fraction in both Bakken and Duvernay shale extracts. There is no indication of the Macro-1 fraction in any shale extract.

Most UV-chromatograms showed two prominent peaks with retention times of 47.2 min (peak 1) and 42.5 min (peak 2) except for the extract from B1 that showed a small shift in peak 2 to retention time of 43.1 min. This extract showed an additional peak (peak 3) at retention time of 39.8 min. The peak 3 is not observable for the extracts from shales with higher maturity than B1 (Fig. 2.4b). These parallel peaks indicate the UV-activity of the extracted organic compounds. As the fractions Macro-2 and Macro-3 contain aromatic and unsaturated structures, they have a good UV response (Jacquemet et al., 2005).

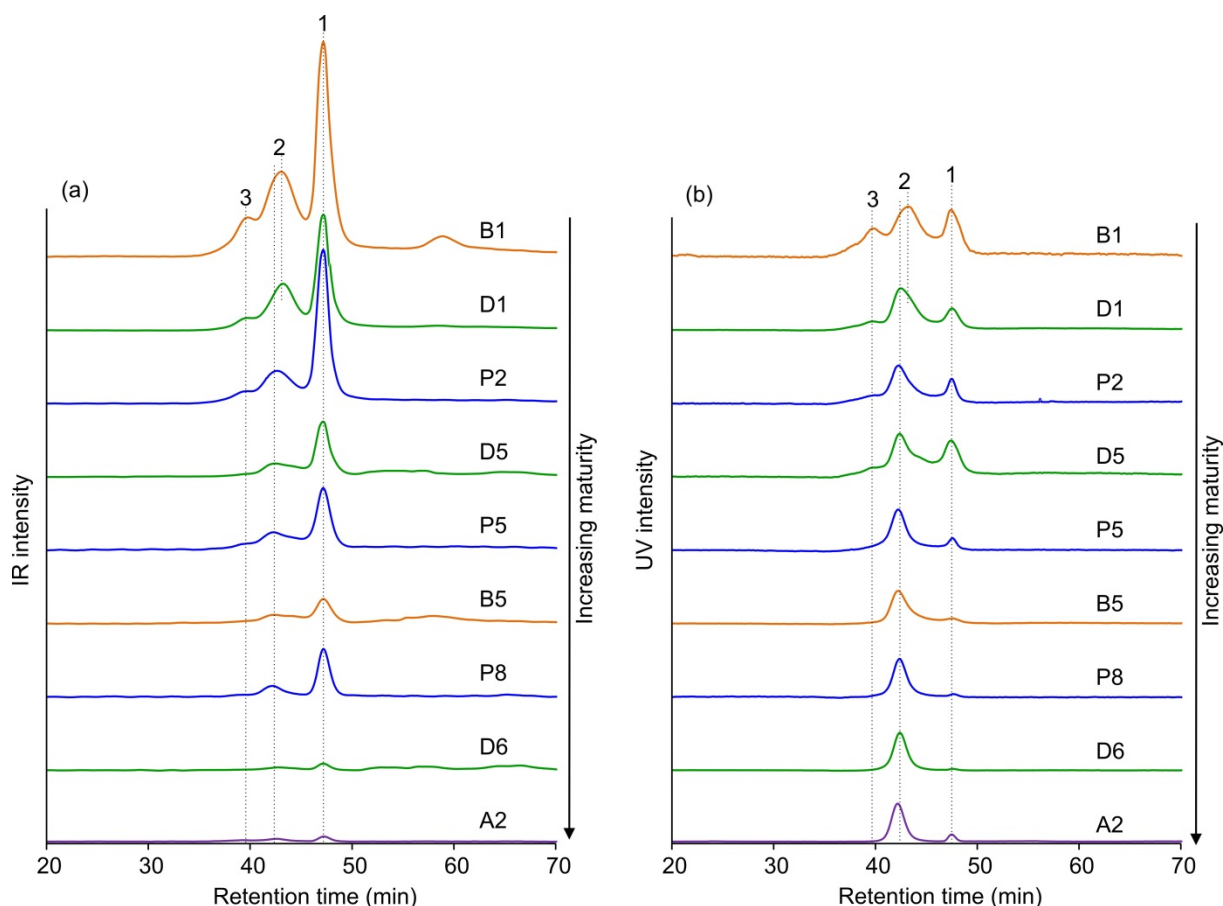


Figure 2.4. SEC chromatograms giving intensity of (a) IR-signal and (b) UV-signal over run time of the analytical separation of shale extracts.

Figure 2.5a shows the IR-intensities of DOC compositions in coal extracts. Generally, the extracts of coals with $T_{\max} \geq 419^{\circ}\text{C}$ (C3, C4 and C5) showed comparable chromatograms to the shale extracts, but the retention times of the peaks were not exactly identical. Peak 1, indicating the Acid fraction, also eluted after 47.2 min. The peak 2, belonging to the Macro-3 fraction, appeared after 42 min, except for the two lignite extracts of C1 and C2 with retention time of 41.7 min. In general, peak 2 eluted a little earlier than in the shale extracts (42.5min). Peak 3, evaluated as belonging to the Macro-2 fraction, showed a shoulder at retention time of 39 min, which was about 1 min earlier than the peak 3 in the shale extracts. The chromatograms of lignite extracts of C1 and C2 were quite different to the other three extracts from coals of bituminous rank. Here, the Macro-2 was the prominent fraction and an additional peak 4 existed, representing the Macro-2 of higher molecular mass. In general, the extracts show decreasing intensities of the IR-signals with increasing T_{\max} for both shale and coal samples.

The corresponding UV-response of the coal extracts is shown in Figure 2.5b. It is obvious that the UV- chromatograms of shale and coal extracts are quite distinct and the intensity of UV-chromatograms decreases with increasing maturity of the coals. The two lignite extracts of C1 and C2 were comparable with one another in UV-peak distribution and shapes. They both showed a dominant peak at 37 min and a shoulder at 39 min. The two coal extracts of C3 and C4 showed a peak at 39 min and two small shoulders (retention times of 37 and 42 min) on both sides while the coal extract of C5 showed the lowest UV-signal. All the coal and shale extracts exhibited a peak at 47.2 minute in the UV-chromatograms, which might correspond to the breakdown products of the Macro-3 fraction or comprise colloidal material where the UV-signal resulted from light scattering rather than absorption (Allpike et al., 2007).

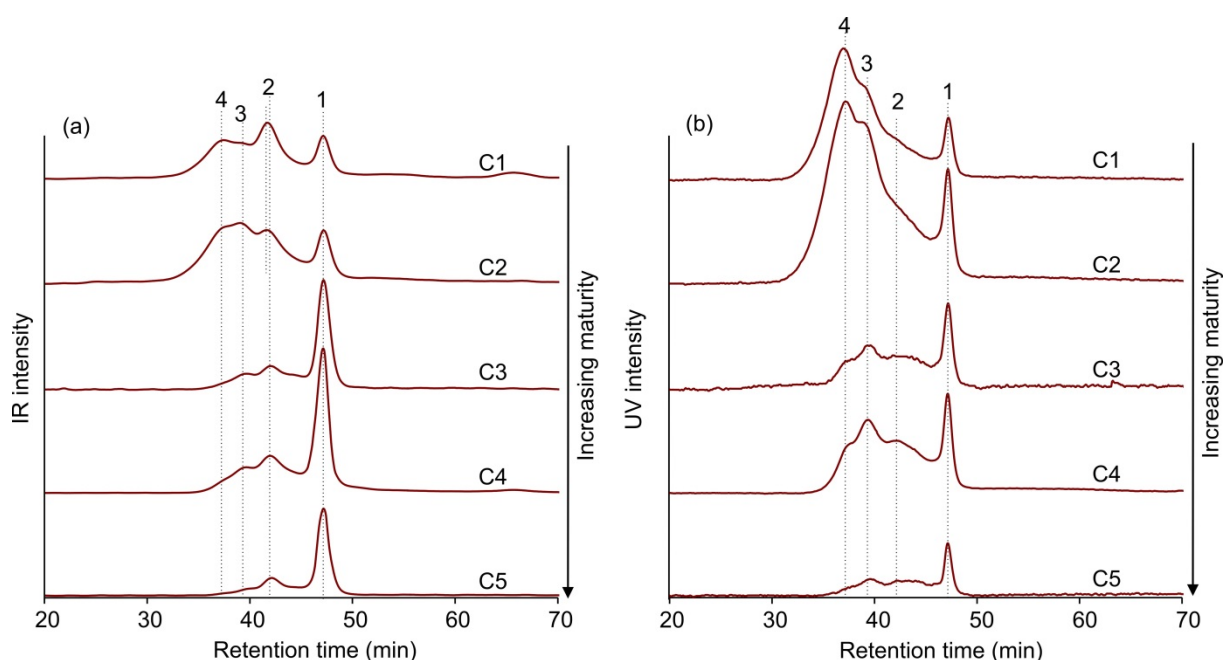


Figure 2.5. SEC chromatograms giving intensity of (a) IR-signal and (b) UV-signal over run time of the analytical separation of coal extracts.

The relative percentages of DOC in the different fractions (Acids, Macro-2+3 and Neutrals) are shown in Figure 2.6. As the boundary between the fractions Macro-2 and Macro-3 was difficult to identify, these two fractions were grouped together. For the Posidonia extracts, the percentages of the Acids decreased with progressive shale maturation up to peak oil window ($T_{\max} = 447^{\circ}\text{C} - 449^{\circ}\text{C}$) and reversed afterwards. The percentages of the Neutral fraction showed the opposite tendency and the percentages of the Macro-2+3 fraction showed slight but steady decrease with increasing maturity of the shales (Fig. 2.6a).

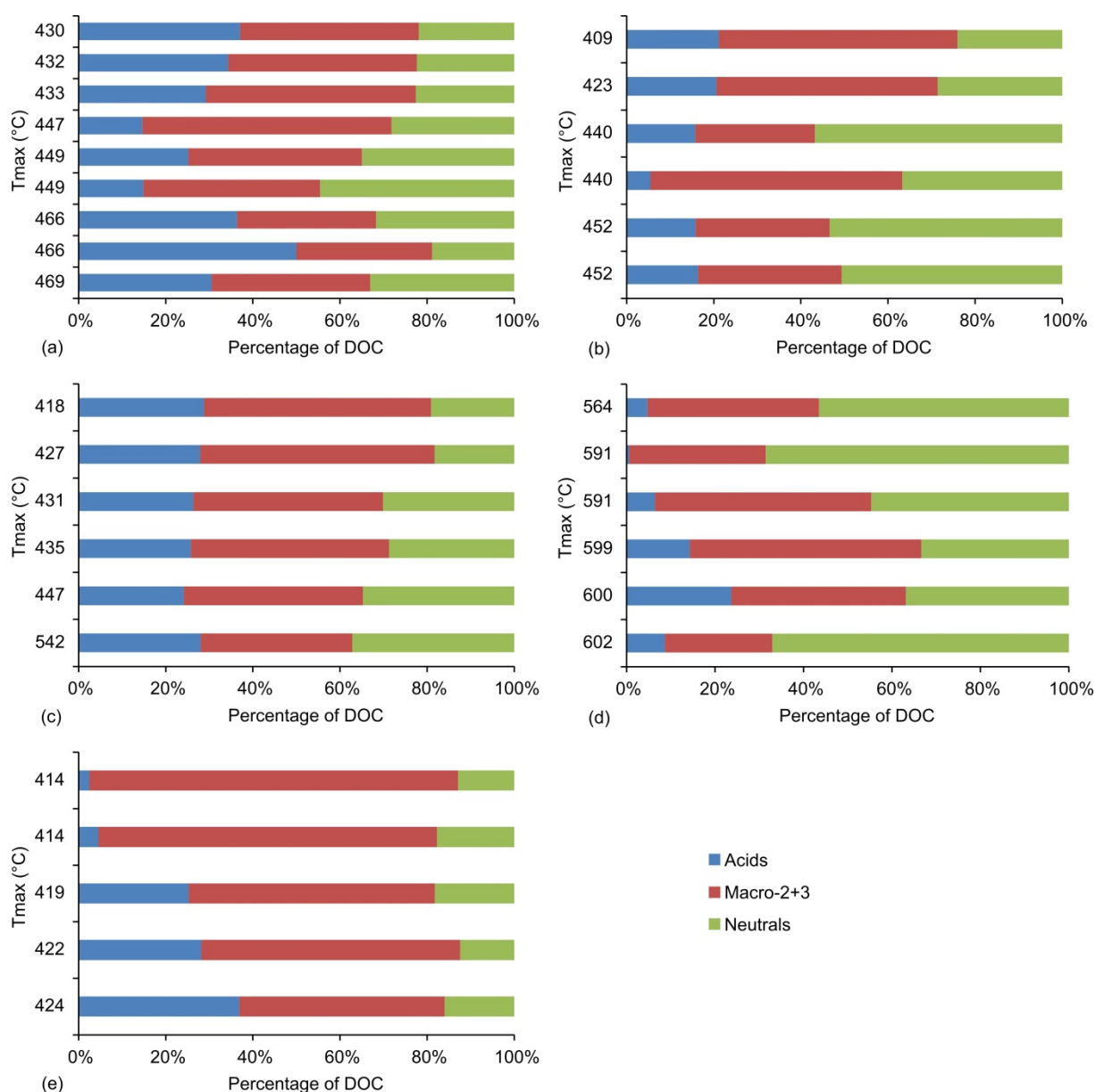


Figure 2.6. The relative percentages of the different DOC fractions extracted from shales and coals, (a) Posidonia shales; (b) Bakken shales; (c) Duvernay shales; (d) Alum shales; (e) New Zealand coals.

The DOC fractions extracted from the Bakken and Duvernay shales showed comparable variation (Fig. 2.6b+c). With increasing maturity of the Bakken and Duvernay shales, the relative percentages of the Neutral fraction showed a progressive increase, the percentages of the Macro-2+3 fraction decreased and the Acid fraction decreased only slightly. However, the percentages of the different fractions were different for Bakken and Duvernay shale extracts. The extracts of the overmature Alum shales generally showed high percentages of the Neutral fraction and low percentages of the Acid fraction. As the total amounts of DOC in the leachates of Alum shales were extremely low, the variations in percentages of different

fractions should not be over-interpreted. For New Zealand coals, the fractions of the two lignite extracts of C1 and C2 showed similar relative distributions of DOC fractions (Neutrals around 15%, Macro-2+3 around 80%, Acids around 5%) while the percentage of the Acid fraction increased up to 37% and the percentage of the Macro2+3 fractions decreased to 47% for the extracts of the other three bituminous coal samples.

2.5.3 Occurrence of individual organic acids in the extracts

2.5.3.1 Organic acids in shale extracts

Formate and acetate were the dominant LMWOAs detected in the water extracts of all shale samples followed by oxalate. Propionate, butyrate and valerate were present in low concentrations in the extracts of immature and some mature samples; none of them were detected in the overmature samples.

The Posidonia shales from the wells Wickensen, Harderode and Haddessen are immature, mature and overmature, respectively (Rullkötter et al., 1988). The concentrations of LMWOAs in the extracts are comparable for samples from the same well, while significant differences can be observed between wells (Fig. 2.7). The concentrations of formate decreased remarkably with increasing maturation of the shales and then remained at a low level for shales reaching the oil window. The concentrations of acetate also decreased with maturity of the shales but surprisingly showed a reversal for shales reaching the gas window – possible explanations for the reversal are discussed later in this paper.

The Bakken shale samples were immature to mature and the concentrations of formate and acetate in the extracts were both negatively correlated to thermal maturity, as was the case for the early mature to mature Posidonia samples. No overmature Bakken shale samples were available. The Duvernay shale samples, which were either immature or mature except for one extremely overmature sample, also showed a trend of decreasing carboxylic acid concentrations with increasing maturity. The extracts of the overmature Alum shale had extremely low concentrations of both formate and acetate, which ranged from 0.02 to 0.5 mg/g TOC and 0.02 to 0.10 mg/g TOC, respectively. The reversal in acetate concentration at high maturity as noted for the Posidonia shale extracts was not seen for either the Alum or the Duvernay extracts.

2.5.3.2 Organic acids in coal extracts

The concentrations of formate were higher than the concentration of acetate in the extracts of the two lignites while in the extracts of three bituminous coals the concentrations of acetate were higher than formate. Except for oxalate showed much high concentration in the extracts of the two lignites, other acids (e.g. propionate, butyrate, valerate) showed only trace amount or were below the detection limit in all coal extracts. Due to the narrow range of the maturity of the coal samples, the concentration of formate and acetate in the coal extracts was not so obviously correlated with thermal maturity compared to the shale extracts. When normalized to TOC, the concentrations of formate ranged from 0.5 to 1.76 mg/g TOC for coals and from 0.34 to 2.44 mg/g TOC for all shale extracts (Fig. 2.7a). The concentrations of formate in the extracts of coals and shales with same maturity were comparable (Fig. 2.7a). The concentrations of acetate in the coal extracts were also within the range detected in the shale extracts, but acetate concentrations were much lower in coal extracts compared to extracts from shales with the same maturity (Fig. 2.7b).

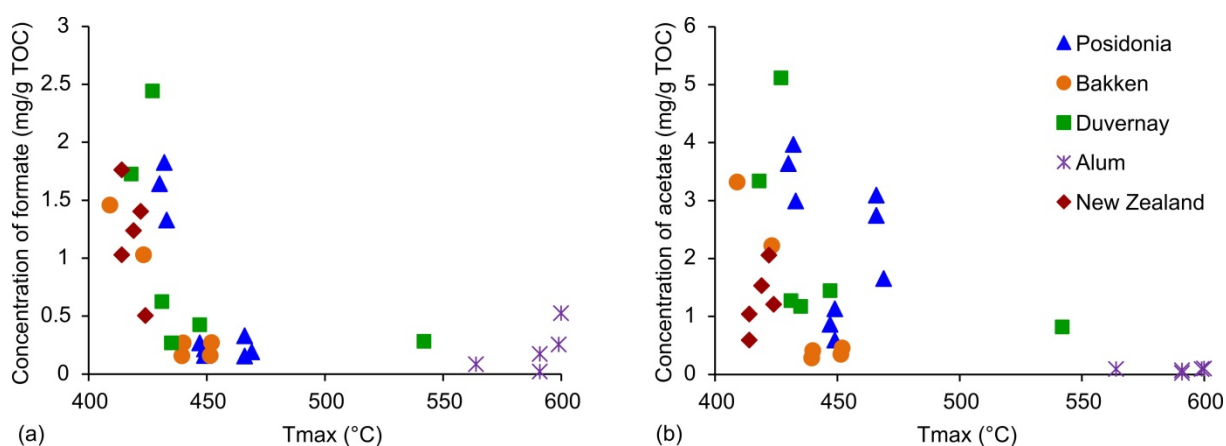


Figure 2.7. The concentrations of formate (a) and acetate (b) extracted from shales and coals of different maturities.

2.6 Discussion

2.6.1 Effect of shale and coal organic matter composition on water extracts

2.6.1.1 Bulk DOC and DOC fractions

As shown in Fig 2.3b, only a few permil of the TOC was extracted as DOC in our experiments. However, the coal samples with higher contents of TOC show higher amount of extracted organic carbon than the shale samples (Fig. 2.3a). When normalized to TOC, the concentrations of DOC in the coal extracts are within the range of the DOC concentrations of the immature shale leachates (Fig. 2.3b). From these experimental results, we can conclude that the total amount of extractable organic compounds from shales and coals was influenced by the amount of TOC and probably not by the kerogen type of the organic matter. Nevertheless, the DOC compositions of shale and coal extracts are clearly influenced by the kerogen types, as shown by the differences in IR-chromatograms of the extracts. The two lignite extracts of C1 and C2 are characterized in their IR-chromatograms by high intensities of the Macro-2+3 fractions while the IR-chromatograms of the other three coal extracts (C3, C4 and C5) show high peaks of the Acid fraction, which are similar to the chromatographic patterns of the immature shale extracts. The organic matter of coals C4 and C5 contains mainly terrestrial higher plant material with a significant contribution of microbial biomass (Vu et al., 2009) and it can be as *previous* sumed that the organic matter of C3 also has a significant contribution of microbial biomass as it belongs to a similar petroleum type organofacies as coals C4 and C5 (Fig. 2.1). Also all selected shales have organic matter that is derived from a mixture of planktonic and microbial sources. Therefore, the similarity of the chromatographic patterns is plausible. However, the retention times of the peak maxima of the Macro-2 and Macro-3 fractions from the coal extracts are shorter than for the shale extracts, which points to the differences in the molecular masses of these DOC fractions from shales and coals. The molecular masses of most constituents included in the fractions Macro-2 and Macro-3 in the coal extracts are heavier than in shale extracts. Even more notable differences between shale and coal extracts can be observed in the UV-chromatograms where coal extracts showed higher intensities. These higher intensities may be related to the presence of aromatic structures in the DOC of coal extracts. Coals with type III kerogen mainly originate from terrigenous higher plant material of lignocellulosic origin while the

shales with type II kerogen originate from marine planktonic material which is comprised of aliphatic structures.

2.6.1.2 LMWOAs

The observed distribution of the individual organic acid concentrations, where acetate is dominant in the shale and bituminous coal extracts, is in accordance with the results from hydrous pyrolysis of kerogen (Kawamura et al., 1986), crude oils (Borgund and Barth, 1994) and source rocks (Barth et al., 1988; Barth and Bjørlykke, 1993). The observed order in concentrations with acetate >> propionate > butyrate > valerate has also been reported for natural deep subsurface waters (Fisher, 1987; Means and Hubbard, 1987). However, no information about formate concentrations was given in these previous studies.

The relation between the concentrations of formate and acetate, extracted from shales and coals is shown in Figure 2.8. The results of Alum shale extracts are not included here due to their extremely low concentrations. A linear correlation between the concentrations of formate and acetate can be observed in all shale extracts except for the three Posidonia extracts of P7, P8 and P9 and the coal extracts. This linear trend indicates that the extraction of these acids might be controlled by the same factors. Discussion about the three outlier points representing the three Posidonia extracts of P7, P8 and P9 is given later in this paper. The linear correlation between the concentrations of formate and acetate in the shale extracts cannot be observed in the coal extracts. This may be due to the fact that the five samples already represent two different petroleum type organofacies. Thus, we can deduce that the correlation between the concentrations of formate and acetate in the extracts of samples with the same organofacies might be similar.

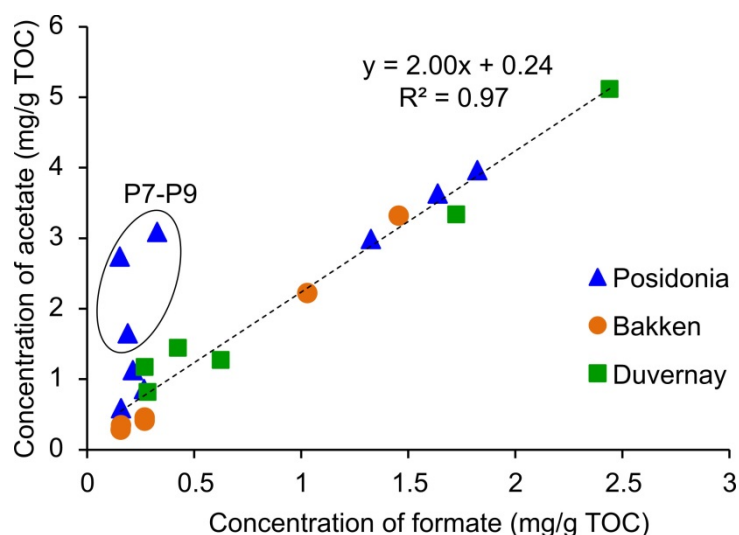


Figure 2.8. Comparison of formate and acetate concentrations in the water extracts. The linear regression excludes the extracts of P7, P8 and P9 and New Zealand coals.

2.6.2 Effect of burial processes on composition of water extracts

2.6.2.1 Influence of maturation on the extracted organic matter

As illustrated in Fig. 2.3, the concentrations of DOC decreased with maturity until T_{\max} reaches 435°C after which low concentrations were maintained. The samples clearly showed a higher potential for DOC extraction at the stage of diagenesis rather than at later stages when thermal cracking reactions became significant. Generally, the concentrations of the individual DOC fractions also decreased with increasing maturity for shale samples from the same formation, which could be indicated by the IR-chromatograms as the intensities of the IR-chromatograms correspond to the concentrations of DOC (Fig. 2.4a). But there was no overall trend of decreasing DOC concentration with increasing maturity. This can be illustrated for shale D1 which is less mature (lower T_{\max}) than shale P2 but the extract of D1 had a lower DOC concentration (lower IR signal intensity). The similar phenomenon can also be observed for samples B5 and P8. Though the coal samples represent only a very narrow range in maturity, the general trend of decreasing DOC concentrations with increasing T_{\max} can also be observed for the coal extracts.

Fig. 2.7 showed the concentrations of formate and acetate in extracts over T_{\max} of the shales/coal. The concentrations of extracted acids decreased with increasing maturity of the samples except for the overmature Posidonia shales from the Haddessen well. Here, acetate concentrations are higher than expected. This similar decreasing tendency of LMWOA

concentrations in extracts with ongoing maturation has already been described in the experiments of soxhlet water extraction and alkaline ester cleavage of coals (Vieth et al., 2008; Glombitza et al., 2009). Thus, it may be assumed that a potential equilibrium exists between kerogen bound LMWOAs and free LMWOAs. Kerogen is generally accepted as the source of LMWOAs and their generation is considered to result from kerogen maturation (Eglinton et al., 1987; Kawamura and Kaplan, 1987). The immature kerogen maturation process simulated by hydrous pyrolysis illustrates that the generation of LMWOAs from kerogen resulted from cracking and hydrolysis reactions and continues at high simulated maturation levels (Kawamura et al., 1986; Barth et al., 1988). In the present experiment, the LMWOAs easily extracted during water extraction were assumed to be mainly the free acids, which assimilated into sedimentary organic matter or dissolved in the in-situ pore water during early diagenesis (Pittman and Lewan, 1994). The immature kerogen contains significant amounts of aliphatic components and oxygen. Their functional groups show higher potential to form LMWOAs compared to the overmature kerogen, which contains fewer aliphatic chains and less oxygen (Bernard et al., 2012; Vu et al., 2013). The defunctionalisation reaction of oxygen containing functional groups and oxidation of *n*-alkanes during geological times might lead to the formation of LMWOAs. So the maturity of the samples is a pivotal factor that influences the concentrations of different acids in the extracts. This is supported by the minor amounts of formate and acetate extracted from overmature Alum shale samples.

2.6.2.2 Influence of OI on the concentration of individual organic acids

The significant decrease of oxygen-containing compounds during diagenesis can be traced using Van Krevelen diagram, which shows the preferential decrease of O/C ratio relative to H/C ratio (Tissot and Welte, 1984). Furthermore, the loss of C=O functionalities with increasing maturity can be revealed by infrared spectroscopy (Lis et al., 2005; al Sandouk-Lincke et al., 2013). A general positive correlation between Oxygen Index (OI) and the concentrations of formate and acetate in the extracts could be observed for the Bakken, Posidonia and Duvernay (Fig. 2.9). This indicates that the amounts of acids extracted from the shales were directly constrained by the initial kerogen oxygen content. When the coals were separated into two groups according to their organofacies, the positive trend between OI of coals and the concentrations of formate and acetate in the extracts also could be observed in each group. The coal samples with type III kerogen, characterized by generally high atomic O/C ratio, were expected to generate a higher concentration of organic acids than type II kerogen (Cooles et al., 1987). But the functionality of the oxygen may be an important factor,

i.e. oxygen in carboxylic acids and esters is assumed to contribute more to LMWOAs than the oxygen in ether bonds and ring systems (Borgund and Barth, 1994). Additionally, the type II kerogen contains more aliphatic moieties that can be oxidized to form carboxylic acids.

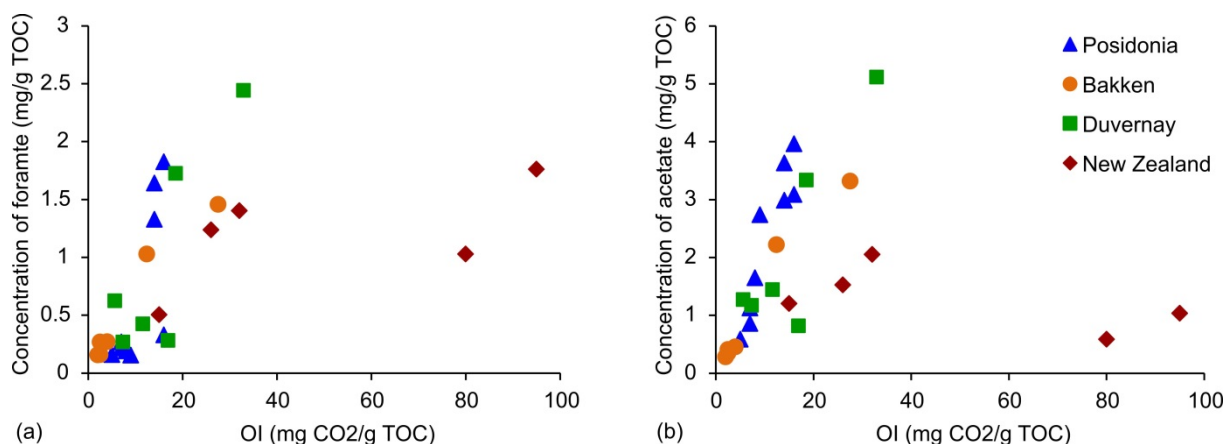


Figure 2.9. Concentrations of formate (a) and acetate (b) in the extracts are plotted over the oxygen index (OI) values of the shales and coals.

2.6.2.3 Possible influence of hydrothermal brines

The unexpectedly high concentrations of acetate extracted from these overmature Posidonia shales might be related to the occurrence of hydrothermal fluid migration along the southern rim of the Lower Saxony Basin (Petmecky et al., 1999). The occurrence of authigenic albite with halite inclusions has been used to argue for hydrothermal activity affecting the mineralogy of the Posidonia shale (Bernard et al., 2012). The hydrothermal brines and iron-bearing minerals may have provided a source of available oxygen to partly oxidize bitumen to form acids (Bernard et al., 2012). The oxidation of hydrocarbons may produce LMWOAs during thermal maturation (Barth, 1987; Eglinton et al., 1987; Surdam et al., 1993; Borgund and Barth, 1994; Seewald, 2001a), and this is speculated to be the main control on the high concentration of acetate in the extracts of samples P7, P8 and P9. The higher concentrations of chloride detected in the extracts of shales from the overmature Haddessen well in comparison to the extracts of other Posidonia shales would support an influence of hydrothermal brines (Fig. 2.10). Hydrothermal activity could have provided both a local heat source to drive the generation reactions which led to the formation of organic acids, and water to act as reaction and transport medium. It should be noted that high geothermal gradients associated with hydrothermal activity might have also increased the rate of acid production from kerogen. The steep gradient in formate/acetate for the Haddessen shales (P7-P9; Fig. 2.8) might signal the selective generation of acetate from bitumen

precursors, possibly accompanied by formate degradation or consumption. Though a heat-flow anomaly existed in the Bakken formation (Kuhn et al., 2012), no obvious influence on the generation of acetate or formate could be observed in our experiments.

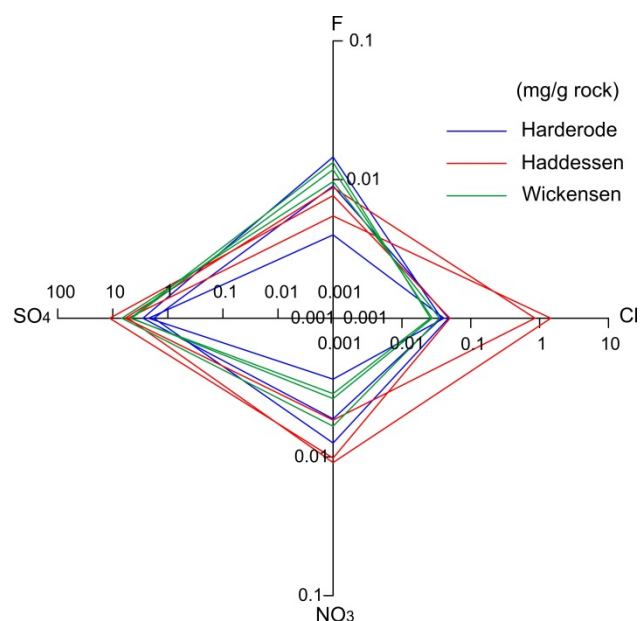


Figure 2.10. The concentrations of inorganic anions in Posidonia extracts. The concentrations of fluoride, sulfate and nitrate are in the same order of magnitude for most Posidonia samples, only extracts of P8 and P9 show extremely high concentrations of chloride.

2.6.2.4 Correlation between concentration of acids and porosity

LMWOAs have been shown to be an important potential contributor to generate secondary porosity by dissolution of aluminosilicate and carbonate minerals (Surdam et al., 1984). That type of porosity could provide more space for storage of generated bitumen in shales, which could then act as a source of acetate afterwards. The total porosity of the Posidonia maturity sequence shows a loss of porosity in going from the immature stage (ca. 10-13%) to the oil window (4-6%) and then an increase again in the gas window Haddessen well (9-12%) (Mathia et al., 2013). The pattern in porosity changes with increasing maturity correlates with the concentration of acetate in the water extracts of the respective shales (Fig. 2.11), but not with formate. According to Bernard et al. (2012), the pores in Posidonia shales of oil window maturity were filled by viscous bitumen during kerogen degradation, and this resulted in the decrease of porosity. In gas window, the porosity increased again because of secondary cracking reactions leading to the generation and exsolution of gaseous hydrocarbons. The creation of nanoporosity within overmature Barnett shale by thermal cracking of retained hydrocarbons has also been reported by Loucks et al. (2009). Based on

the lack of porosity data from other shales, no reliable evaluation of the correlation between extracted acetate concentrations and porosity of Posidonia shales is possible. It is assumed that there is no cause-effect relationship between these parameters.

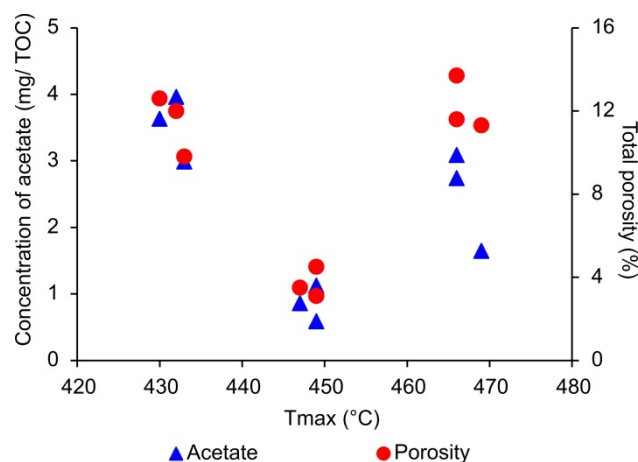


Figure 2.11. The variation of acetate concentrations in Posidonia extracts (left Y axis) and porosities of the shales (right Y axis) with increasing maturity.

2.7 Summary and Conclusions

Extraction of black shales and coals using deionized water resulted in the release of water soluble organic compounds. In general, the concentrations of DOC decreased steeply with progressive maturation and then remained at low values for samples with T_{\max} higher than 435°C. The coal extracts showed much higher DOC concentrations on a per gram sediment basis, but when normalized to TOC, the concentrations of DOC are within the range observed for the immature shale leachates. From this we conclude that maturity of the kerogen and TOC content are two main factors that influence the amount of DOC extracted from sediments. Macro-2, Macro-3, Acids and Neutrals comprise the four DOC fractions that have been detected in the extracts using SEC. The extracts of immature samples have a high content of the Macro-2 and Macro-3 fractions whereas leachates of mature and overmature samples are dominated by the Neutral fraction, which represent the final degradation products of organic matter during geological maturation. The DOC extracted from coal samples is more aromatic than that extracted from shales, which is documented by the higher intensity of UV-signals. According to the retention times in SEC, it can be deduced that the molecular weight of the constituents included in the fractions Macro-2 and Macro-3 of the coal extracts is higher than for the shale extracts.

Acetate and formate represent the dominant acids extracted from shales and coals. Other LMW mono- and di-carboxylic acids like propionate and oxalate are detected in some of the leachates, but in lower concentrations. The linear trend between the concentrations of formate and acetate extracted from shales indicated that the generation of individual LMWOAs is controlled by the same factor. The concentrations of acids also decreased with increasing maturity of the shales except for the overmature Posidonia shales from the Haddessen well. The reason for the high concentrations of acetate in the extracts of the overmature Haddessen shales might be the influence of hydrothermal brines. These brines might provide oxygen and hydrogen to enhance the generation of organic acids.

2.8 Acknowledgments

The financial support from the China Scholarship Council (CSC) for Yaling Zhu is gratefully acknowledged. The authors thank Kristin Günther and Wilma Mierke (GFZ Potsdam) for their excellent technical assistance in the lab. We appreciate the North Dakota Geological Survey and the Canadian Geological Survey for providing samples. The two anonymous reviewers are greatly acknowledged for their useful comments.

3. MOLECULAR CHARACTERIZATION OF EXTRACTED DISSOLVED ORGANIC MATTER FROM NEW ZEALAND COALS IDENTIFIED BY ULTRAHIGH RESOLUTION MASS SPECTROMETRY²

3.1 Abstract

Knowing the composition, molecular size and structure of water soluble organic compounds are the prerequisites for a better understanding of water-rock interactions and of the main controls on their release from natural organic matter in shale environments and coal seams over both geological and human timescales. In this study, extracted dissolved organic matter (DOM) from two lignites and three bituminous coals of New Zealand was analyzed by high-resolution Fourier transform-ion cyclotron resonance-mass spectrometry (FT-ICR-MS) combined with electrospray ionization (ESI) in negative ion mode after solid phase extraction (SPE). Compared to DOM in natural waters, the yields of extracted DOM of New Zealand coals were 10 to 100 times higher while the compounds showed an elevated aromaticity as indicated by lower H/C ratios. Elevated abundances of benzenepolycarboxylic acids (BPCAs) and naphthalenepolycarboxylic acids (NPCAs) with different numbers of carboxyl and hydroxyl groups in the FT mass spectra of all five samples have been confirmed by GC-MS. Oxygen containing compounds are the dominant elemental class in the extracted DOM of bituminous coals and lignites. However, the relative intensity distributions of individual oxygen classes as well as of the double bond equivalents (DBE) in the extracted DOM of the

²This chapter has been published as: Zhu, Y., Vieth-Hillebrand, A., Noah, M., Poetz, S., 2019. Molecular characterization of extracted dissolved organic matter from New Zealand coals identified by ultrahigh resolution mass spectrometry. *International Journal of Coal Geology* 203, 74-86 (postprint), <https://doi.org/10.1016/j.coal.2019.01.007>.

bituminous coals differ from those in the lignites. The low abundance of O9-16 in the bituminous coals might reflect the loss of oxygen via eliminations of carboxyl and carbonyl groups with increasing maturation. Furthermore, the extracted DOM of bituminous coals contains higher percentages of aromatic and condensed aromatic compounds than the extracted DOM of the lignites. A modified aromaticity index (AI_{coal}) was established to evaluate aromaticity of the extracted DOM based on sample-specific calculated fraction of oxygen numbers bound in π -bonds instead of an assumed average of 50%.

3.2 Introduction

Mined coal is exposed to water in many different ways like e.g. coal washing processes, exposure of storage piles to rain, transport of coal-water slurries and disposal of coal. Throughout these processes, water soluble organic compounds can be mobilized from coal into the surrounding water (Reid et al., 1988; Berrueta et al., 1991; Nakajima et al., 2005). During coalbed methane (CBM) exploitation, large volumes of water from coal seams containing DOM can also be brought to the surface (Dahm et al., 2011; Navi et al., 2015). Many organic compound classes including phenols, polycyclic aromatic hydrocarbons (PAHs), long-chain fatty acids and heterocyclic compounds have been detected in the produced and formation water of CBM (Orem et al., 1999; Orem et al., 2007a; Volk et al., 2011; Orem et al., 2014; Stearman et al., 2014; Tang et al., 2014). To simulate groundwater leaching of organic compounds, a number of extraction experiments were performed with distilled water and lignites in laboratories (Orem et al., 1999; Maharaj et al., 2014; Doskočil et al., 2015; Zhu et al., 2015; Kosateva et al., 2017). Different compounds like benzene carboxylic acids and their derivatives as well as low molecular weight organic acids (LMWOAs) and polyols have been detected in the aqueous leachates. High degree of oxygen containing functional groups such as carboxyl groups, alcohols, ethers and esters are attached to the aromatic and aliphatic moieties (Orem et al., 1999; Maharaj et al., 2014; Doskočil et al., 2015; Kosateva et al., 2017). Up to now, a large fraction of the water extracts remains uncharacterized at the molecular level.

Due to the high complexity, low concentration and high polarity of DOM in natural samples, the investigation of its chemical composition is an analytical challenge. Elemental analyses, infrared and ultraviolet spectroscopy only provide bulk characteristics of DOM. Other approaches like pyrolysis and chemolysis are destructive for most of DOM. Traditional GC-MS targets at specific compounds (e.g., PAHs, heterocycles) making up only a small

portion of DOM. The advent of Fourier transform ion cyclotron resonance mass spectrometry (FT-ICR-MS) combined with electrospray ionization (ESI) has expanded the current knowledge about DOM composition by resolving thousands of molecules and providing elemental composition of individual compounds. ESI FT-ICR-MS is a powerful tool to characterize medium- to high-molecular-weight organic compounds of different polarity within a mass range from 100 to 10,000 Da. This technique has been successfully applied to characterize the molecular composition of DOM from marine and different terrestrial water systems (Stenson et al., 2002; Tremblay et al., 2007; Koch et al., 2008; Sleighter and Hatcher, 2008; D'Andrilli et al., 2010; Minor et al., 2012) as well as groundwater (Longnecker and Kujawinski, 2011; Islam et al., 2016), pore water (Tremblay et al., 2007; Schmidt et al., 2009; D'Andrilli et al., 2010; Seidel et al., 2014; Rossel et al., 2016; Schmidt et al., 2017) and water extracts of marine sediments (Schmidt et al., 2014). However, to the best of our knowledge, it has never been used for the molecular characterization of extracted DOM from coals.

In addition, clarification is missing, which properties of the coal organic matter are the controlling factors for the molecular composition of the extracted DOM. Generally, lower rank coals contain a greater abundance of easily cleaved bridge structures compared to higher ranked coals (Volk et al., 2011). It has been reported that both, the concentrations of dissolved organic carbon (DOC) as well as concentrations of LMWOAs leached from coals gradually decrease with increasing maturity of the coals (Vieth et al., 2008; Zhu et al., 2015). With increasing maturation, the organic matter within coals is subjected to thermal decarboxylation, decarbonylation and demethoxylation (Kelemen et al., 2002; Kelemen et al., 2007; Salmon et al., 2009). As the dominant heteroatom in coal organic matter, oxygen makes up 10 - 28% weight of kerogen type III in immature sediments (Tissot and Welte, 1984). The loss of oxygen content is significant with increasing coalification and can be detected by the decrease of oxygen index (OI) and atomic O/C ratio, the decrease in infrared adsorption intensities of -OH, -COOH, C=O and C-O-R as well as the increase of water and CO/CO₂ generation (Tissot and Welte, 1984; Behar et al., 1995; Ibarra et al., 1996; Vu et al., 2013). Based on this, we assume that the variation of the oxygen containing compounds in coal organic matter is reflected in the extracted DOM.

The main goals of this study were to identify the molecular composition of the extracted DOM from a variety of coal samples and to decipher the correlation between properties of the original coal organic matter and the water soluble organic compounds. For this goal we applied high-resolution ESI FT-ICR MS paying attention to the medium to high molecular

weight oxygen containing compounds of the extracted DOM. The selected coal samples are known to show a range in thermal maturity, but also represent significant differences in organofacies. Coal organic matter has been characterized by pyrolysis GC as well as GC-MS analysis of solvent extracts of the coals. This work is dedicated to the characterization of the water-soluble and labile part of the coal organic matter (extracted DOM) and this will provide additional insight into fluid-rock interactions taking place in coal seams over both geological and human timescales.

3.3 Samples and methods

3.3.1 Sample set

Five New Zealand coal samples of Eocene to middle Pleistocene age were selected for this study (Table 3.1). Three of them were taken from different coal horizons of the DEBITS-1 well located at Ohinewai in the Waikare Coalfield of the Waikato Basin on the North Island of New Zealand. The well was drilled in 2004 within the scope of the “deep biosphere in terrestrial systems” (DEBITS) project (Kallmeyer et al., 2006). Along the drilled cores an unconformity occurred at a depth of ca. 76 m. Above this unconformity, poorly consolidated gravels, sands, muds and imbedded lignite layers were deposited, forming the Tauranga group. Two of the coal samples taken from different depths of this group were lignites with a thermal maturity of $R_o = 0.29\%$. Below the unconformity are moderately indurated sediments consisting of sandstone, mudstone and imbedded coal layers, forming the Te Kuiti Group. The third sample taken from this coal layer of the Te Kuiti Group is a sub-bituminous coal with $R_o = 0.39\%$ (Table 3.1). Two other opencast mine samples were also included that have already been investigated in detail by Vu (Vu et al., 2008; Vu et al., 2009). One outcrop sample being in the sub-bituminous rank range ($R_o = 0.45\%$), was taken from the Rotowaro mine of Waikato Basin, which also belongs to the Te Kuiti Group. The other sample was taken from the Welcome mine of West Coast Basin representing high volatile bituminous coal ($R_o = 0.52\%$). Generally, the TOC values of the coal samples increase with increasing maturation, which might be related to the loss of moisture and oxygenated compounds as the oxygen index (OI) shows a notable decrease (Vu et al., 2013). The sulfur content is generally low in the coal samples, only lignite G004543 shows higher sulfur content, which might indicate the influence of marine incursions (Sykes, unpublished data).

Table 3.1. General information of the coal samples. Hydrogen Index (HI) and Oxygen Index (OI) are measured in mg hydrocarbon/g organic carbon and mg CO₂/g organic carbon, respectively (Zhu et al., 2015).

Sample	Basin	Location	Stratigraphic group	Age	Depth (m)	TOC (%)	Sulfur (%)	OI	HI	R _o (%)
G004541	Waikato Basin	DEBITS-1 well	Tauranga	Middle Pleistocene	18.9	45.1	0.42	95	192	0.29
G004543	Waikato Basin	DEBITS-1 well	Tauranga	Early-mid Pliocene	62.5	35.9	1.64	80	366	0.29
G004547	Waikato Basin	DEBITS-1 well	Te Kuiti	Late Eocene	140.5	58.2	0.23	26	172	0.39
G001981	Waikato Basin	Rotowaro Mine	Te Kuiti	Eocene-Oligocene	Outcrop	61.2	0.15	32	154	0.45
G001997	West Coast Basin	Welcome Mine	Brunner Coal Measures	Eocene	Outcrop	67.4	0.24	15	209	0.52

The selected samples show differences in their palynofloras. Within the Tauranga group, where the two lignites have been taken from, five pollen zones have been recognized (Nelson et al., 1988). By comparing the geological time, it can be speculated that the lignite G004541 belongs to the zone dominated by pollen of *Restionaceae* and *Podocarpus families*. It has been observed that the pollens of the lignites are composed of dominant herbaceous plant pollens and low proportion of tree pollens (Mildenhall, unpublished report). The lignite G004543 belongs to the *Nothofagidites cranwellae* Zone, where major pollens are derived from trees and only a small portion are derived from herbaceous plants (Mildenhall, unpublished report). Thus, the two lignites from the DEBITS well show the same maturation, but the palynofloras of the input organic matter are different. The Te Kuiti Group of the Waikato basin, where the sub-bituminous coals (G004547 and G001981) have been taken from, can be divided into four biozones (Pocknall, 1991). These two samples belong to the *Myrtaceidites* subzone of the *Nothofagidites matauraensis* Assemblage Zone. This subzone overlaps with the Brunner Coal Measure of West Coast Basin that also has been described as *Nothofagidites matauraensis* Assemblage (Raine, 1984), where sample G001997 was collected from. Therefore, the three bituminous coals show similar palynofloras with the dominant pollen type of *N. matauraensis*.

3.3.2 Methods

3.3.2.1 Open-system pyrolysis gas chromatography (Py-GC)

Open-system pyrolysis gas chromatography (Py-GC) was applied to the coal samples to characterize the labile kerogen on a molecular level. Each sample aliquot (ca. 4 mg) was placed into a small glass capillary tube and inserted into a Quantum MSSV-2 Thermal

Analyzer interfaced with an Agilent GC-6890A (Horsfield et al., 1989; Horsfield et al., 2015). The glass tubes were flushed with helium at 300 °C for 5 min to get rid of volatile constituents and pollutants. Pyrolysis was then performed at a heating rate of 50 °C/min from initial 300 °C to 600 °C and maintained for 2 min at the final temperature. The generated products were collected in a liquid nitrogen-cooled trap, from which they were later liberated by heating the trap to 300 °C for 10 min. A HP-Ultra 1 dimethylpolysiloxane capillary column (50 m length, inner diameter 0.32 mm, film thickness 0.52 mm) connected to a flame ionization detector (FID) was used with helium as the carrier gas for GC analysis. Quantification of individual compounds and boiling ranges was conducted by external standardization with *n*-butane.

3.3.2.2 Solvent extraction, fractionation and GC-MS analysis of coal samples

Around 5 g finely ground coals were Soxhlet extracted with an azeotropic mixture of chloroform, methanol and acetone for 72 h. After concentration and asphaltene precipitation, the extracts were fractionated into aliphatic, aromatic and polar fractions using Medium Pressure Liquid Chromatography (MPLC) (Radke et al., 1980). GC-MS measurements were carried out on the aliphatic fractions for the identification and quantification of individual *n*-alkanes and isoprenoids (pristane and phytane). The experiments were performed using an Agilent 6890 Series gas chromatograph (GC) coupled with a Finnigan MAT 95SQ mass spectrometer (MS). The GC was equipped with a programmable temperature vaporizer (PTV) injector and a BPX5 fused silica capillary (50 m × 0.22 mm i.d., film thickness = 0.25 µm). Helium was used as carrier gas at a constant flow rate of 1.0 ml/min. The injector temperature was set to 50 °C with a rate of 10 °C/s heating up to 300 °C (held for 10 min). The GC oven was programmed from 50 °C with 1 min, then raised to 310 °C at a heating rate of 3 °C/min and held for 30 min at the final temperature. Biomarkers were quantified in the total ion current (TIC) chromatogram by relating the peak area of the target compound to the peak area of the internal standard (5 α -androstane) of known concentration.

3.3.2.3 Water extraction

A detailed description of the extraction procedure and the evaluation of the reproducibility have been provided in Zhu et al. (2015). In brief, 10 g ground coals were extracted with 125 ml deionized water in reaction vessels equipped with a reflux condenser. The extraction lasted for 48 hours under atmospheric pressure and 100 °C. The water extracts were vacuum filtered with 0.45 µm polypropylene filters and stored at 4 °C until further

preparation. A blank experiment was performed with deionized water simultaneously covering the whole extraction, purification and detection procedures.

3.3.2.4 Solid phase extraction (SPE)

Salts are known to cause ionization suppression (King et al., 2000). To obtain salt free samples with high concentrations of extracted DOM, SPE was applied using Bond Elut-PPL cartridges (1 g sorbent, 6 ml cartridge; Agilent Technologies, Germany) (Dittmar et al., 2008). In order to avoid overloading of the cartridges, the volume of the water extract was adjusted to contain approx. 1 mg dissolved organic carbon (DOC). DOC concentrations of the water extracts were determined by liquid chromatography coupled to organic carbon detection (LC-OCD) (Huber et al., 2011) as described in Zhu et al. (2015). Prior to extraction the cartridges were rinsed with methanol and acidified deionized water (pH 2, hydrochloric acid) for cleaning. Water extracts were acidified to pH 2 with hydrochloric acid (suprapur, Merck) and passed through cartridges. The remaining salts were removed by rinsing the cartridge with 3 x 6 ml acidified deionized water (pH 2). Afterwards, the cartridge was dried by vacuum pump for 5 min. Extracted DOM was eluted with 6 ml methanol into pre-combusted glass vials, dried under N₂ atmosphere and stored at -24 °C in the dark until FT-ICR-MS analysis. A procedural blank was prepared with the extracted deionized water to check for possible contaminations during extraction.

3.3.2.5 FT-ICR-MS analysis, mass calibration and data analysis

Extracted DOM was dissolved in methanol to produce a 1 mg/mL solution for each sample, to which a concentrated aqueous ammonium hydroxide solution was added to facilitate the deprotonation of the sample constituents. Extracted DOM samples were analyzed on a Bruker Solarix FT-ICR-MS equipped with a 12 T refrigerated actively shielded superconducting magnet and an Apollo II ESI source from Bruker Daltonik GmbH (Bremen Germany). Samples were ionized using electrospray ionization (ESI) in negative ionization mode at an infusion flow rate of 150 µL/h using a syringe pump (Hamilton). The capillary voltage was set to 3000 V and an additional collision-induced dissociation (CID) voltage of 70 V in the source was applied to avoid cluster and adduct formation. Nitrogen was used as drying gas at a flow rate of 4.0 L/min and a temperature of 220 °C and as nebulizing gas at 1.4 bars. Spectra were recorded in broadband mode using 4 mega word data sets. Ion accumulation time was set to 0.05 s and 200 scans were collected and added to each mass

spectrum. For the extracted DOM samples, the mass range of the measurements was set between 150 Da and 1000 Da.

Mass spectra were calibrated externally using an in-house calibration mixture for ESI negative ion mode containing fatty acids and polyethylene glycol sulfates (Shipkova et al., 2000). Internal calibration was performed using the homologous fatty acids series with a quadratic calibration mode. The root mean square deviations of the five internal calibrations were between 0.05 and 0.013 ppm. Peaks identified in the blank sample were subtracted from the peak lists of the extracted DOM samples. Data evaluation was done with the software packages Data analysis 4.0 SP5 (Bruker Daltonik GmbH, Germany) and Excel 2010 (Microsoft Corporation, Redmont, WA). Only m/z values with a signal to noise ratio ≥ 12 were exported for formula assignment. Molecular formulas were calculated by considering the following elemental isotopes ^1H , ^{12}C , ^{13}C , ^{16}O , ^{32}S , ^{14}N and ^{23}Na , with the upper thresholds $\text{O} \leq 30$, $\text{S} \leq 2$, $\text{N} \leq 2$ and $\text{Na} \leq 1$, C and H were unlimited. A mass tolerance of ± 0.5 ppm was considered as a valid formula and molecular formulas containing ^{13}C were excluded from the final dataset. In ESI FT-ICR-MS, the relative intensity is the joint product of the initial concentration, the ionization efficiency and ion suppression effects. Although the measurements with ESI FT-ICR-MS are not quantitative, samples were compared semi-quantitatively based on their relative proportion of individual peaks and classes relative to the total monoisotopic ion abundance (TMIA).

Double bond equivalents (DBEs) are a measure of hydrogen deficiency and express the number of double bonds and rings. They are calculated from the molecular formula ($\text{C}_c\text{H}_h\text{N}_n\text{O}_o\text{S}_s$) using the equation $\text{DBE} = c - (h/2) + (n/2) + 1$, which are restricted to integer values. In order to evaluate the unsaturation and aromaticity of the molecules that contain heteroatoms, the modified aromaticity index (AI_{mod}) as described by Koch and Dittmar (2006) has been used. The AI_{mod} was calculated based on the molecular formula and expressed as:

$$\text{AI}_{\text{mod}} = \frac{1 + C - 0.5O - S - 0.5(N + P + H)}{C - 0.5O - N - S - P} \quad (\text{Koch and Dittmar, 2016}). \quad (1)$$

Molecules with values of $\text{AI}_{\text{mod}} \geq 0.5$ are described as aromatic compounds; values of $\text{AI}_{\text{mod}} \geq 0.67$ are unambiguous indicators for condensed aromatic compounds (Koch and Dittmar, 2006; D'Andrilli et al., 2010). Following this, values $\text{AI}_{\text{mod}} < 0.5$ can be used to identify nonaromatic (unsaturated and saturated aliphatic) compounds (Šantl-Temkiv et al., 2013; Seidel et al., 2014; Oni et al., 2015).

3.3.2.6 Derivatization and GC-MS of SPE samples

To verify the possible molecular structures of the prominent peaks identified in FT-ICR-MS, GC-MS analysis of the SPE samples was performed. Prior to GC-MS analysis, the SPE samples (in methanol) were derivatized. The acids were methylated by adding diazomethane in ether. Analysis was performed using the same GC-MS equipment and the oven temperature program as described in chapter 2.2.2.

3.4 Results and discussion

3.4.1 General characterization of coal organic matter

3.4.1.1 Organofacies

To gain information about the organofacies of the coals, the chain length distributions of *n*-alkanes (C_{1-5} , $n-C_{6-14}$, $n-C_{15+}$) found in their pyrolysates were plotted in the ternary diagram (Horsfield, 1989) (Fig. 3.1). The two lignites plot in the field of high wax paraffinic oil prone kerogens/coals rich in long-chain *n*-alkanes and *n*-alkenes. The slight variation between the two lignites indicates subtle differences in organofacies, which is in accordance to the different palynofloras observed in the Tauranga group (Nelson et al., 1988). The pyrolysates of the three bituminous coals are plotting very close to each other and show higher amounts of short chain *n*-alkanes indicating the potential to produce high wax paraffinic-naphthenic-aromatic oils. This similarity in organofacies for the three bituminous coals is in accordance with our assumption that they have been derived from the same palynoflora.

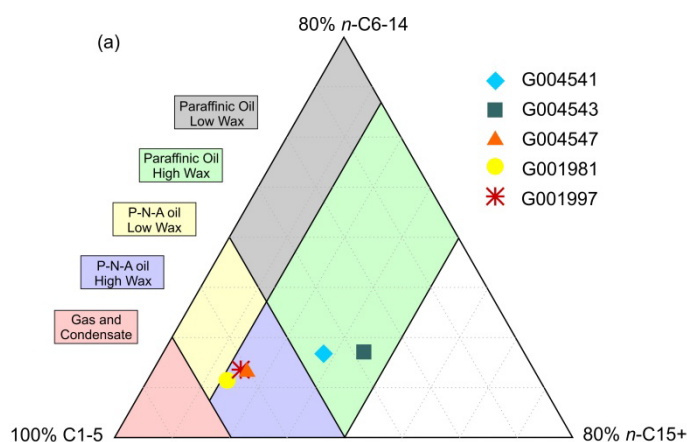


Figure 3.1. Ternary diagram showing petroleum type organofacies assessment according to Horsfield (1989) based on molecular compositions from open-system pyrolysis GC-FID analysis.

3.4.1.2 Depositional environment and level of coalification

To get insights into the depositional environment of the coal organic matter, coal samples were extracted with organic solvent. The yields of the solvent extractions vary between 112 and 212 mg/g TOC (Table 3.2). The three bituminous coals and lignite G004541 have comparable amounts of solvent extractable organic matter (SEOM), which are lower than the SEOM yield of lignite G004541. The yields of *n*-alkanes in these SEOM are one order of magnitude higher for the lignites than for the bituminous coals. The *n*-alkane distribution of the coals is characterized by a predominance of long-chain *n*-alkanes ($> nC_{23}$) with odd carbon numbers (Fig. 3.2), which is typically found in terrestrial organic matter. The values of the CPI (Carbon Preference Index) (Bray and Evans, 1961) range from 2.79 to 3.49 for the bituminous coals and are 7.92 and 16.15 for the lignites (Table 3.2) displaying their different diagenetic stages but also the differences in palynoflora for the two lignites. The ratio of pristane and phytane (Pr/Ph) can be used to evaluate the redox conditions and the depositional environment of the organic matter (Didyk et al., 1978), though it is also influenced by thermal maturity. The bituminous coals contain significant amounts of isoprenoids while the lignites do not contain pristane and phytane (Table 3.2). One possible explanation for this might be that the release of isoprenoid alkanes only occurs after thermal maturation has proceeded to about sub-bituminous rank (Vu et al., 2009). The high Pr/Ph ratios (2.9-10.98) of the bituminous coals confirm their high terrigenous matter input and an oxic depositional environment (Peters et al., 2007).

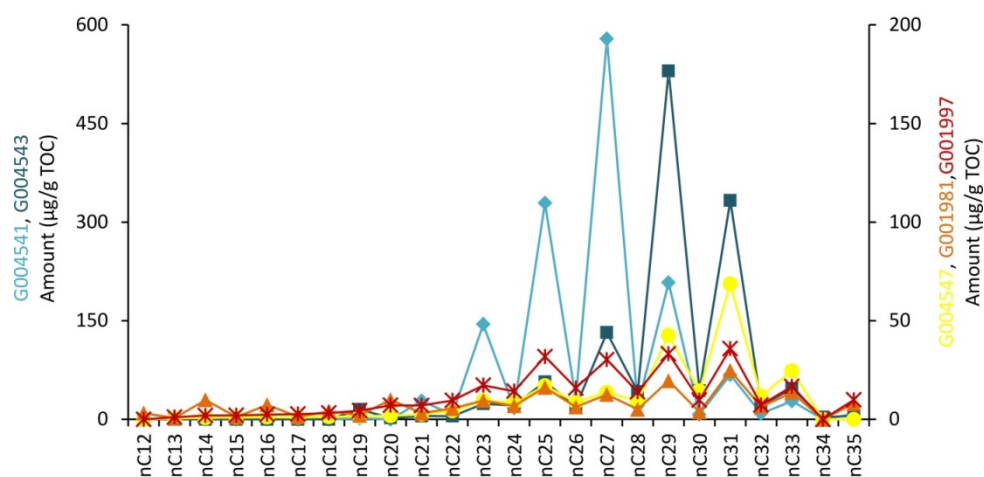


Figure 3.2. The amounts of *n*-alkanes in the solvent extracts of the five New Zealand coals.

3.4.2 Composition of the extracted DOM

3.4.2.1 Water extraction yields (content of extracted DOM)

The extracted DOM contents of the five coals have been investigated in our previous study (Zhu et al., 2015), which ranged from 66 to 187 mg C/l or from 1.1 to 5.7 mg C/g TOC (Table 3.2). The concentrations of the extracted DOM are higher than published data for natural DOM. It has been reported that concentrations of DOM vary from approximately 0.5mg C/l for sea water, 2 to 10 mg C/l for rivers and lakes as well as 10 to 60 mg C/l for swamps, marshes, and bogs (Thurman, 1985). The high concentrations of the extracted DOM are related to the low fluid to solid ratio that was realized during our extractions. The yields of the water extraction are about two orders of magnitude lower than the yields of solvent extraction, clearly indicating that only a small proportion of the coal organic matter can be mobilized by water extraction.

3.4.2.2 Molecular composition of extracted DOM

a) Comparison of extracted DOM of coals with other natural DOM samples

The Van Krevelen diagram is a useful tool for visualizing hydrogen and oxygen content of organic compounds and has often been applied for characterization of natural DOM. It has been reported that DOM with a high input of terrestrial organic matter has high O/C and low H/C values and is more aromatic while the marine DOM with high amount of aliphatic structures, shifts to low O/C and high H/C values (Sleighter and Hatcher, 2008; Schmidt et al., 2009). Van Krevelen diagrams are widely used for FT-ICR-MS data analysis of different natural DOM types (Kim et al., 2003a; Kujawinski et al., 2004; Sleighter and Hatcher, 2007, 2008; Schmidt et al., 2009; Minor et al., 2012). Within the Van Krevelen diagram, different regions/areas have been defined and linked to different chemical compound groups like lipids, proteins, lignin and condensed aromatic compounds (Kim et al., 2003a; Sleighter and Hatcher, 2007; Ohno and Ohno, 2013). To get first insights into the characteristics of the extracted DOM, Van Krevelen diagrams were prepared for extracted DOM of lignite G004541 and bituminous coal G001997 (Fig. 3.3A and 3.3B). To simplify the comparison, we define four groups of compounds with different ranges of O/C and H/C values (I: $H/C > 1$ and $O/C < 0.5$ including lipids, proteins and part of the lignins, II: $H/C > 1$ and $O/C > 0.5$ including amino sugars, carbohydrates and part of the tannins, III: $H/C < 1$ and $O/C < 0.5$ including condensed hydrocarbons and part of the lignins and IV: $H/C < 1$ and $O/C > 0.5$ including partly condensed

hydrocarbons and tannins). Extracted DOM of lignite and bituminous coal are quite similar with majority of formulas plotting in areas III and IV. There are only differences in two groups of formulas, one with high O/C (>0.7) and medium H/C ($0.4 < \text{H/C} < 1.0$) values and one with high O/C and high H/C values that are only present in extracted DOM of the lignite (Fig. 3.3A). The lignites are known to contain more oxygen-containing functional groups than the bituminous coals (Murata et al., 2001). These compositional differences between lignites and bituminous coals are also reflected in their extracted DOM as the lignite extracts have additional formulas with high O/C values. The Van Krevelen diagrams of the extracted DOM of coals vary fundamentally from those of natural DOM samples (Fig. 3.3C). The majority of peaks in almost all natural DOM samples belong to groups I and II (Koch et al., 2005; Sleighter and Hatcher, 2008; Schmidt et al., 2009; Minor et al., 2012; Schmidt et al., 2017), whereas the extracted DOM of coals consists mainly of compounds in groups III and IV indicating an elevated aromaticity of the extracted DOM. While in natural DOM compounds in group III have been assigned as black carbon derived from incomplete combustion of fossil fuels and biomass (Kim et al., 2004; Hockaday et al., 2006; Dittmar, 2008), it is obvious that group III compounds in the extracted DOM of coals are not derived from black carbon but directly from the coal organic matter. The group IV compounds mainly consist of tannin-like compounds. Tannins are polyphenolic compounds that normally occur in higher plants and some algae (De Leeuw and Largeau, 1993). The extracted DOM of coals resembles terrestrial-derived DOM with high amounts of lignin- and tannin-like and condensed hydrocarbon formulas. Compared to natural DOM with a high fraction of terrestrial organic matter input like pore waters from fens, bogs and peatland soils (D'Andrilli et al., 2010; Tfaily et al., 2013), additional formulas with O/C value below 0.2 can be observed in the extracted DOM of the coals. This might be due to the loss of oxygen during the burial and coalification process of coals.

b) Does the extracted DOM composition of the coals reflect the differences in organofacies and coalification?

The ESI broadband mass spectra of extracted DOM of the five coal samples are shown in Fig. 3.4. The number of assigned monoisotopic peaks ranges between 1432 and 2903 (Table 3.3). The extracted DOM of the lignites covers a broader mass range and contains more peaks than the bituminous coal extracts. Compounds consisting of only C, H and O (O_x compounds) predominated in number followed by O_xN_y compounds in all samples. The calculated overall mean values for DBE, carbon numbers and oxygen numbers as well as the

number-averaged molecular weight (M_n) and the weight-averaged molecular weight (M_w) are much higher in the extracted DOM of the two lignites than in the extracted DOM of the three bituminous coals (Table 3.3). For the extracted DOM of the bituminous coals, the numbers of assigned peaks, O_x compounds, M_n as well as M_w slightly decrease with increasing coal rank. But the variations observed within the extracted DOM of the bituminous coals are less significant than the differences between extracted DOM of lignites and bituminous coals.

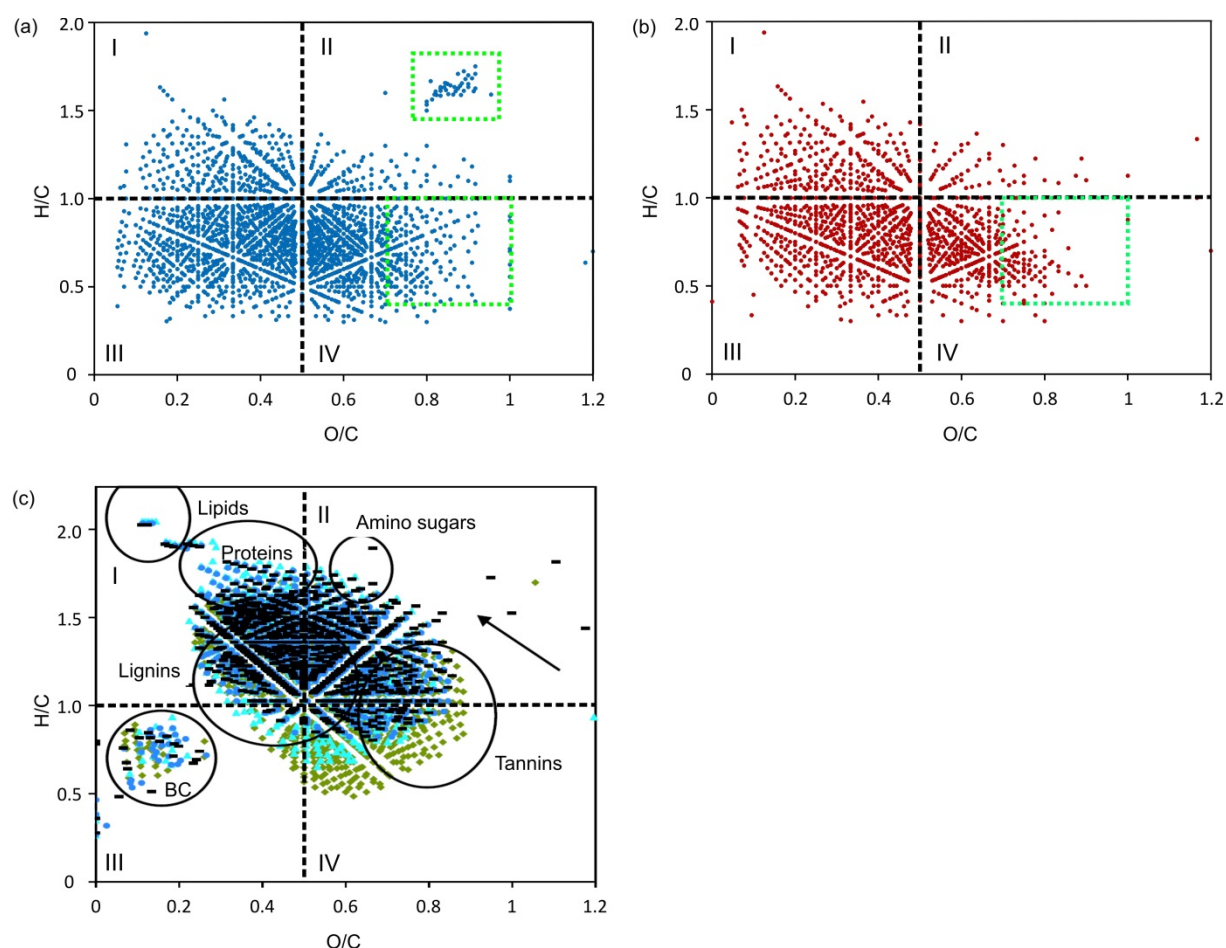


Figure 3.3. Van Krevelen diagrams for the extracted DOM of lignite G004541 (a) and of bituminous coal G001997 (b) as well as DOM from shelf (c) as detected by negative ion mode ESI FT-ICR-MS analysis. The compounds are divided into four groups according to the O/C and H/C values (I: $H/C > 1$ and $O/C < 0.5$ including lipids, proteins and part of the lignins, II: $H/C > 1$ and $O/C > 0.5$ including amino sugars, carbohydrates and part of the tannins, III: $H/C < 1$ and $O/C < 0.5$ including condensed hydrocarbons and part of the lignins and IV: $H/C < 1$ and $O/C > 0.5$ including partly condensed hydrocarbons and tannins). The differences between extracted DOM of the lignite and the bituminous coal are indicated by light green rectangles. Figure (c) is adapted from (Schmidt et al., 2009).

Table 3.2. Concentrations of solvent extractable organic matter and *n*-alkanes, carbon preference index (CPI) and pristane/phytane (Pr/Ph) ratios as well as the extracted DOM in terms of mg C/l and mg C/g TOC of the five coal samples.

	SEOM (mg/g TOC)	n-alkane (µg/g TOC)	*CPI ₂₅₋₃₃	Pr/Ph	DOM (mg C/l)	DOM (mg C/g TOC)
G004541	138	1487	16.15	-	153	3.7
G004543	212	1307	7.92	-	187	5.7
G004547	112	244	3.48	6.46	137	2.6
G001981	123	180	3.56	2.90	144	2.6
G001997	124	278	2.79	10.98	66	1.1

$$* \text{CPI}_{25-33} = \frac{1}{2} \left(\frac{\text{C}_{25} + \text{C}_{27} + \text{C}_{29} + \text{C}_{31} + \text{C}_{33}}{\text{C}_{24} + \text{C}_{26} + \text{C}_{28} + \text{C}_{30} + \text{C}_{32}} + \frac{\text{C}_{25} + \text{C}_{27} + \text{C}_{29} + \text{C}_{31} + \text{C}_{33}}{\text{C}_{26} + \text{C}_{28} + \text{C}_{30} + \text{C}_{32} + \text{C}_{34}} \right)$$

Table 3.3. Total numbers of assigned peaks and their distribution in the main elemental classes, total mass range as well as average values of DBE, elemental numbers (carbon, hydrogen, oxygen) and molecular weight.

Sample	Total	No. formulas				Mass range (Da)	Mean				M _n Total	M _w Total
		O _x	O _x N _y	O _x S _z	O _x Na _v		DBE	C	H	O		
G004541	2253	1806	371	29	46	159-869	11.08	16.95	12.79	8.51	353.7	387.24
G004543	2903	1836	567	487	11	159-827	10.65	17.52	14.87	8.16	360.71	389.96
G004547	1818	1241	403	15	156	159-587	9.64	13.12	13.12	6.90	314.44	337.47
G001981	1805	1186	390	19	203	159-594	9.48	15.20	12.50	7.03	310.76	333.88
G001997	1432	1001	316	15	97	159-585	9.54	14.84	11.69	6.97	304.18	328.65

Number of formulas: number of assigned monoisotopic signals. M_n: number-averaged molecular weight. M_w: weight-averaged molecular weight.

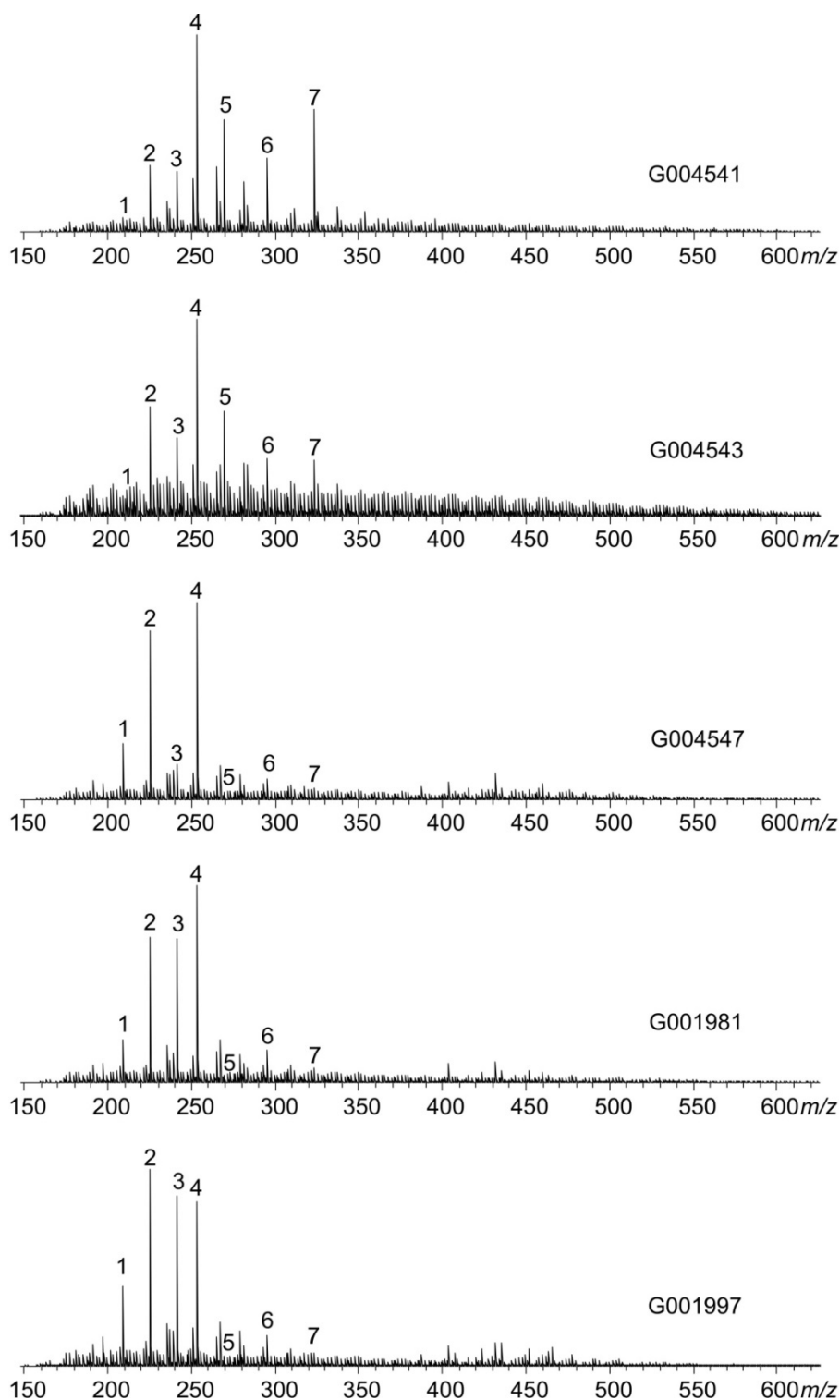


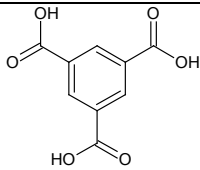
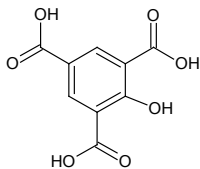
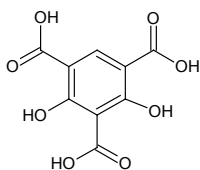
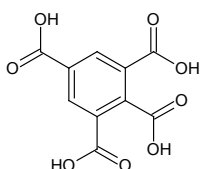
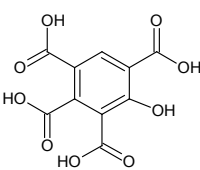
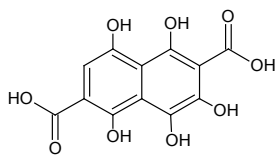
Figure 3.4. ESI negative FT-ICR mass spectra of the extracted DOM from the five coal samples. Prominent peaks are numbered and represent these formulas: 1 - $C_9H_5O_6$; 2- $C_9H_5O_7$; 3 - $C_9H_5O_8$; 4 - $C_{10}H_5O_8$; 5 - $C_{10}H_5O_9$; 6- $C_{12}H_7O_9$; 7- $C_{13}H_7O_{10}$.

All spectra show a number of prominent peaks between m/z 200 and 350 (no. 1-7) but with different relative intensities from sample to sample (Fig. 3.4). These seven peaks were not detected in the spectrum of the blank sample confirming that they did not represent

contaminants. The exact masses and calculated formulas of these peaks as well as possible structures are listed in Table 3.4. All these elevated peaks very likely refer to different benzenepolycarboxylic acids (BPCAs) and naphthalenepolycarboxylic acids (NPCAs) varying in their numbers of carboxyl and hydroxyl groups. The high number of carboxyl groups leads to an increased response of these compounds in electrospray in negative ion mode. Since FT-ICR-MS does not allow structure elucidation or detection of distinct isomers, GC-MS measurements have been performed on coal extracts with the focus on BPCAs and their derivatives. GC-MS measurements confirmed that the prominent peaks (no. 1-5 in Fig. 3.4) were corresponding to benzene tricarboxylic acids (B3CA), hydroxybenzene tricarboxylic acids (OH-B3CA), dihydroxybenzene tricarboxylic acids (2OH-B3CA), benzene tetracarboxylic acids (B4CA) and hydroxybenzene tetracarboxylic acids (OH-B4CA) as shown in Fig. 3.5. The extracted ion chromatograms of all detectable BPCAs and their hydroxyl and di-hydroxyl derivatives detected in extracted DOM of lignite G004541 as an example are shown in Fig. S3.1. B2CA, B3CA, B4CA and B5CA appeared in all extracted DOM samples but with minor amount of B5CA in the extracted DOM of the bituminous coals. Furthermore, B1CA and B6CA were only present in extracted DOM of the lignites in low amounts. The relative abundances of the detected BPCAs were compared (Fig. 3.6). The extracted DOM of the two lignites was rich in B4CA and B5CA while the extracted DOM of the three bituminous coals shows a high abundance of B2CA and B3CA. It has been reported that oxidation of coals results in BPCAs with decreasing number of carboxyl-groups relative to increasing coal rank (Yang et al., 2017). Thus, the difference in relative abundance of BPCAs in the extracted DOM might relate to the coalification degree of the coal samples.

BPCAs and their derivatives have also been detected by FTIR spectra in the leachates from lignites (Doskočil et al., 2015; Kosateva et al., 2017). BPCAs were described as oxidation products of coals (Gong et al., 2011; Wang et al., 2013; Yang et al., 2017), but harsh chemical oxidation treatments have been applied in these studies. Coals contain aromatic clusters with alkyl side chains that can be easily transformed to BPCAs via chemical oxidation (Murata et al., 2001). Indeed, BPCAs have been detected as constituents of fulvic acids extracted from weathered coal (Zhou and Zhang, 1994). This led to the hypothesis that BPCAs can also be formed from coals in a natural system under soft oxidative and/or diagenetic conditions. The coals extracted in this study are known to be deposited in oxic environments. Thus, the BPCAs and the hydroxyl-substituted BPCAs detected in the extracted DOM might be related to the oxidation of coal organic matter over geological time.

Table 3.4. General information of the seven elevated peaks.

	Assigned formula $[M - H]^-$	Measured compounds [M]	Calc. m/z $[M - H]^-$	DBE	Possible structure [M]	Abbreviation
Peak 1	$C_9H_5O_6$	$C_9H_6O_6$	209.009161	7		B3CA
Peak 2	$C_9H_5O_7$	$C_9H_6O_7$	225.004076	7		OH-B3CA
Peak 3	$C_9H_5O_8$	$C_9H_6O_8$	240.998991	7		2OH-B3CA
Peak 4	$C_{10}H_5O_8$	$C_{10}H_6O_8$	252.998991	8		B4CA
Peak 5	$C_{10}H_5O_9$	$C_{10}H_6O_9$	268.993905	8		OH- B4CA
Peak 6	$C_{12}H_7O_9$	$C_{12}H_8O_9$	295.009555	9		4OH- N2CA

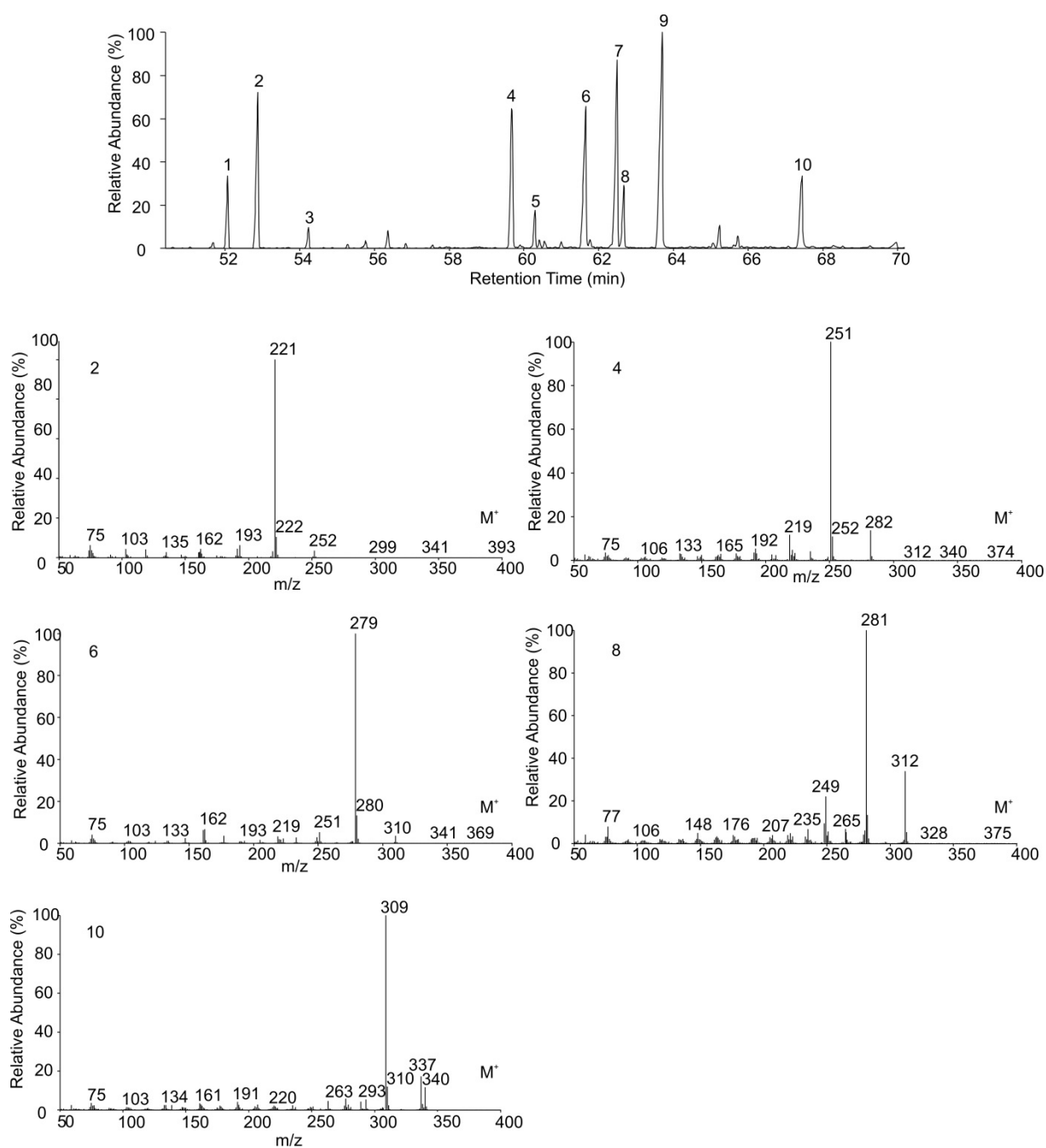


Figure 3.5. Extracted ion chromatograms (m/z 221 + 251 + 279 + 281 + 309) from GC-MS analysis of the methyl esters of BPCAs and hydroxyl-substituted BPCAs in the extracted DOM of coal sample (G004541): methyl esters of benzene tricarboxylic acids (1, 2, 3; m/z 221), hydroxybenzene tricarboxylic acids (4, 5; m/z 251), benzene tetracarboxylic acids (6, 7, 9; m/z 279), dihydroxybenzene tricarboxylic acids (8; m/z 281), hydroxybenzene tetracarboxylic acids (10; m/z 309).

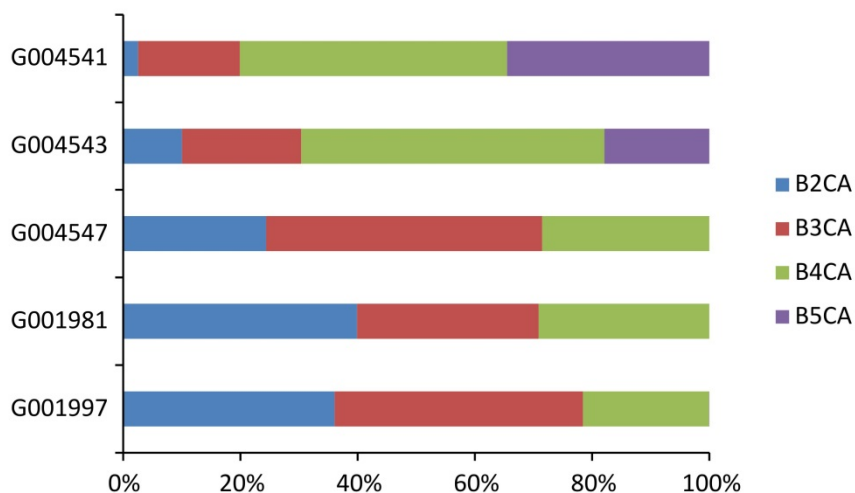


Figure 3.6. The relative abundance of BPCA groups in the extracted DOM of the five coal samples as calculated from GC-MS results.

3.4.2.3 Elemental class distribution

The relative intensity distribution of elemental classes in extracted DOM of the coals is illustrated by a bar chart (Fig. 3.7). The O_x class is the dominant elemental class in all samples (77.8% to 91.9% of the TMIA). Such dominance of only C, H and O atoms containing molecular formulas ($> 80\%$) has also been described for humic acids extracted from peats with 0.5 M sodium hydroxide (NaOH) (Hartman et al., 2015). The O_xN_y class is present in lower intensity and varies between 6.7% TMIA and 12.8% TMIA. The O_xS_z class shows even less than 1% TMIA except for extracted DOM from lignite G004543 where it accounts for 10.2% TMIA, which correlates well with the higher sulfur content of this lignite (Table 3.1). The O_xNa_w class rises from below 1% TMIA in the lignite extracts to 4.6-6.1% TMIA in the bituminous coal extracts. The sodium containing molecular formulas might be sodium adducts that are formed during ionization. Overall, the relative intensity distribution of the elemental classes shows no obvious systematic variation with maturation or with organofacies except for the O_xNa_w class, which shows higher TMIA proportion in extracted DOM of bituminous coals.

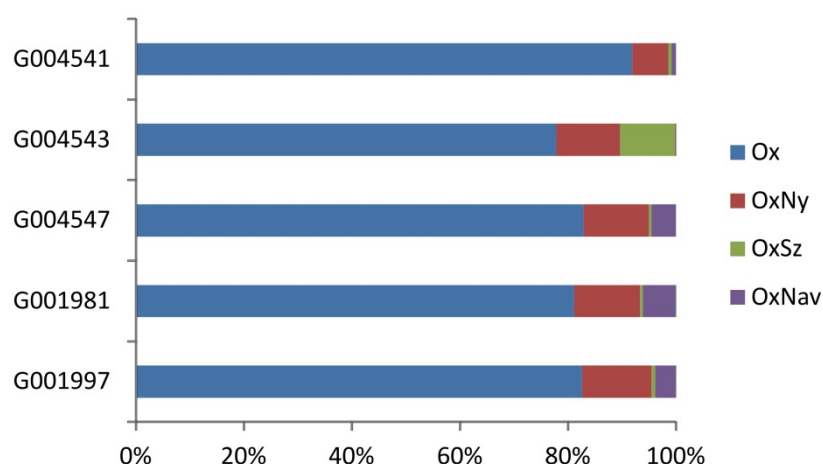


Figure 3.7. Bar chart displaying the percentage of individual elemental classes in the extracted DOM of the five coals as detected in negative ion ESI spectra.

3.4.3 Detailed characterization of the oxygen containing compounds

3.4.3.1 Compound class distributions

The number of oxygen atoms in the compounds ranges from 1 to 16 for the bituminous coal extracts and from 1 to 22 for the lignite extracts (Fig. 3.8). High numbers of oxygen atoms (>13) in the oxygen containing compounds have also been reported for DOM in river, creek, and bay water (Dubinenkov et al., 2015), offshore coastal water (Bae et al., 2011) as well as lacustrine, marine and estuarine water samples (Melendez-Perez et al., 2016). The relative intensities of all individual oxygen classes are quite similar for the extracted DOM of the two lignites on the one hand, and the extracted DOM of the three bituminous coals on the other hand (Fig. 3.8). Generally, the relative intensities of O_1 to O_8 classes increase with increasing number of oxygen atoms and then decrease for the classes with higher oxygen numbers ($O_{>8}$). In extracted DOM of the bituminous coals the relative intensities of the O_{1-8} classes are higher than in extracted DOM of the lignites, while it is the other way round for oxygen classes with $O_{>8}$. The differences in the relative intensities of the oxygen classes between lignite and bituminous coal extracts are coincident with the organofacies differences of the samples. The lower intensities in O_{9-16} classes of the bituminous coal extracts might be related to the defunctionalisation reactions, such as thermal decarboxylation and decarbonylation, which lead to the loss of oxygen from the original coals during diagenesis to moderate catagenesis (Schenk and Horsfield, 1998; Kelemen et al., 2002; Vu et al., 2013),

which is also reflected by significantly decreased OI values of bituminous coals compared to lignites (Table 3.1).

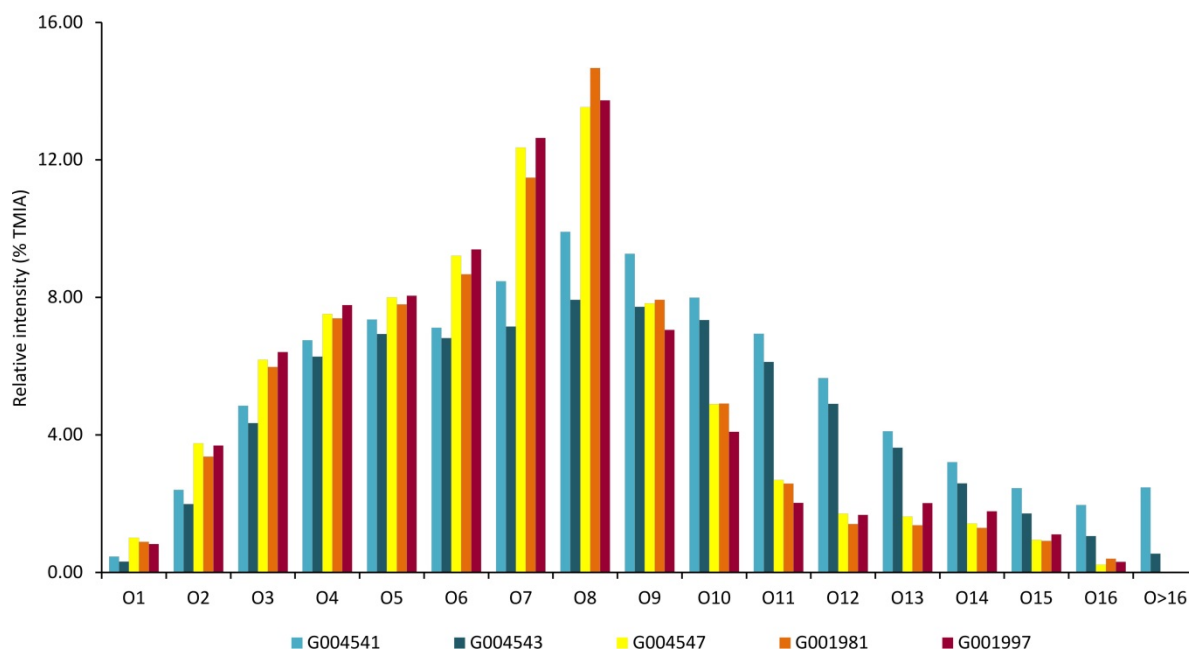


Figure 3.8. Relative intensities of the different O_x classes in the extracted DOM of the coal samples.

3.3.2 DBE distributions of the oxygen containing compounds

The DBE distributions of the O₃, O₆, O₈ and O₁₁ classes are given in Fig. 3.9. DBE distributions of all O_x classes are shown in Fig. S3.2. In most cases, monomodal DBE distributions can be observed in all oxygen classes of all extracted DOM samples. The range of DBE values present in the O₁ class is 4-13 and shifts to 12-23 in the O₁₆ class (Fig. S3.2). In the O₁₋₈ classes, compounds with 7 to 9 DBEs are the most abundant species, while compounds with 9 to 16 DBEs have maximum intensity in the O₉₋₁₆ classes. A broader range in DBE distribution by extension to higher DBE values can be observed for the extracted DOM of the two lignites. The DBE distributions for individual O_x classes are nearly similar for the lignite extracts on the one hand and the bituminous coal extracts on the other hand. The relatively high intensities of the compounds with DBE of 7-10 in the O₆₋₁₀ classes were mostly contributed to the seven compounds with relatively high intensities as shown in the mass spectra (Fig. 3.4, Table 3.4). The exception for O₈ class in the extracted DOM of lignite G004541 is due to relatively high intensities of the compounds corresponding to the prominent peaks no. 3 and 4 (Fig. 3.4).

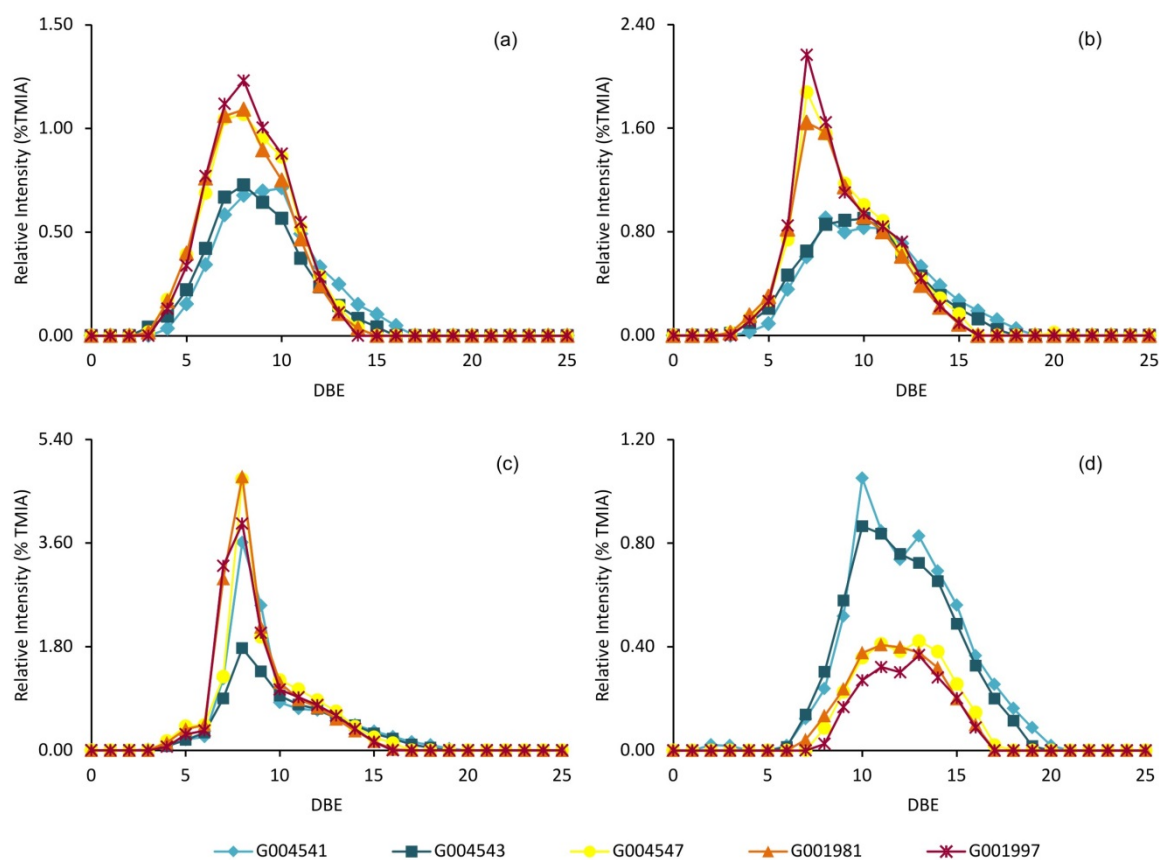


Figure 3.9. DBE class distributions found in the O₃ (a), O₆ (b), O₈ (c), and O₁₁ (d) classes.

3.4.3.2 Structure information provided by average DBE

The overall DBE distribution of a selected compound class can be described by its intensity-weighted average DBE (DBE_{average}), calculated as

$$\text{DBE}_{\text{average}} = \frac{\sum_i I_i * (\text{DBE})_i}{\sum_i I_i} \quad (\text{Bae et al., 2011}) \quad (2)$$

where I_i and $(\text{DBE})_i$ are the relative abundance and DBE value of peak i , respectively. The relative abundance was calculated as the percentage of TMIA.

The number of oxygen atoms in a molecule is not included in the calculation of DBE values. However, oxygen bound in carboxyl or carbonyl groups contributes to the DBE of a compound, while oxygen bound in alcohol or ether functionalities does not. The change in the average DBE values with the number of oxygen atoms can be used to assess the contribution of oxygen atoms to DBE in different oxygen classes. Therefore, the average DBE was plotted against the number of oxygen atoms in each oxygen class for all extracted DOM (Fig. 3.10)

and for the individual samples (Fig. S3.3). We identified three different types of slope for all five samples (Fig. 3.10). The R^2 values are very close to 1 for both O_{1-5} classes and O_{9-16} classes of the five extracted DOM (Fig. S3.3), which indicate a strong correlation between the number of oxygen atoms and the $DBE_{average}$ values of the extracted DOM molecules. In O_{1-5} classes, the average DBE increases only slightly with increasing number of oxygen atoms in the molecular formulas. For the O_{6-8} classes, average DBE remains more or less constant. And in the O_{9-16} classes, the average DBE shows again a linear increase with increasing number of oxygen atoms, but with a higher slope. Thus, a newly added oxygen atom makes a significantly lower contribution to the average DBE value in the O_{1-5} classes than in the O_{9-16} classes, while it does not seem to influence average DBE in the O_{6-8} classes. It therefore can be speculated that the compounds in the O_{9-16} classes consist of more carbonyl and carboxyl groups than those in the O_{1-5} classes, the latter contain more hydroxyl and ether functional groups (Bae et al., 2011). The constant DBE values with increasing number of oxygen atoms in O_{6-8} classes are probably related to the four compounds corresponding to the prominent peaks (no. 1-4) with relatively high intensities and low DBE values (Fig. 3.4, Table 3.4). Knowing that the extracted DOM of the bituminous coals contains relatively higher abundances of O_{1-8} classes than of O_{9-16} classes, it can be speculated that the extracted DOM contains more hydroxyl and ether functional groups and lower amounts of carboxyl and carbonyl functional groups. Hydroxyl groups as the most abundant oxygen moieties have also been reported in the solvent extracts of subbituminous coals (Kong et al., 2016). From pyrolysis experiments of type III kerogen, it is known that the decrease in oxygen content is due to the elimination of the carbonyl and carboxyl groups but not of hydroxyl and ether groups (Durand, 1980). A preferential loss of oxygen fixed in carboxylic acids and esters prior to oxygen in ethers and phenolic groups with increasing maturation of coal has been reported by Vu et al. (2013). It therefore can be speculated that the relatively low abundance of O_{9-16} classes of the extracted DOM of the bituminous coals compared to the lignite extracts might be due to the loss of oxygen via eliminations of carboxyl and carbonyl groups with increasing maturation.

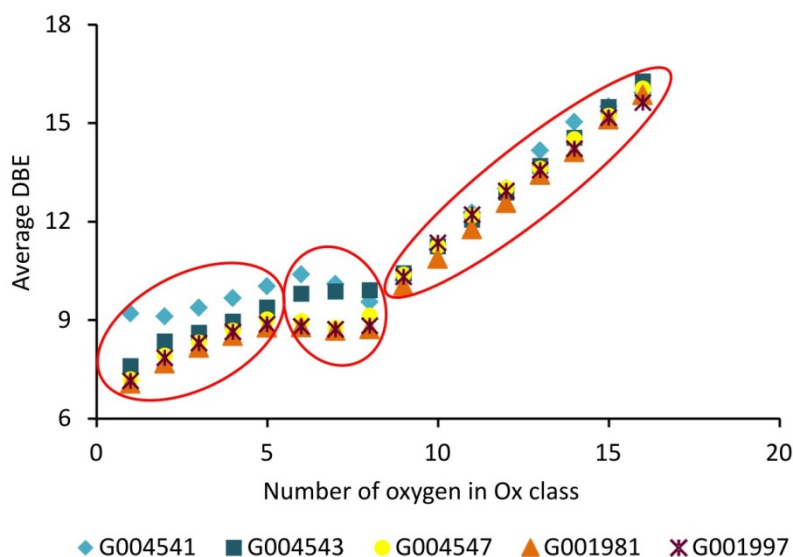


Figure 3.10. Average DBE of each O₁₋₁₆ class is plotted over the respective oxygen number. The plots can be divided into three groups, O₁₋₅, O₆₋₈ and O₉₋₁₆ as indicated by the elliptical frames.

3.4.3.3 Aromatic structure of oxygen containing compounds

The modified aromaticity index (AI_{mod}) can be used for the evaluation of aromaticity and unsaturation of the assigned molecular formula (Koch and Dittmar, 2006). The AI_{mod} was developed based on the assumption that approximately half of the oxygen is bound with π -bonds in carboxyl groups, which is a valid assumption for marine DOM (Benner, 2002). However, the amounts of oxygen involved in π -bonds are various in different oxygen classes for the coal extracts. The gradients of average DBE over oxygen number are equal to the percentage of oxygen atoms involved in π -bonds that can make contribution to DBE value (Fig. S3.3). Therefore, an improved equation for the calculation of the aromaticity index for the extracted DOM of coal extracts is proposed:

$$AI_{\text{coal}} = \frac{1 + C - mO - S - 0.5(N + P + H)}{C - mO - N - S - P}, \quad (3)$$

m value represents the percentage of oxygen atoms bound in π -bonds. The m value is 0.5 in AI_{mod}. For the extracted DOM of coals, the m values are different in the O₁₋₅ classes, O₆₋₈ classes and O₉₋₁₆ classes and equal to the slopes of the linear regressions of DBE_{average} vs. O_x (Table 3.5). To divide the molecular formulas into three aromaticity groups (aliphatic, aromatic and condensed aromatic), the threshold values for AI_{mod} were also used for AI_{coal}.

For the extracted DOM of lignite G004541, the molecular formulas in O₁₋₅, O₉₋₁₆ classes were plotted in Van Krevelen diagram and calculated AI_{coal} for the individual formulas is

indicated by color code (Fig. 3.11). AI_{coal} divides molecular formulas into aliphatic, aromatic and condensed aromatic compound groups where more aliphatic compounds and less condensed aromatic compounds are existing in O_{9-16} classes compared to O_{1-5} classes. The relative intensities of the three aromaticity groups for the oxygen containing compounds of the five extracted DOM are shown in Fig. 3.12. The relative intensities of the condensed aromatic compounds gradually increase from 23% to 40% while the relative intensities of the aliphatic compounds decrease from 51% to 30% with increasing coalification. The relative intensities of the aromaticity groups between the two lignites are different, which might correlate to their organofacies difference. The total proportion of condensed aromatics and aromatics is slightly higher for extracted DOM of the bituminous coals than for the lignites. This may indicate that the extracted DOM of the bituminous coals is more aromatic than the extracted DOM of the lignites, which is consistent with the increase in aromaticity of the original organic matter of the New Zealand coals with increasing maturation (Zhu et al., 2015).

Table 3.5. Equations and R^2 values of the linear regressions when plotting average DBE vs oxygen number for O_{1-5} , O_{6-8} and O_{9-16} classes. The x values are equal to the number of oxygen atoms in the molecular formula. The y values are equal to the average DBE values in each oxygen class.

	O_{1-5} classes	O_{6-8} classes	O_{9-16} classes
G004541	$y = 0.22x + 8.82$ $R^2 = 0.87$	$y = -0.42x + 12.95$ $R^2 = 0.97$	$y = 0.85x + 2.84$ $R^2 = 0.98$
G004543	$y = 0.42x + 7.32$ $R^2 = 0.97$	$y = 0.05x + 9.48$ $R^2 = 0.97$	$y = 0.84x + 2.84$ $R^2 = 1.00$
G004547	$y = 0.44x + 6.90$ $R^2 = 0.97$	$y = 0.08x + 8.37$ $R^2 = 0.21$	$y = 0.80x + 3.29$ $R^2 = 1.00$
G001981	$y = 0.43x + 6.76$ $R^2 = 0.97$	$y = -0.03x + 8.93$ $R^2 = 0.29$	$y = 0.83x + 2.57$ $R^2 = 1.00$
G001997	$y = 0.42x + 6.89$ $R^2 = 0.96$	$y = 0.01x + 8.70$ $R^2 = 0.04$	$y = 0.75x + 3.82$ $R^2 = 1.00$

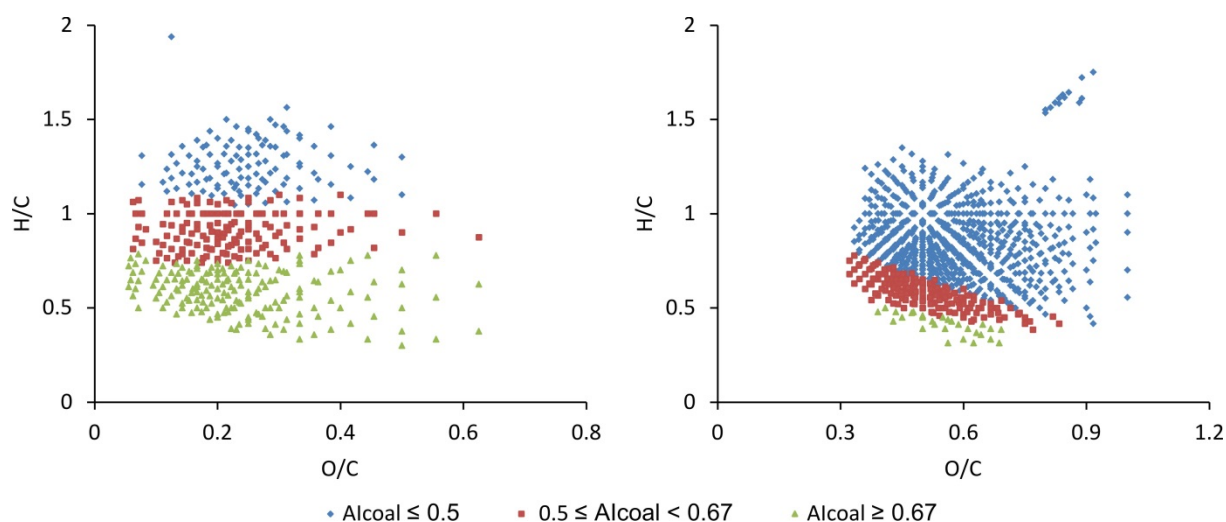


Figure 3.11. Van Krevelen diagrams show the molecular formulae in O1-5 (left), O9-16 (right) classes of the sample G004541. Aliphatic, aromatic and condensed aromatic structures can be identified with threshold criteria of the $\text{Alcoal} \leq 0.5$, $0.5 \leq \text{Alcoal} < 0.67$ and $\text{Alcoal} \geq 0.67$, respectively.

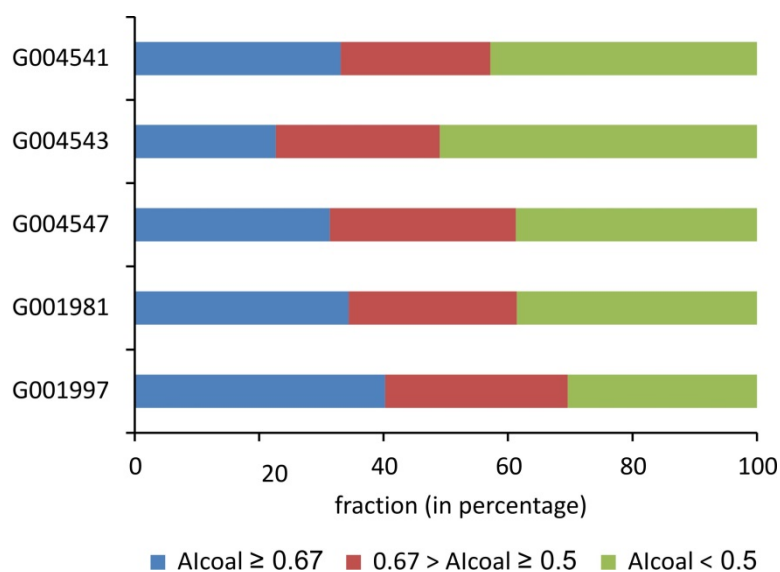


Figure 3.12. Relative intensities of the oxygen compounds classified as condensed aromatic, aromatic and aliphatic fractions based on the calculation of Al_{coal} for the extracted DOM of five coals.

3.5 Summary and Conclusions

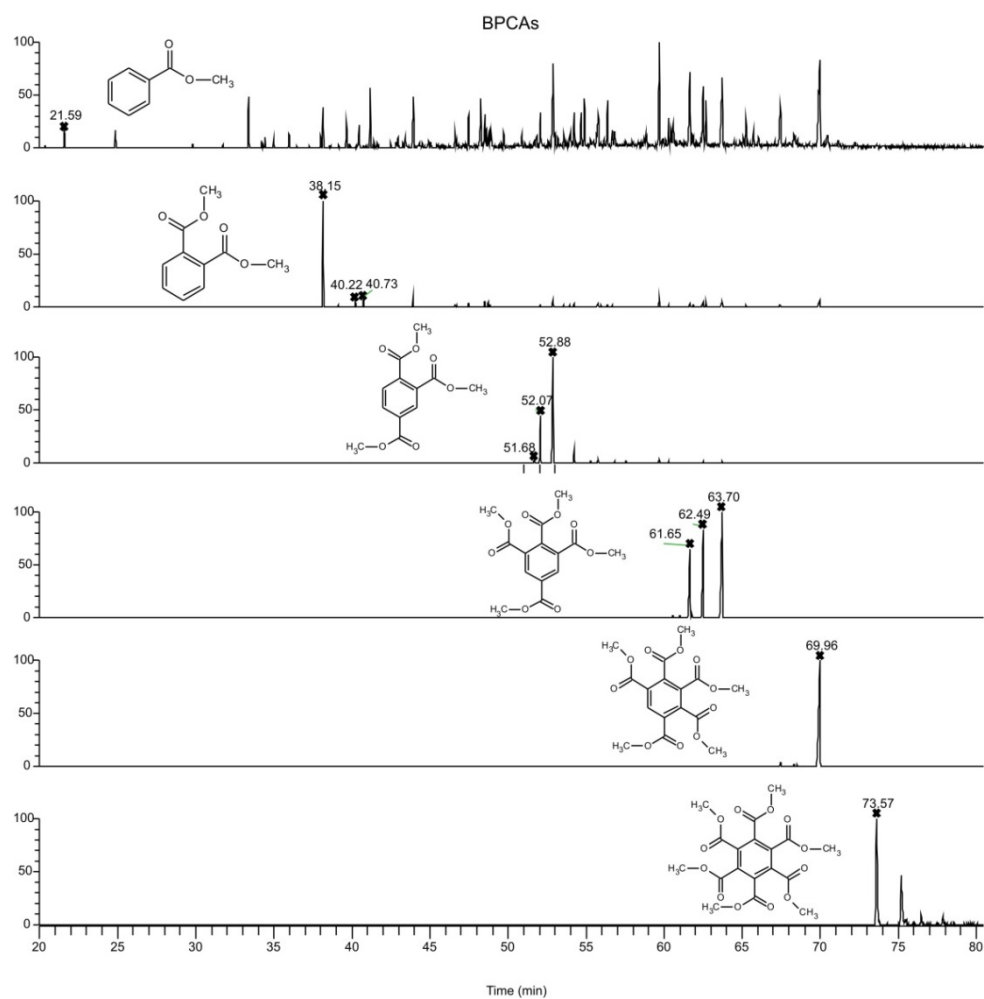
Five New Zealand coal samples as well as their water extracts were investigated using conventional geochemical analysis and ultrahigh resolution mass spectrometry to characterize the extracted DOM composition, its relation to coal organic matter properties and compare extracted DOM with natural DOM. The amounts of extracted DOM are generally lower than the amount of SEOM from the same samples but higher than the amount of DOM found in

natural water samples. The composition of extracted DOM differs from natural DOM with respect to high aromaticity of individual compounds. Extracted DOM from lignites contains a higher number of organic compounds than the extracted DOM from bituminous coals. The prominent peaks in the mass spectra of the extracted DOM have been identified as BPCAs and NPCAs with different numbers of carboxyl and hydroxyl groups. The compositional differences of BPCAs in extracted DOM from lignites and bituminous coals can be related to the coalification process. In general, oxygen containing compounds are the dominant elemental class in the extracted DOM of all coals. The extracted DOM of the lignites shows different oxygen class and DBE distribution than the bituminous coals. When plotting the average DBE of each oxygen class over the oxygen number, the slopes of the linear correlations are equal to the contribution that oxygen has to the DBE. In both sample types, the majority of oxygen atoms in the O₁₋₅ classes are chemically bond in hydroxyl and ether groups while more oxygen atoms are chemically bound in carboxyl and carbonyl groups in the O₉₋₁₆ classes. We used this information to modify the aromaticity index for natural DOM (AI_{mod}) to AI_{coal}. This modified parameter helps to evaluate the aromatic and aliphatic structures of oxygen-containing compounds. The higher proportions of aromatic compounds in extracted DOM of bituminous coals are in accordance with the higher aromaticity of the bituminous coals in comparison to lignites. As a summary, organofacies and coalification/maturation are the main drivers for the compositional differences found in the extracted DOM of investigated lignites and bituminous coals from New Zealand and have to be taken into account for the molecular investigation of water extracts as well as natural DOM samples from coal systems.

3.6 Acknowledgements

The financial support from the China Scholarship Council (CSC) for Yaling Zhu is gratefully acknowledged. We thank Cornelia Karger, Kristin Günther and Anke Kaminsky (GFZ Potsdam) for their excellent technical assistance in the lab.

3.7 Supplementary material



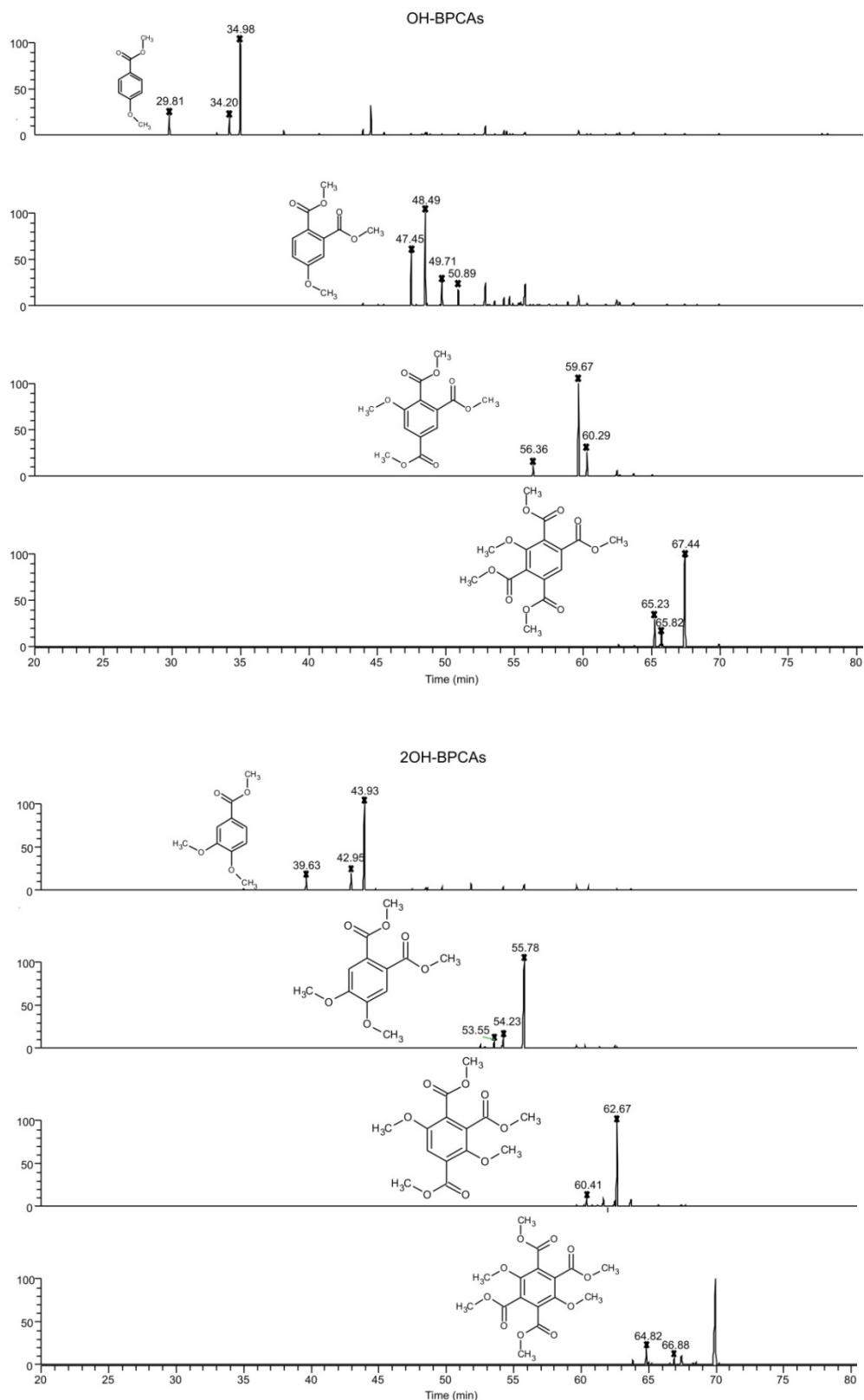
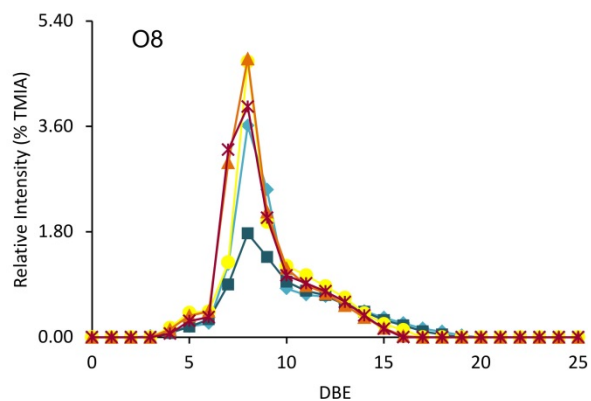
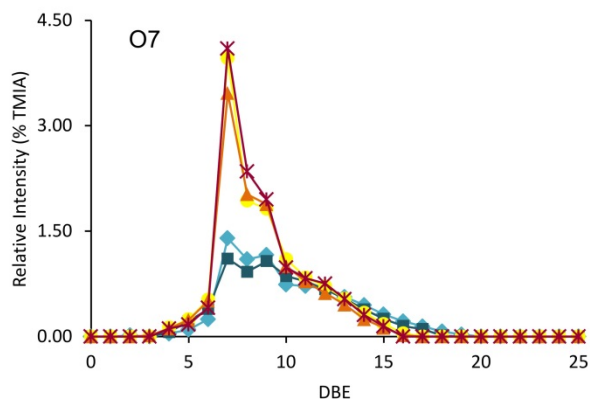
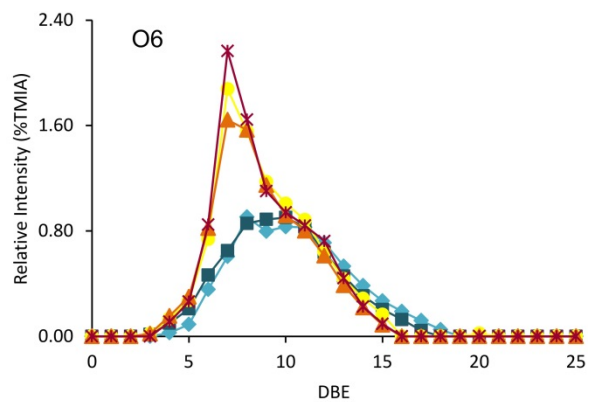
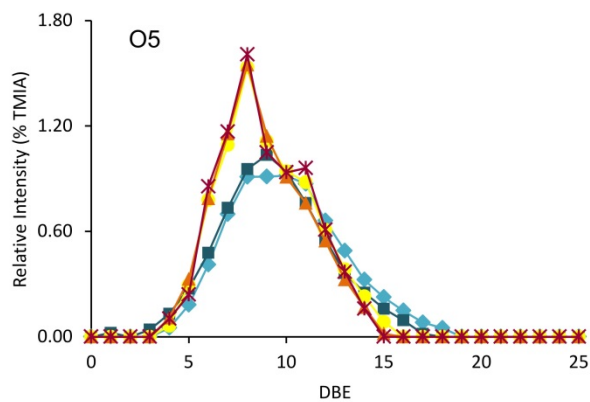
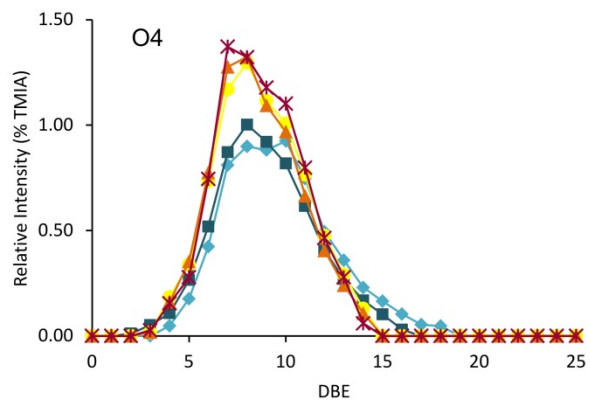
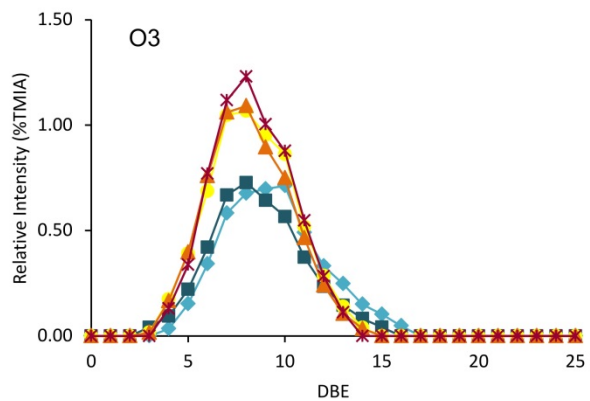
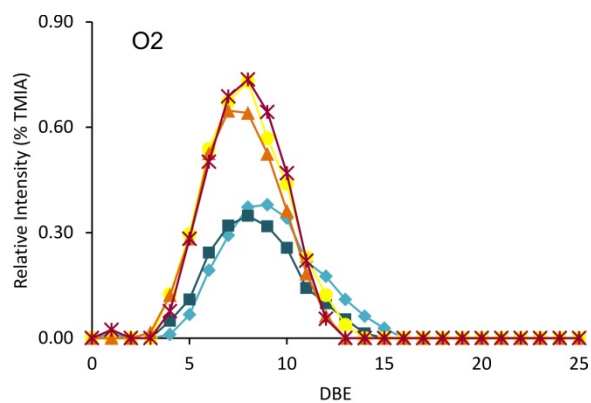
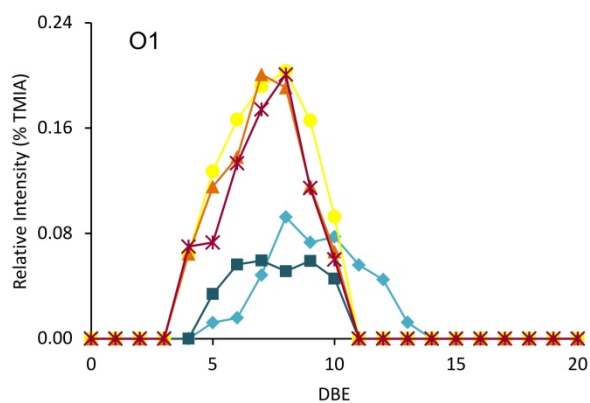


Figure S3.1. Extracted ion chromatograms of BPCAs (m/z 105 + 163 + 221 + 279 + 337 + 395), OH-BPCAs (m/z 135 + 193 + 251 + 309) and 2OH-BPCAs (m/z 165 + 223 + 281 + 339) in the extracted DOM of lignite G004541.



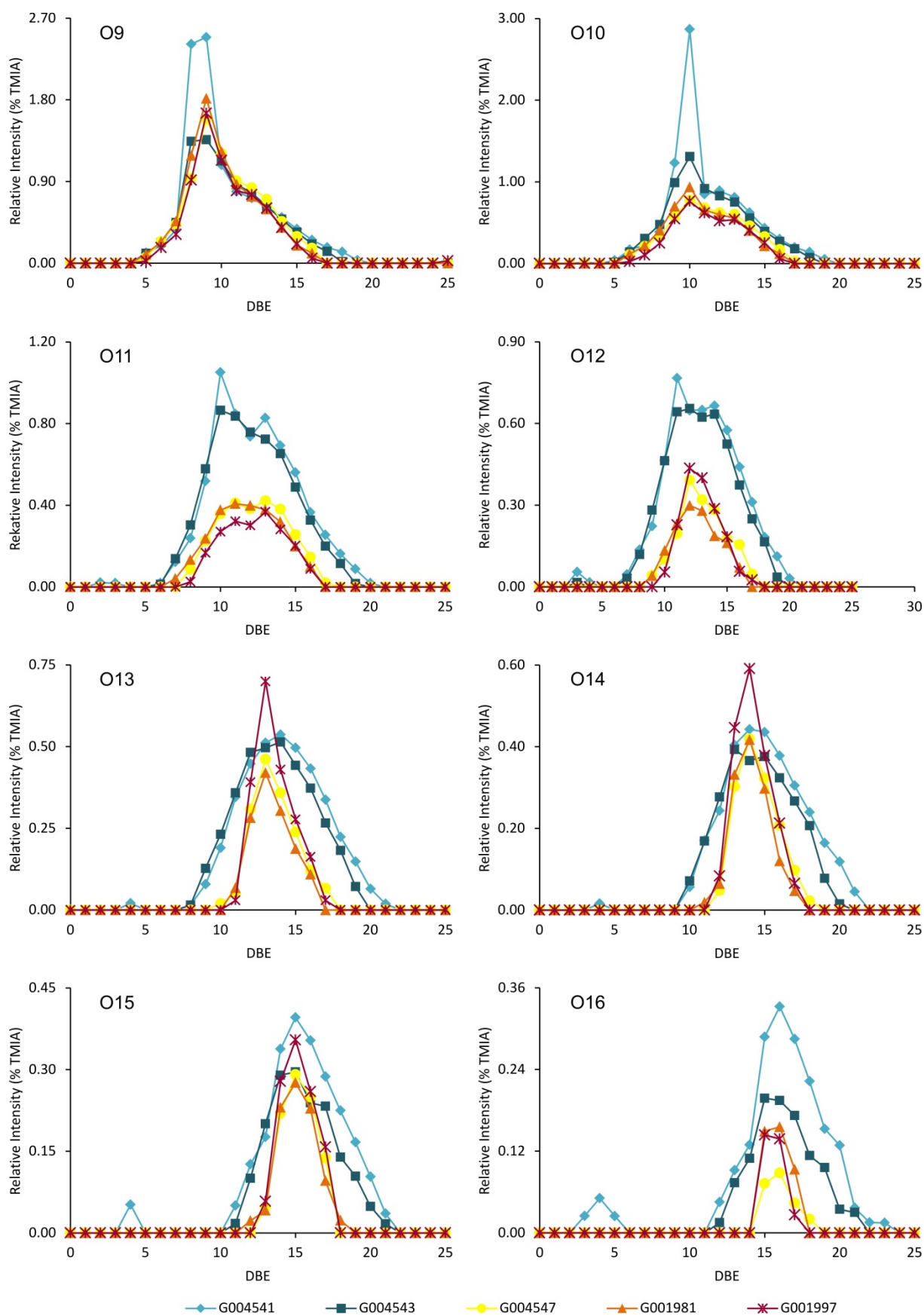


Figure S3.2. DBE distribution of the O_x classes in the extracted DOM of the coal samples.

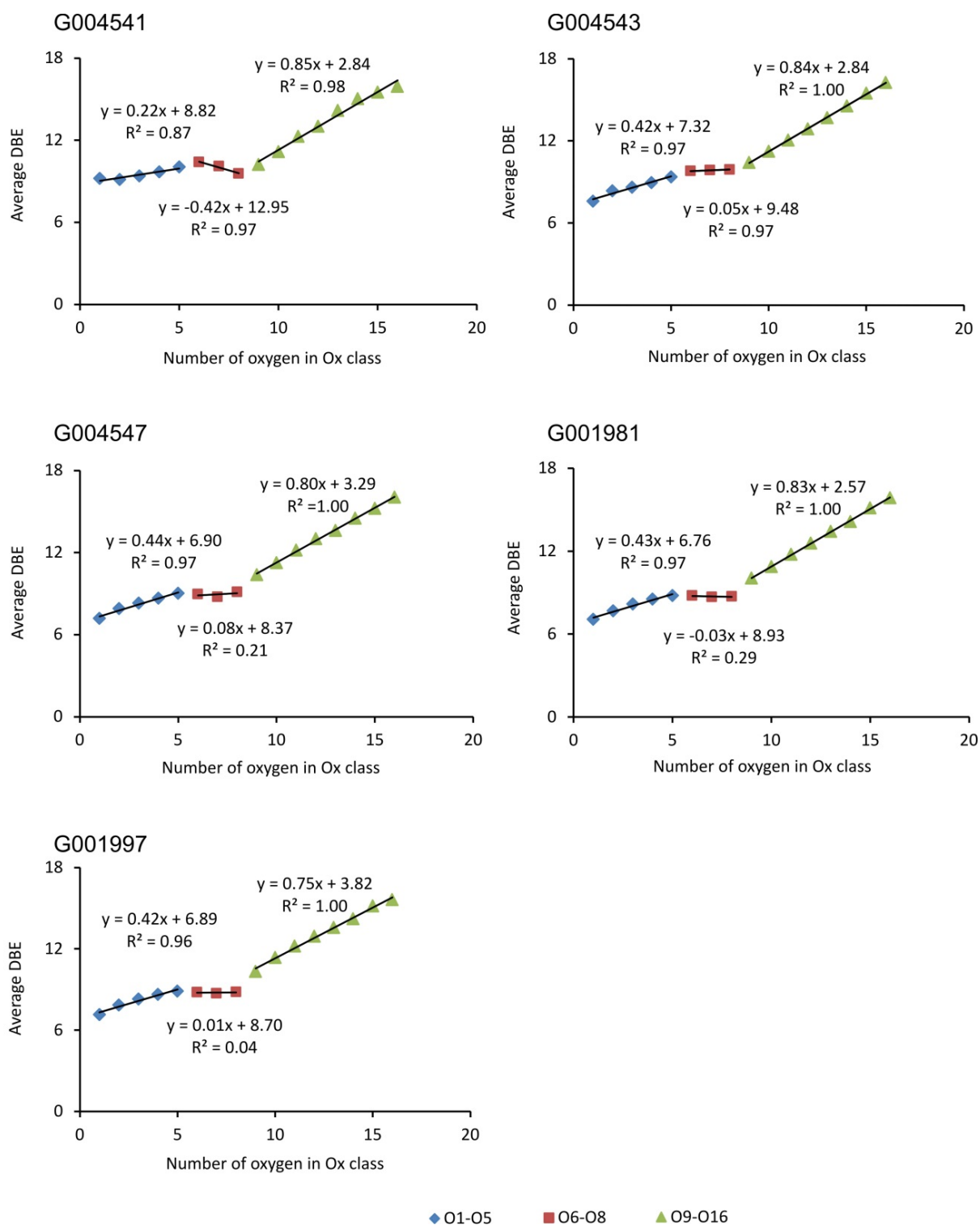


Figure S3.3. Variation of average DBE of each oxygen class. The plots are divided into three groups, O₁₋₅, O₆₋₈ and O₉₋₁₆ as indicated by different symbols.

4. MOLECULAR CHARACTERIZATION OF THE WATER-SOLUBLE ORGANIC COMPOUNDS FROM POSIDONIA SHALES USING ULTRA-HIGH RESOLUTION MASS SPECTROMETRY³

4.1 Abstract

Posidonia shale from the Hils syncline is well-known to represent an excellent natural case study for thermal maturation. Here, the maturity influence on water-soluble organic compounds released from six Posidonia shale samples was investigated by Fourier transform ion cyclotron resonance mass spectrometry (FT-ICR-MS) combined with electrospray ionization (ESI) in the negative ion mode. The changes in the distribution of elemental and compound classes, double-bond equivalents (DBE) and carbon number of the extracted dissolved organic matter (DOM) are described in detail. The general composition of extracted DOM is also compared with the organic solvent extracts of the same Posidonia samples. The differences between the water extracts of shale and coal samples with similar thermal maturity indicate that the kerogen type is a significant factor in shaping the extracted DOM composition. In the water extracts, S_1O_x class is the dominant elemental class followed by O_x class for all the six shale extracts. The relative intensities of S_1O_x classes show a normal Gaussian distribution for all the samples. However, the immature samples show the highest intensity in O_4 class and it shift to O_2 class for the mature samples and to O_5 class for the overmature samples within the O_x classes. The molecular structures of the compounds in O_x and S_1O_x classes are speculated based on their DBE and carbon number distributions. It is likely that an additional benzene ring exists in the core structure of most compounds released

³ This chapter is currently under review by co-authors and will be submitted afterwards: Zhu, Y., Vieth-Hillebrand, A., Noah, M., Poetz S., Molecular characterization of the water-soluble organic compounds from Posidonia shales using ultra-high resolution mass spectrometry.

from the mature samples. The aromaticity of the DOM increases from the immature sample to the oil window samples and then decreases for the gas window sample. Thus, thermal maturity of the original sample also shows an influence on the extracted DOM composition.

4.2 Introduction

The term “Black shale” is widely used to describe the sedimentary rock deposited in stagnant aquatic environments that usually contains a high amount of organic material and sulfides (Vine and Tourtelot, 1970). A large number of chemical reactions are involved in black shale maturation and decomposition in sediments, which promotes the release of nitrogen, sulfur and oxygen containing compounds (Tissot and Welte, 1984; Eglinton et al., 1992; Vandenbroucke and Largeau, 2007); thereby causing an increase in aromatization and condensation as well as a decrease in the degree of alkylation of the organic matter (Tissot and Welte, 1984; Schenk and Horsfield, 1998; Lis et al., 2005). When black shales are exposed to the earth’s surface or to drilling process, significant amount of inorganic and organic compounds can be released to solutions (Jaffe et al., 2002; Tuttle and Breit, 2009; Jin et al., 2013; Maguire-Boyle and Barron, 2014; Ziemkiewicz and Thomas He, 2015). Here, we conduct leaching experiments to black shales with the intent to unravel the effect of thermal evolution process of the shale organic matter on the composition of the mobile water-soluble organic fraction.

The underlying hypothesis of the study is that the leaching experiments performed in the lab can provide fundamental understanding of the mobilization of organic compounds released during water - rock reactions. In previous studies, leaching experiments were mostly applied for detection of trace elements and metals (Falk et al., 2006; Lavergren et al., 2009; Piszcz et al., 2014; Phan et al., 2018). Research on water soluble organic components primarily focused on naphthenic acids and pure hydrocarbons that have been detected by gas chromatography (GC) based analytical methods (Holowenko et al., 2002; Gordalla et al., 2013; Maguire-Boyle and Barron, 2014). However, the heterocyclic/aromatic NSO compound characterization is fundamentally necessary for investigating the organic aspect of the water extracts. The NSO-containing functional groups greatly enhance the polarity of organic compounds and therefore, the solubility of NSO containing compounds is orders of magnitude higher than those of pure aromatic hydrocarbons. For example, the aqueous solubility of phenanthrene is 1.1 mg L^{-1} while acridine has a solubility in water of 46.6 mg L^{-1} (Broholm et al., 1999).

In this study, we provide insight into the variation of water-soluble organic compounds released from a series of black shales with different maturation. Detailed investigations have shown previously that the Posidonia shale samples from the Hils Syncline are uniform with respect to organofacies and depositional environment (Littke et al., 1988; Rullkötter et al., 1988; Littke et al., 1991). The effect of thermal maturation on the composition and transformation of NSO compounds in solvent extracts and pyrolysates was shown before (Poetz et al., 2014; Mahlstedt et al., 2016). This sample sequence from the Posidonia shale may therefore be considered ideal for the investigation of maturity effects on the extracted DOM composition.

Ultra-high resolution Fourier Transform ion cyclotron resonance mass spectrometry (FT-ICR-MS) coupled with electrospray ionization (ESI) has been shown to be a powerful tool to resolve thousands of constituents in complex DOM mixture by yielding exact molecular masses (Mopper et al., 2007). Although FT-ICR-MS analysis cannot provide the exact molecular structure, the tentative structure assignment for isolated molecules has provided substantial information about DOM on the molecular level (Kim et al., 2003a; Hertkorn et al., 2006; Koch et al., 2008). ESI FT-ICR-MS has been already successfully used to characterize DOM from a wide range of environments, including terrestrial and marine aquifers (Tremblay et al., 2007; Schmidt et al., 2009; Longnecker and Kujawinski, 2011; Schmidt et al., 2011; Seidel et al., 2014; Schmidt et al., 2017; Valle et al., 2018) as well as the water column (Koch et al., 2005; Sleighter and Hatcher, 2008; Kellerman et al., 2015; Seidel et al., 2015; Gonsior et al., 2016). It has also been utilized to investigate DOM released from crude oils (Stanford et al., 2007; Ray et al., 2014; Liu and Kujawinski, 2015; Islam et al., 2016). However, to our knowledge, it has never been utilized for molecular characterization of DOM leached from black shales.

In our recent paper, the relation between concentrations of bulk extracted DOC (dissolved organic carbon) as well as concentrations of low molecular weight organic acids leached from black shales and the origin of the organic matter and its thermal maturity was presented (Zhu et al., 2015). This study will now continue this work by providing molecular insights into the composition of polar high molecular weight organic compounds in the extracted DOM of Posidonia black shales and characterizing the effect of thermal maturation of the shale organic matter on the extracted DOM.

4.3 Materials and methods

4.3.1 Geological setting and samples

Lower Toarcian Posidonia Shale is regarded as one of the most widespread and economically important petroleum source rocks of Western Europe. The black shale was deposited in a restricted epicontinental sea of moderate depth extending from the Yorkshire Basin (UK) over the lower Saxony Basin and the Southwest German Basin into the Paris Basin (Rullkötter et al., 1988; Littke et al., 1991). The depositional environment was assumed to be oxygen depleted or anoxic (Jenkyns, 1980; Littke et al., 1991; Jenkyns and Clayton, 1997). The samples investigated in this study were taken from the Lias ϵ level of the Lower Toarcian Posidonia Shales in the Hils Syncline of Lower Saxony Basin, Northern Germany. The same six samples from the wells Wenzen (WE), Wickensen (WI), Dielmissen (DI), Dohnsen (DO), Harderode (HAR), and Haddessen (HAD) as investigated by Poetz et al. (2014) and Mahlstedt et al. (2016) were chosen for this study. Bulk source rock characterizations of the six samples are summarized in Table 4.1. The samples cover a maturity range from immature to overmature with vitrinite reflectance values and T_{\max} values increasing from 0.48% to 1.45% and 423°C to 457°C, respectively. Accordingly, the hydrogen index values (HI) decrease from 663 to 77 mg HC/g TOC and the total organic carbon contents decrease from 13.4% to 6.9% with increasing maturity. However, the total sulfur (TS) contents of the samples are variable and no direct relationship between the TS content and the maturity of the samples can be observed.

Table 4.1. Bulk source rock characterization of the Posidonia Shale samples from six boreholes in the Hils Syncline, Northern Germany^a.

Borehole	Wenzen	Wickensen	Dielmissen	Dohnsen	Harderode	Haddessen
Abbreviation	WE	WI	DI	DO	HAR	HAD
R_o (%)	0.48	0.53	0.68	0.73	0.88	1.45
T_{\max} (°C)	423	427	438	445	444	457
HI (mg HC/g TOC)	663	617	574	429	363	77
TOC (%)	12.2	13.4	8.1	9.4	6.3	6.9
TS (%)	3.44	2.79	3.08	2.35	4.81	5.45

^aDate are average values for a different number of samples per well from Rullkötter et al. (1988) (WI, DI, HAR, HAD) and Wilkes et al. (1998) (WE, DO). R_o : vitrinite reflectance. T_{\max} : temperature

of the maximum hydrocarbon generation from kerogen cracking during pyrolysis. HI: hydrogen index. TOC: total organic carbon content.

4.3.2 Sample preparation for FT-ICR-MS analysis

Sample preparation for FT-ICR-MS analysis, mass calibration and data analysis were described in detail in Zhu et al., (submitted). In brief, 10g ground shale samples were extracted with 125ml deionized water at 100°C and atmospheric pressure for 48 hours. After filtration, DOM was isolated and concentrated by solid phase extraction (SPE) with Bond Elut-PPL cartridges (1 g sorbent, 6ml cartridge; Agilent Technologies, Germany) according to the protocol published by Dittmar et al. (2008). Finally, the DOM was eluted from the cartridge with methanol and dried under N₂ atmosphere and stored at -24°C in the dark until further analysis. A procedural blank was conducted with ultra-pure water to check for possible contaminations during water extraction and SPE procedures.

4.3.3 FT-ICR-MS analysis

DOM samples were analyzed on a 12 Tesla solarix FT-ICR mass spectrometer equipped with an Apollo II ESI ion source, both from Bruker Daltonik GmbH (Bremen Germany). Each sample was dissolved in methanol to produce a 1 mg/mL solution for, to which a concentrated aqueous NH₃ solution was added (10 µL/mL sample solution) in order to facilitate the deprotonation of the sample constituents. Samples were then fused with the Apollo II electrospray source in the negative mode at a flow rate of 150 µL/h using a syringe pump. The capillary voltage was set to 3000 V and an additional CID (collision-induced dissociation) voltage of 70 V was applied in the source to avoid cluster and adduct formation. Nitrogen was used as drying gas at a flow rate of 4.0 L/min and a temperature of 220 °C and as nebulizing gas at 1.4 bars. Spectra were recorded in broadband mode using 4 mega word data sets. Ions were accumulated in the collision cell for 0.05 s and transferred to the ICR cell within 1 ms. For each mass spectrum, a number of 200 scans were accumulated in a mass range from m/z 150 to 1000 Da.

4.3.4 Mass Calibration and Data Analysis

External calibration was performed using an in house calibration mixture containing fatty acids and polyethylene glycol sulfates. Internal recalibration was performed using known homologous series and a quadratic calibration mode. Elemental formulae were assigned to the recalibrated m/z values with a maximum error of 0.5 ppm allowing 0 -100 C, 0

- 200 H, 0 - 30 O, 0 - 2 N, and 0 - 2 S atoms. Only single negative charged species were found in the spectra; m/z and mass thus are used synonymously in this study. Data evaluation was done with the software packages Data analysis 4.0 SP5 (Bruker Daltonik GmbH, Germany). Molecular formulae were classified in different classes according to the type of heteroatoms (elemental class), to the number of heteroatoms (compound classes) and to the number of double bond equivalent (DBE) (DBE class). For a given compound, $C_cH_hN_nO_oS_s$, the DBE was calculated according to the formula $DBE = c - h/2 + n/2 + 1$. The DBE is a measure for the degree of unsaturation and expresses the number of double bonds and/or rings (Poetz et al., 2014).

4.4 Results and discussion

4.4.1 General composition of DOM in aqueous shale extracts

4.4.1.1 ESI Negative Mass Spectra

The ESI broadband mass spectra of the water extracts from the Posidonia shales are shown in Figure 4.1. The mass spectra of the samples are dominated by peaks with odd nominal masses attributed to O_xS_z containing compounds by their exact masses. For the water extracts of the immature ($R_o = 0.48-0.53\%$) and mature samples ($R_o = 0.68-0.88\%$), between 2300 and 3000 monoisotopic peaks have been assigned and the number decreased to 1125 for the overmature sample ($R_o 1.45\%$). In general, decreasing number of assigned monoisotopic peaks with increasing maturation has been reported for both the solvent extracts (Poetz et al., 2014) and the pyrolysates (Mahlstedt et al., 2016) of the same samples. The total number of assigned monoisotopic peaks is highest in the solvent extracts (4635 – 2307), followed by water extracts and pyrolysates (3253 – 254). The weight-average molecular weight (M_w) and number-average molecular weight (M_n) of the assigned peaks ranges from m/z 310-349 (M_w) and m/z 293-334 (M_n) (Fig. 4.1), which tends to be slightly lower than the calculated average molecular weights of the solvent extracts (Poetz et al., 2014) and the pyrolysates (Mahlstedt et al., 2016). This indicates that the hydrophilic compounds have a lower molecular weight than the lipophilic compounds within the labile organic matter of the Posidonia shales.

Four peaks with high relative abundance are marked with cycles in the spectra (Fig. 4.1). These are anions $C_{16}H_{25}O_3S^-$ (m/z 297.1530), $C_{17}H_{27}O_3S^-$ (m/z 311.1686), $C_{18}H_{29}O_3S^-$ (m/z 325.1843) and $C_{19}H_{31}O_3S^-$ (m/z 339.1999) in S_1O_3 class and they have 4 DBEs. It is very likely that these compounds are linear alkylbenzene sulfonic acids (LAS), which belong to the

common groups of anionic surfactants (Lara-Martín et al., 2010; Melendez-Perez et al., 2016). The total relative intensities of the four peaks correlate with the volume of the water extracts used for SPE (Fig. S4.1). These volumes were determined with respect to the known concentrations of DOC in the water extracts to prevent overloading of SPE. As these four formulae were not detectable in the spectrum of the blank sample these compounds might be introduced into the samples already before the water extractions. Therefore, these four formulae were excluded from the mass list.

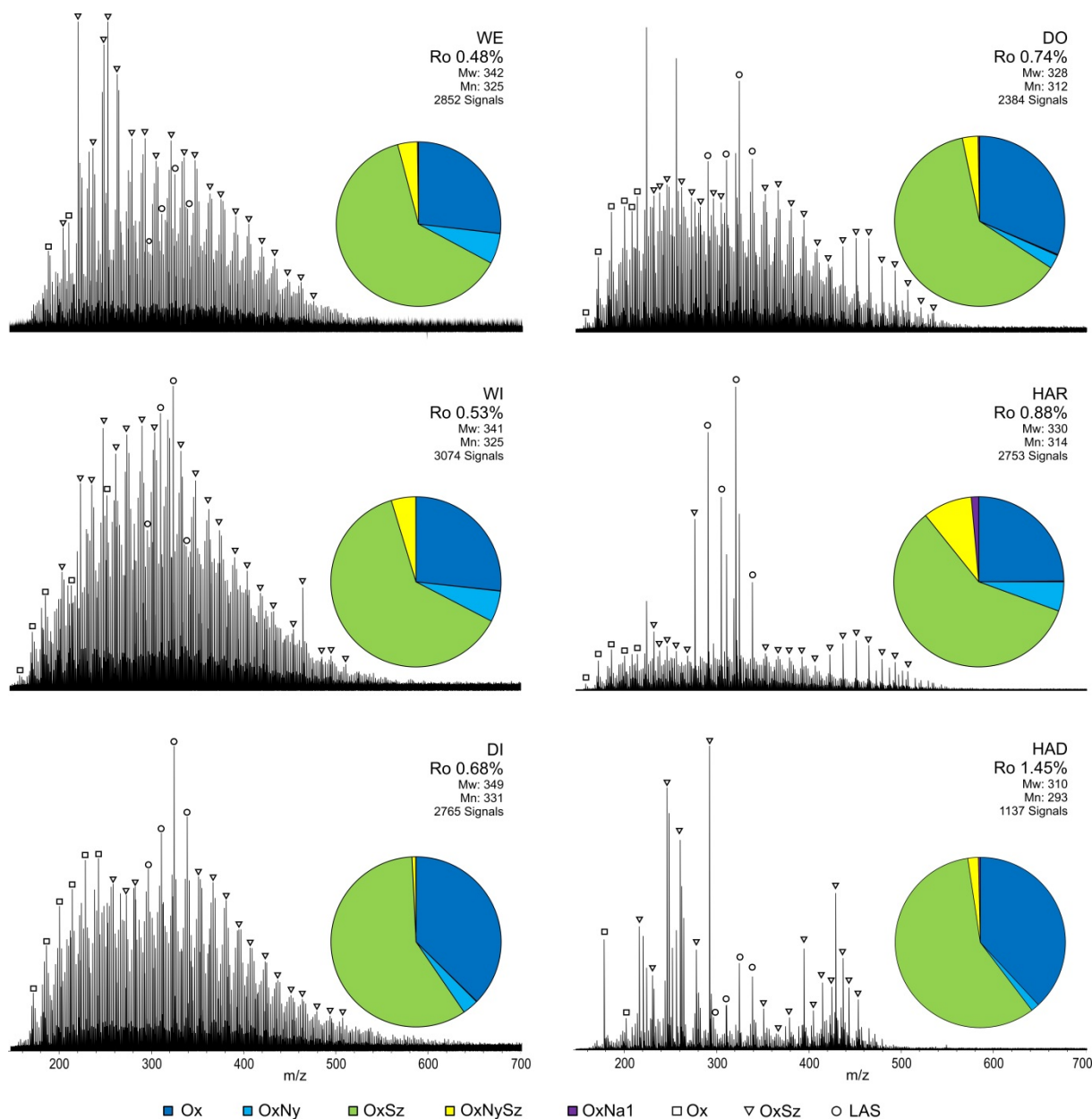


Figure 4.1. Broadband negative ion ESI FT-ICR mass spectra of water extracts DOM of the six Posidonia shale samples with increasing maturity (as indicated by the R_0 values). The pie charts

display the elemental class distribution. Symbols refer to different elemental classes. O_xS_z compounds are depicted with triangles, O_x compounds with squares. LAS compounds are indicated by open circles.

4.4.1.2 Van Krevelen diagrams

To extend the observations, the entire datasets for the water extracts were analyzed with Van Krevelen diagrams, namely, a plot of H/C vs. O/C atomic ratio (Kim et al., 2003a). Van Krevelen diagrams are based upon the elemental ratios of individual formula and do not include the relative peak height information. To simplify the comparison, compounds were divided into four groups with the O/C ratio of 1 and the H/C ratio of 0.5 as limit values (Zhu et al., submitted). The Van Krevelen diagram for the extracted DOM of the WI shale is shown in Fig. 4.2a. The Van Krevelen plots for all extracted DOM of the immature and mature shales were quite similar (Fig. S4.2). Though the extracted DOM of the overmature shale only consists of a low number of assigned formulas, the DOM disperses in the similar area as extracted DOM of the other samples. Most molecular formulas belong to groups I and II with a dominance of lignin-like components. The Van Krevelen diagram of extracted DOM from shale WI is quite different to that of the New Zealand coal with comparable thermal maturity (Fig. 4.2a, 4.2b). The extracted DOM of the coal shows a high abundance of condensed aromatic-like formulas. There is a shift to lower H/C and higher O/C ratios from the shale extract to the coal extract. Similar trends were observed in other studies by comparing DOM from offshore and onshore environments (Sleighter and Hatcher, 2008; Schmidt et al., 2009), or by comparing marine DOM and terrigenous DOM (Koch et al., 2005). The variations in the oxygen and hydrogen content in the different DOM samples are likely linked to the compositional difference of the extracted organic matter. The Posidonia shale organic matter is derived from phytoplankton-derived alginite and bituminite particles (Littke et al., 1991) with high amount of aliphatic compounds. This is reflected in lower O/C and higher H/C ratios. The extracted DOM of the coal is more oxygenated and contains less hydrogen, which is related to the higher aromaticity of the terrestrial organic matter due to the high input of lignins or tannins. The Van Krevelen diagram for the solvent extract from the same shale WI is much condensed with very low O/C values compared to the water extract (Fig. 4.2a, 4.2c). This indicates that plenty of molecular formulas in the water extract contain more oxygen atoms compared to the solvent extract. High amounts of oxygen containing functional groups are likely to exist in extracted DOM as these functional groups promote the polarity and aqueous solubility of the organic compounds. In contrast, the compounds in the solvent extract with low content of oxygen atoms are unpolar and lipophilic.

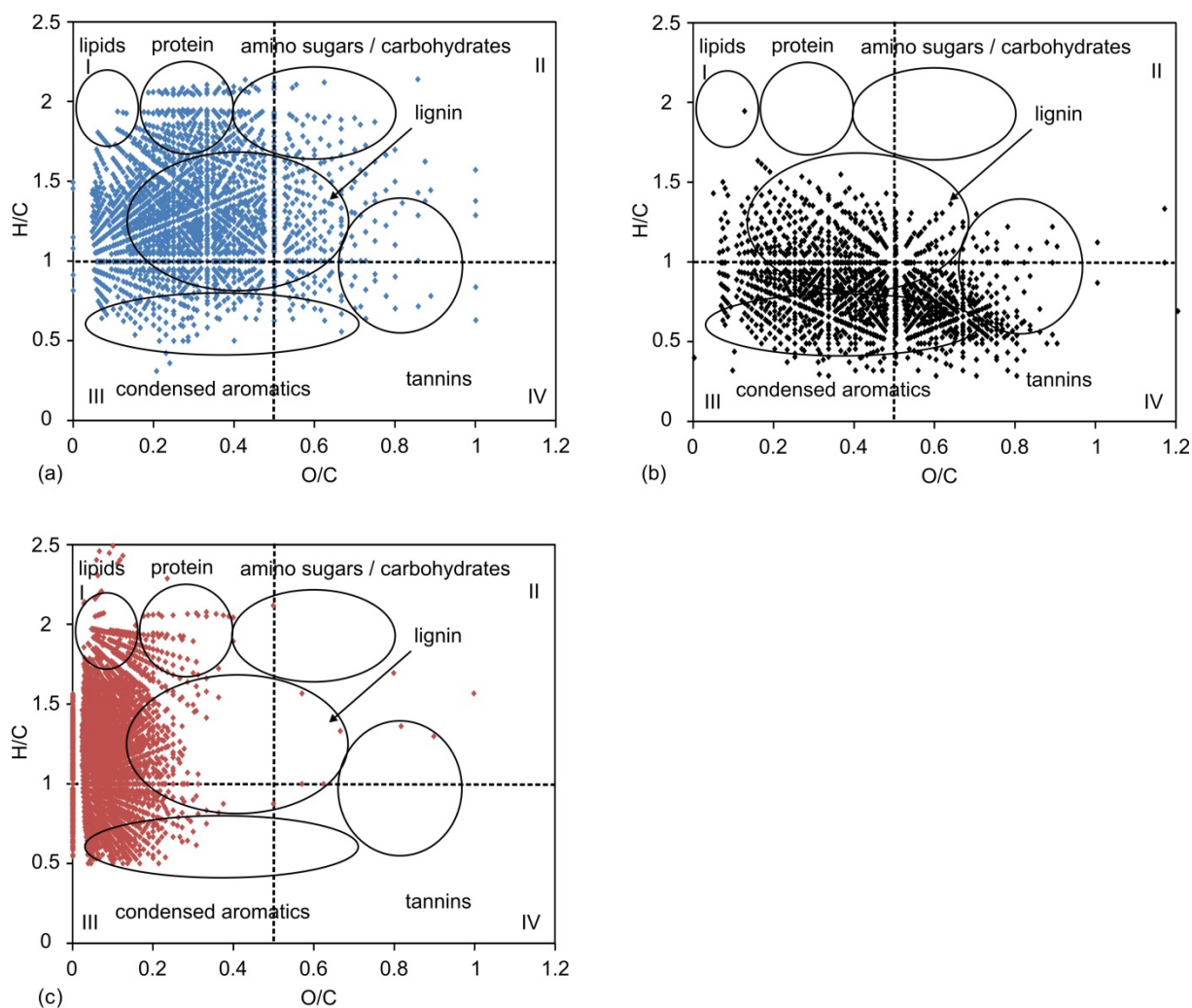


Figure 4.2. Van Krevelen diagrams comparison for (a) all formulae observed in DOM of water extracts from black shale WI, $R_o = 0.53\%$, (b) formulae observed in DOM of water extracts from a New Zealand coal sample, $R_o = 0.52\%$, (c) formulae observed in DOM of solvent extracts from the same black shale WI. Ellipses indicate elemental ratios consistent with compound classes listed (Sleighter and Hatcher, 2007; Hockaday et al., 2009). The compounds are divided into four groups according to the O/C and H/C values (I: $H/C > 1$ and $O/C < 0.5$ including lipids, proteins and part of the lignins, II: $H/C > 1$ and $O/C > 0.5$ including amino sugars, carbohydrates and part of the tannins, III: $H/C < 1$ and $O/C < 0.5$ including condensed aromatics and part of the lignins and IV: $H/C < 1$ and $O/C > 0.5$ including partly condensed aromatics and tannins).

4.4.2 Elemental Class Distribution

The elemental class compositions of the Posidonia shale extracts (illustrated with pie charts in Figure 4.1, data in Table 4.2 reveal a predominance of O_xS_z class followed by oxygen containing compounds (O_x). These two elemental classes comprise roughly 80-95% of the total monoisotopic ion abundance (TMIA) for all the six shale extracts at different thermal

maturity stages. They have also been reported to largely exist in the water impacted by oil (Headley et al., 2011; Islam et al., 2016). No systematic variation trend of the relative intensities for O_xS_z class and O_x class can be observed with increasing maturation of the original shale samples. However, in the solvent extracts, the relative intensities of species in O_xS_z class and O_x class decrease with increasing maturity (Poetz et al., 2014). The abundances of the O_xN_y class and $O_xN_yS_z$ class in the DOM are quite low between 1.6 to 6% and 0.7 to 9.4% TMIA, respectively. In contrast, the relative abundances of O_xN_y class are much higher in the solvent extracts (Poetz et al., 2014). Another obvious difference in elemental class composition is the dominance of the N_y class in the solvent extracts and the pyrolysates of the Posidonia shales (Poetz et al., 2014; Mahlstedt et al., 2016), but this elemental class is completely missing in the water extracts.

Table 4.2. General characterization of the ESI FT-ICR mass spectra for extracted DOM of Posidonia shale samples^a.

Sample	No. of signals					TMIA (%)			
	Total	O_x	O_xN_y	O_xS_z	$O_xN_yS_z$	O_x	O_xN_y	O_xS_z	$O_xN_yS_z$
WE	2852	784	318	1525	215	26.7	6.0	63.1	3.9
WI	3074	850	340	1617	567	26.7	5.9	62.7	4.7
DI	2765	1047	191	1478	46	37.3	3.0	58.8	0.7
DO	2384	770	144	1324	136	31.4	2.6	62.5	3.0
HAR	2753	706	258	1427	354	24.8	5.6	58.7	9.4
HAD	1125	518	39	523	45	38.1	1.6	58.0	2.0

^aNumber of signals: number of assigned, monoisotopic signals. TMIA: total monoisotopic ion abundance.

It is obvious that the water soluble organic compounds cover a different but new analytical window of the labile organic matter compared to the solvent extracts. As mentioned before, the differences between the solvent extracts and water extracts of the same samples are strongly related to the physico-chemical properties of the organic substances. The octanol-water partition coefficient, $\log K_{ow}$, is a widely used parameter that can provide a measure of the lipophilic vs. hydrophilic behavior of a compound (Meylan et al., 1996). A higher $\log K_{ow}$ value indicates higher hydrophobicity and hence lower aqueous solubility. In general, $\log K_{ow}$ values tend to be large for compounds with extended non-polar structures (such as long chain or multi-ring hydrocarbons) and small for polar compounds. Additionally, the heteroatom content in the polar compounds, the molecular mass and carbon numbers also have a significant impact on $\log K_{ow}$ (Liu and Kujawinski, 2015). The higher number of heteroatoms

and the lower M_w and M_n values of the extracted DOM compared to the solvent extracts are indicative for low $\log K_{ow}$ and with this favored partitioning to the aqueous phase.

4.4.3 Compound class distribution

O_x class and O_xS_z class are the most important elemental classes as they comprise most of the TMIA (Fig. 4.1, Table 4.2). The O_xS_z class consists of O_xS_1 and O_xS_2 compounds. The O_xS_1 classes have higher relative intensities (49-60% TMIA) than the O_xS_2 classes (2.5-9.6% TMIA) at the different maturity levels (Fig. S4.3). Therefore, this study is focusing on the compound class distributions of O_x class and O_xS_1 class.

Figure 4.3 illustrates the changes in relative intensity of oxygen containing compound classes with the increase in oxygen number. The O_1 to O_8 classes are present in all extracted DOM samples at all maturity levels, but O_9 class is absent at peak oil window (DO) and late oil window (HAR) and compounds with up to 12 oxygen atoms were only released from overmature sample (HAD). In general, the intensities of the oxygen classes show a continuous increase to the highest value and then decrease gradually. Interestingly, water extracts of the two immature samples show the highest intensity at O_4 class, the three extracted DOM from mature samples are featured with highest values at O_2 class whereas the extracted DOM of the overmature sample is characterized by the highest intensity at O_5 class. The composition of extracted DOM from coal samples with comparable low maturity has also been reported before (Zhu et al., submitted). The oxygen classes in the coal extracts are featured by high abundance of O_8 class and with maximum oxygen numbers up to 16. The oxygen class distribution differences between the shale and coal extracts are related to the different sources of organic matter. Higher OI value of the coal samples than the shale samples have been shown before (Zhu et al., 2015). In the solvent extracts of the same Posidonia shales, O_2 class is the most abundant O_x class for all samples irrespective of maturity (Poetz et al., 2014). This clearly indicates that the water soluble organic compounds derived from shales are not similar to the solvent extracts, as the partitioning into the aqueous phase is governed by compound-specific physio-chemical properties. Although the relative intensity of the O_5 class in DOM of the overmature sample HAD is the highest among the six extracts, the absolute intensity is the lowest one. The relatively high intensities of $O_{>5}$ classes for the overmature sample might be an indication of oxidation processes that are related to the influence of hydrothermal brines to the Haddessen well samples, the brines may favor the formation of oxygen-containing compounds (Bernard et al., 2012; Zhu et al., 2015). However,

the pyrolysates of the overmature sample shows extraordinarily high intensity of O₂ class (Mahlstedt et al., 2016), which might be due to the dehydration and decarboxylation of the multi-oxygen containing compounds during the pyrolysis at high temperature (Derenne et al., 1990).

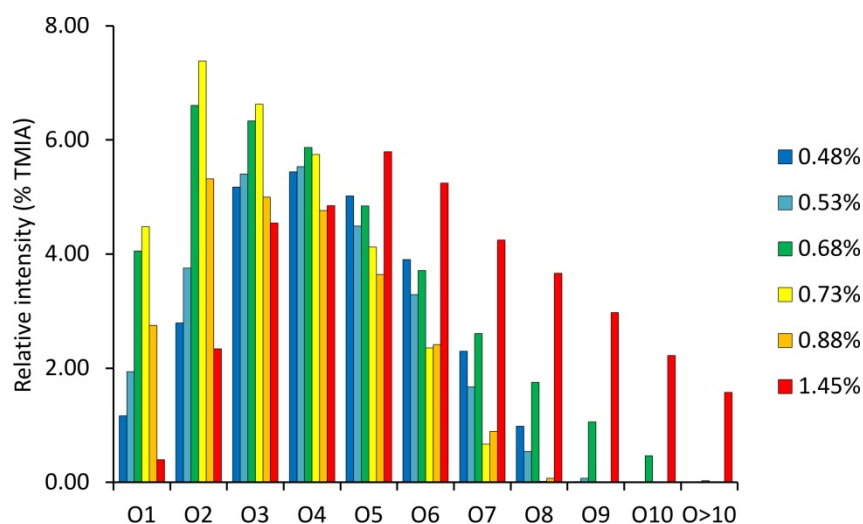


Figure 4.3. Relative intensities of the different O_x classes in DOM of the Posidonia shale extracts.

The relative intensities of S₁O_x classes in extracted DOM of Posidonia shales were shown in Figure 4.4. For all the extracted DOM samples, S₁O_x containing compounds have relative abundance between 47.5 and 60.0% TMIA. This high abundance is probably related to the high sulfur amount of the original shale samples (Table 4.1). High dissolved organic sulfur (DOS) content has been reported in pore water of anoxic coastal sediments before, which is enriched in H₂S and reduced sulfur species (Schmidt et al., 2009; Schmidt et al., 2014; Seidel et al., 2014). Also, around 10% TMIA S₂O_x containing compounds have been detected in the DOM of a New Zealand lignite sample, which contains lower amount of sulfur than the shale samples (Zhu et al., submitted). Sulfur can be covalently and unselectively bound to DOM via sulfurization reactions (Pohlabein et al., 2017), these may also happen during water-rock interactions..

The majority of S₁O_x containing compounds are distributed in a normal Gaussian profile with maxima in class S₁O₅ or S₁O₆ (Fig. 4.4), indicating a direct relationship of similar origin and precursor structure of these compounds. Probably the thermal maturity of the original shale samples cannot be reflected in the relative intensity variations of different S₁O_x classes in water extracts. In the solvent extracts, the relative abundances of S₂O_x containing

compounds decrease with increasing maturity of the original samples and remain at minor amount after entering the oil window (Poetz et al., 2014). It is obvious that the S_zO_x containing compounds in the water extracts and the solvent extracts show different characteristics.

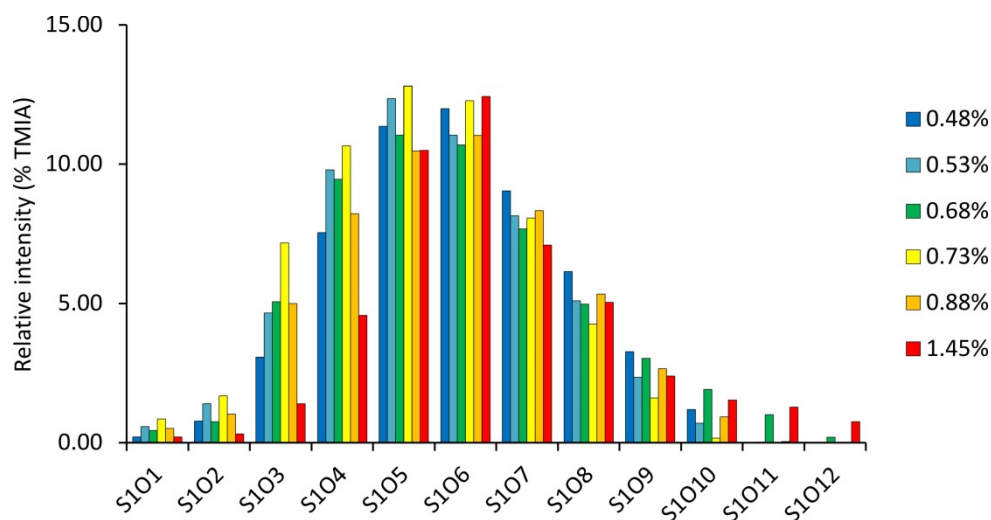


Figure 4.4. Relative intensities of the different S_1O_x classes in DOM of Posidonia shale extracts.

4.4.4 Detailed characterization of selected compound classes

In the following sections, the O_{1-6} and S_1O_{3-8} classes are described in detail as they show much higher intensities compared to other compound classes (Fig. 4.3, Fig. 4.4). These compound classes are described with respect to its DBE and carbon number distributions.

4.4.4.1 O classes

The DBE distributions of the selected O_{1-6} classes of the six shale water extracts are illustrated in Figure 4.5. With increasing number of oxygen atoms the range in DBE values is enlarged slightly. Generally, the extracted DOM of the two immature samples (WE and WI) shows quite similar DBE distribution in each oxygen class but is different to the DBE distribution of the extracted DOM from of the three oil window samples (DI, DO and HAR). The extracted DOM of the gas window sample (HAD) shows a narrow DBE range and is very different from other samples. The observed changes in the oxygen class distribution of the six sample extracts indicate that the generation and expulsion of hydrocarbons in the shales influence the composition of O-containing compounds in extracted DOM.

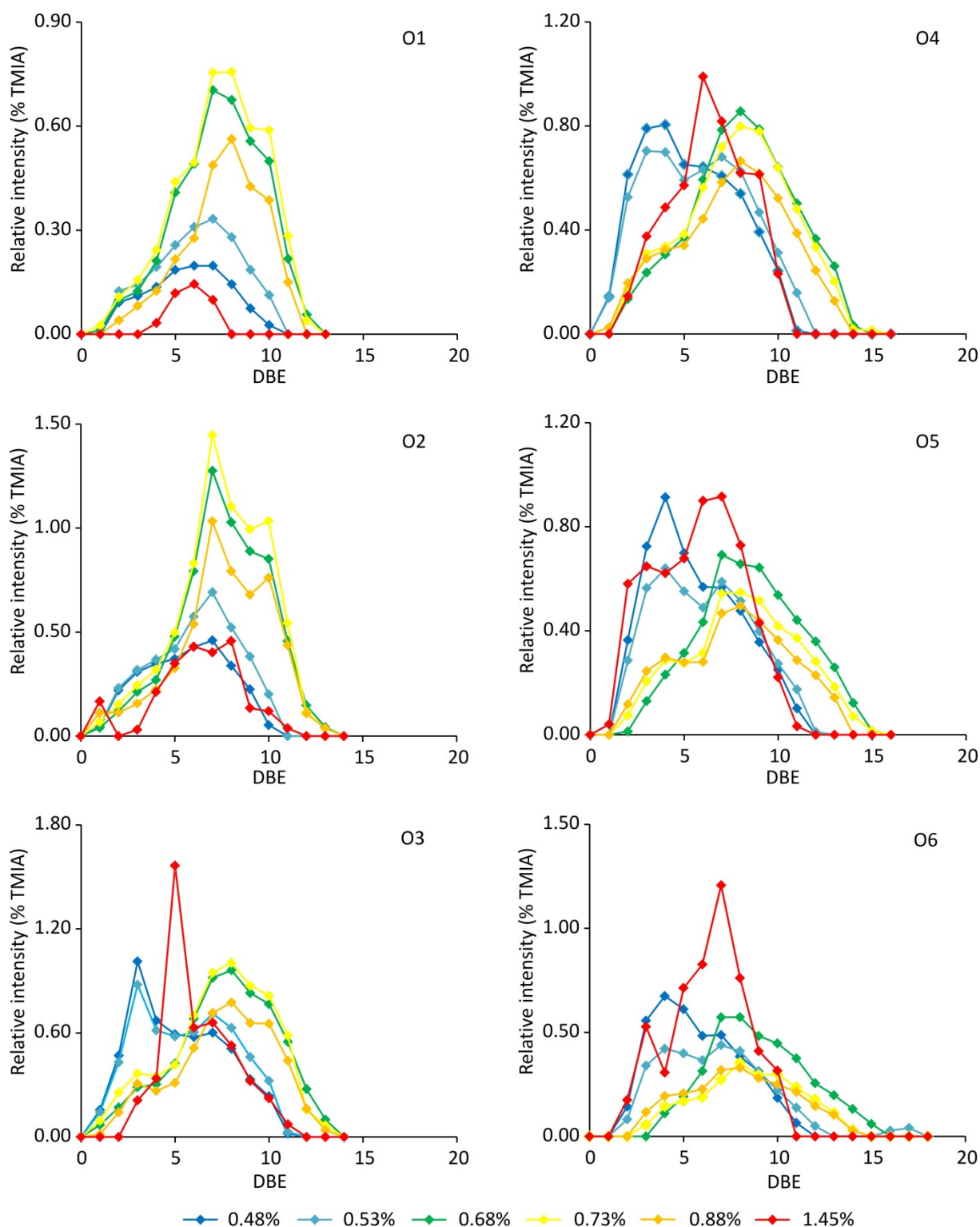


Figure 4.5. DBE distribution of the O_{1-6} classes in the DOM of Posidonia shale extracts.

In O_1 and O_2 classes, the formulas are spread over a DBE range from 1 to 12 and exhibit a more or less unimodal distribution for the six extracts (Fig. 4.5). DBE distribution show maximum at DBE 7 for extracted DOM from immature shales (0.48 - 0.53% R_o) and at DBE 7, 10 (compared to 11) at oil window (0.68-0.88% R_o) with the exception of the sample HAR

(0.88% R_o) showing DBE maxima of 8 in O_1 class. The extracted DOM of the gas window sample (1.45% R_o) shows maximum at DBE 6 for O_1 class and DBE 8 for O_2 class. In O_1 class, less than 25 carbon atoms can be observed in all detected formulas. The carbon number distributions of compounds with DBE 7 and DBE 10 in O_1 class range from 12 to 21 and 14 to 24, respectively (Fig. 4.6). It has been reported that steroidal compounds mainly show carbon numbers between 27 and 29 with the predominance of C_{27} homologues for marine sourced oils (Mackenzie et al., 1982). The hopanoid compounds normally contain 28-36 carbon atoms (Watson and Farrimond, 2000; Poetz et al., 2014). Regardless of the water solubility, the steroidal and hopanoid compounds with four and five naphthenic rings should not be involved in the DOM of O_1 classes due to their high number of carbon atoms. It has been reported that the acyclic saturated compounds show water solubility 1 to 3 orders of magnitude lower than the aromatic hydrocarbons with the similar molecular weight due to the higher polarity of aromatic compounds (Wilkes and Schwarzbauer, 2010). The O_1 species could consist of compounds with a hydroxyl functional group that can be deprotonated (Oldenburg et al., 2014). The species with DBE of 5 and 6 are thought to be indanols and indenols (Pan et al., 2013), while those with DBEs of 7 and 10 could probably be compounds like hydroxyl naphthalene and hydroxyl anthracene, respectively.

In O_2 class, the species with DBE 1 show high relative abundance at carbon numbers 16 and 18, which are mostly corresponding to hexadecanoic acid ($C_{16}H_{32}O_2$) and octadecanoic acid ($C_{18}H_{36}O_2$) (Fig. 4.7a). As the most common fatty acids in nature, the two acids might be artificially introduced into the samples during the sampling processes (Shi et al., 2010a; Shi et al., 2010b; Zhang et al., 2011; Liu et al., 2015). The possible core structure for O_2 compounds with DBE 5 and 6 might be aromatic acids and diols with 1 or 2 additional naphthenic rings (Zhang et al., 2011). The compounds with DBE 10 have a carbon number range from 13 to 24 while those with 13 to 17 carbon atoms are more prominent in the extracted DOM of the oil window samples (Fig. 4.7e). Possible chemical core structures are fluorine-9-carboxylic acid, 2-hydroxy-fluorene-9-one and anthracene-9, 10-diol (Fig. S4.4). As the fluorine-9-carboxylic acid shows the lowest calculated $\log K_{ow}$ value among the three compounds, it is more likely to be part of the extracted DOM. The O_2 class with DBE 7 is the most abundant DBE class for all extracted DOM from immature and mature samples showing a carbon number range from 10 to 23. Relatively high intensity can be observed for the compounds with 11 to 17 carbon atoms (Fig. 4.7d). Since an additional benzene ring attached to the original aromatic core is related to an increase in DBE by 3, the core structure of compounds in O_2 DBE 10 class might

contain an additional benzene ring compared to the core structures of compounds in O₂ DBE 7 class.

Unlike the O₁₋₂ classes, the relative intensities of the O₃₋₆ classes with different DBE values display bimodal distributions for both immature and mature samples (Fig. 4.5). In O₃₋₆ classes, the extracted DOM from the two immature samples is characterized by prominent intensities at DBE 3 or 4 and a shoulder at DBE 7. In contrast, the extracted DOM of the three oil window samples exhibits the highest intensities at DBE 7 or 8 and a shoulder at DBE 3 or 4 for different oxygen classes. The extracted DOM of the overmature sample shows very different DBE distribution pattern with highest intensity at DBE 5 to 7. From immature to oil window samples, the relative abundance of the compounds with low number of DBEs decreases and the relative abundance of the compounds with higher number of DBEs increases. The variation is indicative of an increased degree of condensation and aromatization of the extracted DOM with increasing maturation of the original samples. As carboxyl and carbonyl functional groups both may contribute to the DBE, it is difficult to deduce the molecular structure of the detected compounds in the O₃₋₆ classes. However, using the carbon number distributions, we can speculate that the compounds in O₃ class with DBE 3 might be attributed to hydroxylated fatty acids with two naphthenic rings or polyols with three naphthenic rings (Fig. 4.8). Compounds in O₄ class with DBE 3 and 4 could be hydroxylated fatty acids or dicarboxylic acids with naphthenic rings. The O₄ class with DBE 4 might also consist of polyols with phenol or a benzene ring. With increasing number of oxygen atoms involved in the molecular formula, the number of possible structures increases. As the compounds with DBE 3 (4) and 7 (8) in each oxygen class show quite similar range in carbon number distributions (Fig. 4.8, Fig. 4.9), it can be speculated that the molecular structure of the compounds with DBE 7 (8) contains similar oxygen containing functional groups as the molecular structures of compounds with DBE 3 (4) plus one additional benzene ring.

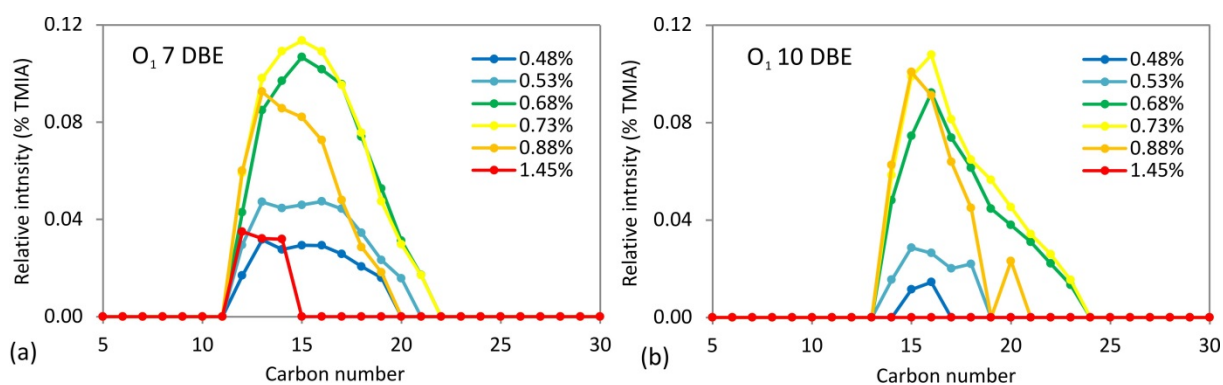


Figure 4.6. Carbon number distribution of O_1 class with 7 and 10 DBEs.

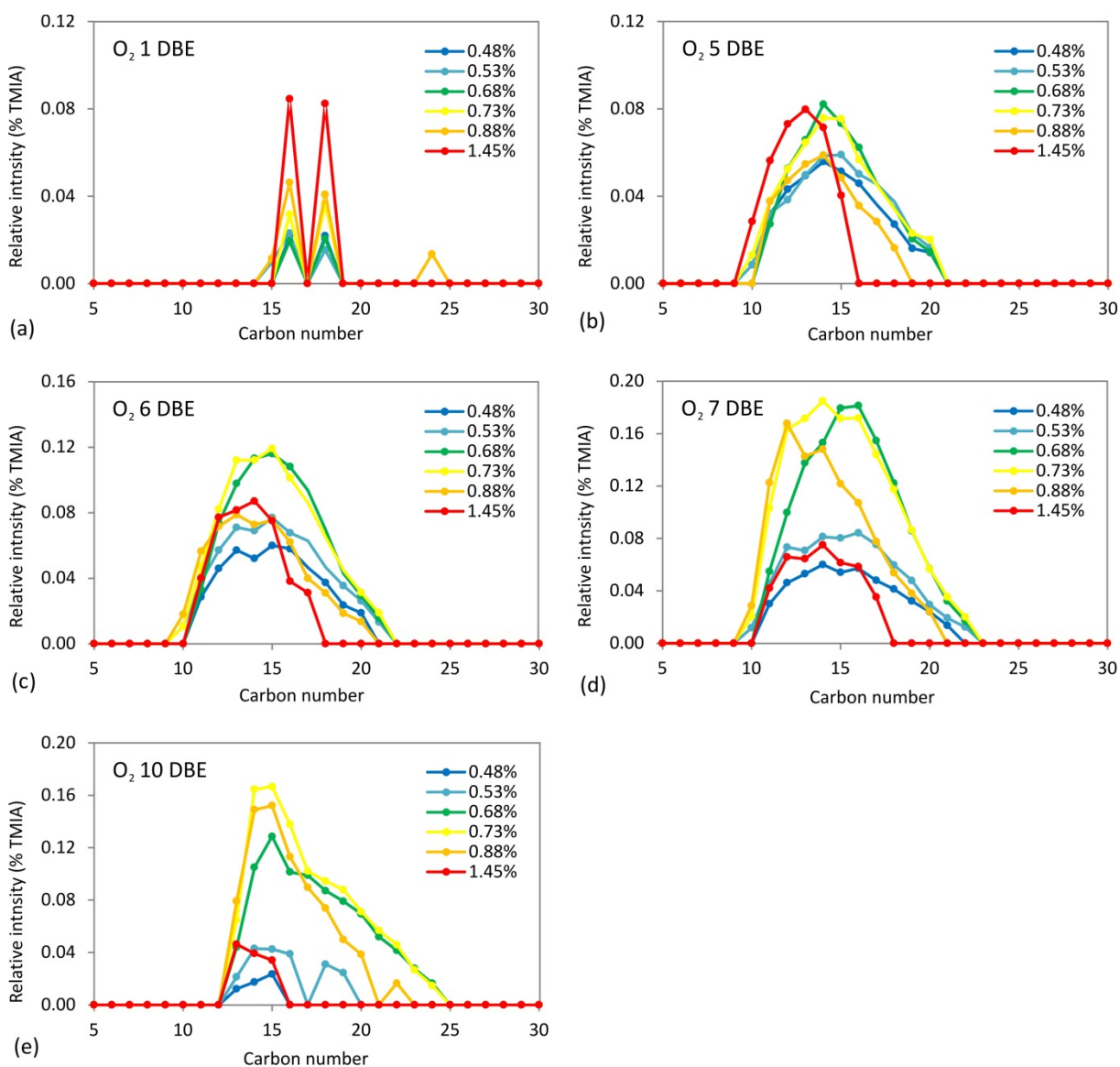


Figure 4.7. Carbon number distribution of O_2 class with different DBEs.

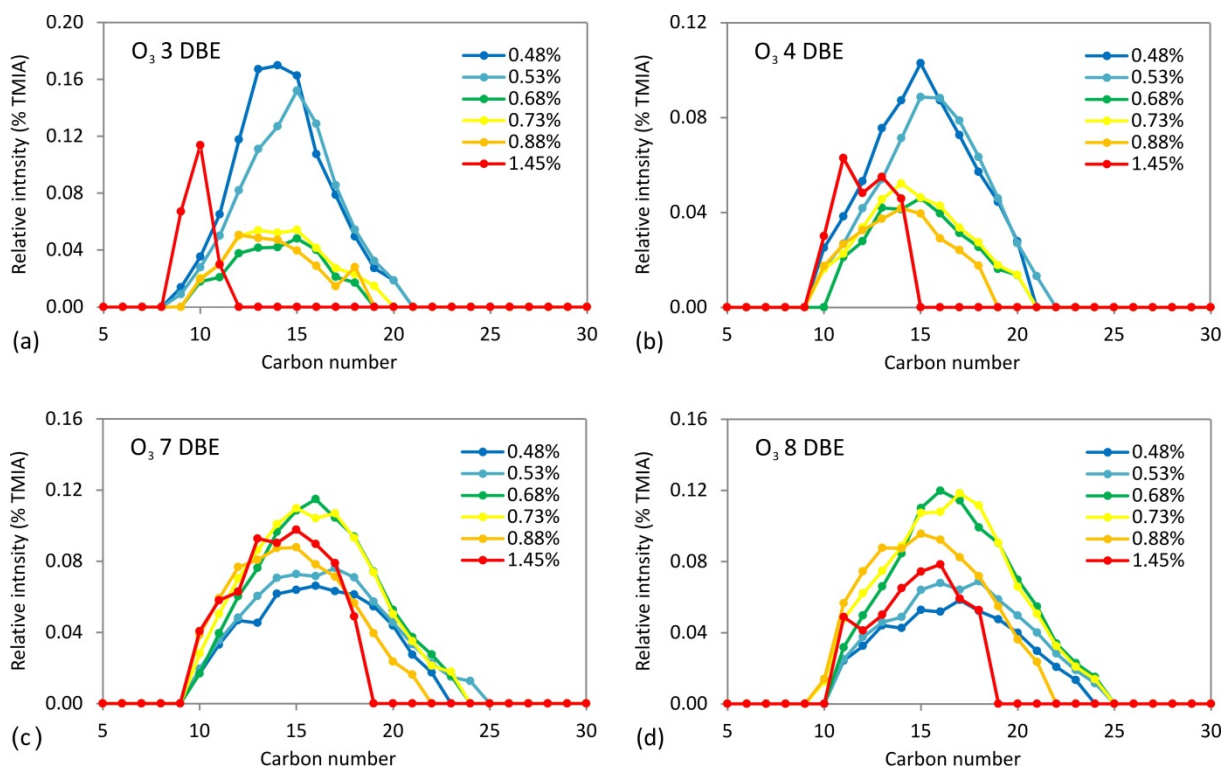


Figure 4.8. Carbon number distribution of O_3 class with different DBEs.

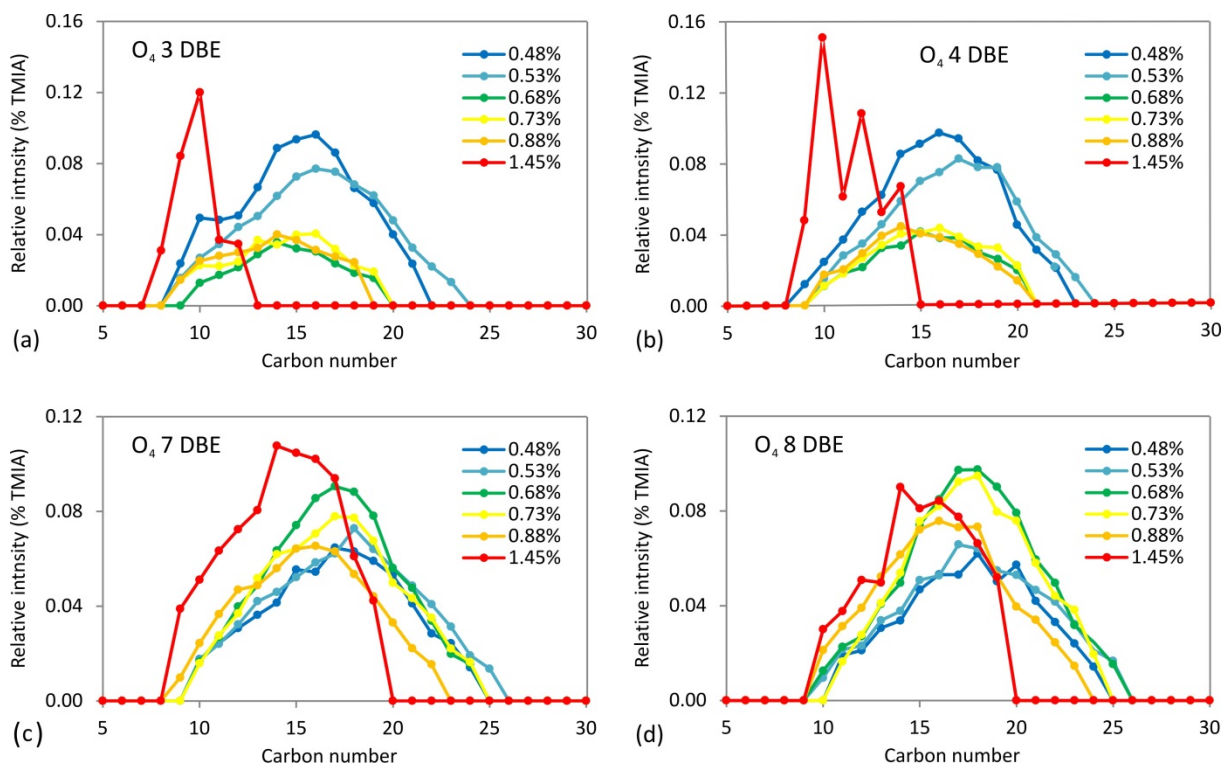


Figure 4.9. Carbon number distribution of O_4 class with different DBEs.

4.4.4.2 OS classes

The relative intensities of the S_1O_{3-8} species for extracted DOM of the six Posidonia shales are presented as a function of DBE in Fig. 4.10. The overall DBE range of the S_1O_{3-8} species increases from the immature samples (0-12) to the mature samples (0-14) and then decreases for the overmature samples (0-9). This variation in DBE range strongly resembles that of the O_{1-6} species.

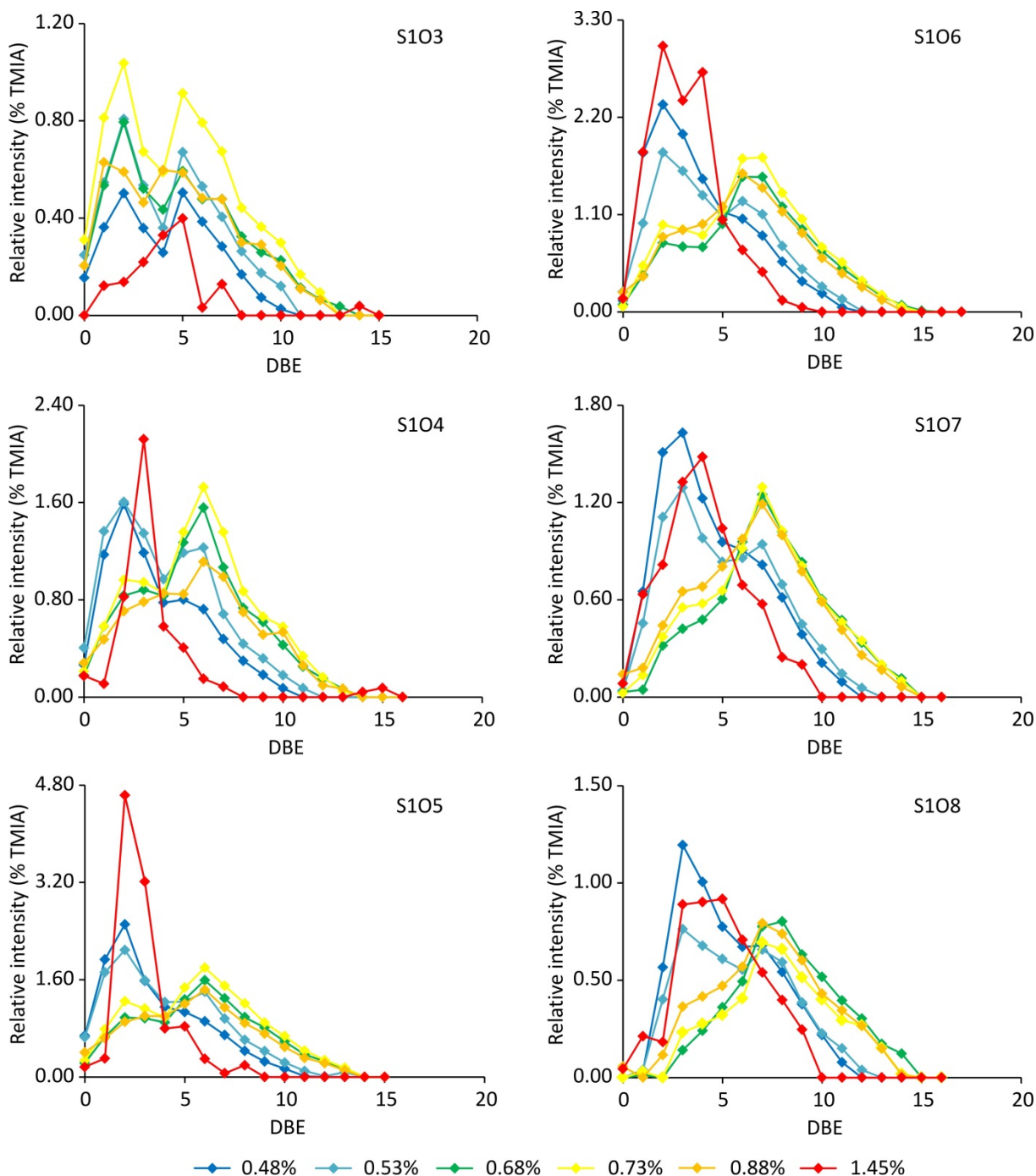


Figure 4.10. DBE distribution of the S_1O_{3-8} classes in the DOM of Posidonia shale extracts.

In S_1O_3 class, a bimodal DBE distribution can be observed for extracted DOM of the immature and mature shales with peak maxima at DBE 2 and 5 while the extracted DOM of the overmature sample show the highest relative intensity at DBE 5. With the limited number of carbon atoms, the compounds in S_1O_3 class with DBE 5 most probably consist of benzene or thiophenic ring in the molecular structure (Fig. 4.11). The variation of DBE distributions in S_1O_{4-8} classes appear to be very similar to that in O_{3-6} classes for both extracted DOM from immature and mature samples. In S_1O_4 to S_1O_8 classes, the extracted DOM of the two immature samples is featured by peak maxima at DBE 2 or 3 and a shoulder at DBE 6 or 7. Inversely, the extracted DOM of three oil window samples is characterized by highest relative intensity at DBE 6 or 7 and a shoulder at DBE 2 or 3. The extracted DOM of the gas window sample exhibited the maximum peak at DBE 2 or 3 in S_1O_{4-6} classes, which indicates that no aromatic ring can be involved in most of the compounds. Thus, extracted DOM of the oil window samples probably consists of higher amount of double bonds or/and rings than the immature samples. It is possible that the molecular structure of most compounds with DBE 6 and (7) contain similar functional groups as the compounds with DBE 2 and (3) plus an additional benzene ring.

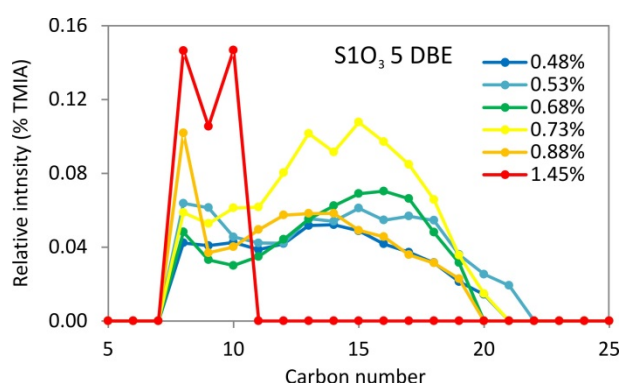


Figure 4.11. Carbon number distribution of S_1O_3 class with 5 DBEs.

It is generally accepted that organic sulfur containing compounds can be abiotically formed in sulfidic sediments during early diagenesis (Sinninghe Damsté et al., 1989; Vairavamurthy et al., 1995; Schmidt et al., 2009). As Posidonia shale was deposited in an anoxic environment with inorganic sulfur mainly fixed as pyrite (Fisher and Hudson, 1987; Littke et al., 1991; Röhl et al., 2001), part of the sulfur could be incorporated into organic matter at early diagenesis. Some of the sulfur containing functional groups like thiols and thioesters has been reported to be formed by sulfurization of organic matter (Schneckenburger et al., 1998; Hertkorn et al., 2013; Sleighter et al., 2014). However, they are in general unstable in the presence of oxygen (Dupont et al., 2006) and can be quickly oxidized to

sulfonic acids (Pohlabein and Dittmar, 2015). Sulfonic acids have been reported to be the predominant functionality in pore water DOS (dissolved organic sulfur) while only minor or undetectable amounts of thiols, thioester, sulfonic acid esters, alkylsulfates or sulfoxides can be detected (Pohlabein et al., 2017). Composition of marine dissolved organic sulfur (DOS) has been investigated in detail by Pohlabein and Dittmar (2015). They reported that sulfonic acids are the main component in DOS for the oxic marine water column. In marine sediments, organic sulfur accumulated as strongly oxidized compounds like sulfonates (Eglinton et al., 1994; Vairavamurthy et al., 1994; Zhu et al., 2014). Thus, it is reasonable to speculate that the sulfonic acid is the common functional group of the compounds in $S_1O_{\geq 3}$ classes. Sulfonic acid functions might be formed during early diagenesis or when the shales were exposed to air or during the extraction process as the experimental setup contains atmospheric oxygen. DOS can also exist in the form of thiophenes and sulfones (Pohlabein and Dittmar, 2015), which might explain the existence of sulfur in S_1O_1 and S_1O_2 classes. The steep increase in the relative intensities from S_1O_2 class to S_1O_3 class (Fig. 4.4) might indicate this difference in the functional groups as the applied electrospray ionization is very sensitive for sulfonic acids (Thurman et al., 2001).

It is obvious that the aromaticity of the extracted DOM from oil window shales is much higher than for immature shales regarding both the O_x classes and the S_1O_x classes. The accumulation of extractable aromatic compounds in the oil window shales can be explained in different ways. First, the aromatic compounds are retained in the shale to a high amount while the aliphatic compounds migrated out the source rock during expulsion. Second, a large number of aromatic structures were released from kerogen at higher maturity levels. However, according to the literature a depletion of aromatic components has not been observed in the expelled crude oils and this contradicts the first assumption (Hughey et al., 2004; Hughey et al., 2007; Shi et al., 2010b; Liao et al., 2012; Mahlstedt et al., 2016). The decreasing aromaticity of the extracted DOM released from the overmature shale was observed. One explanation might be the progressive formation of coke from the aromatic compounds in gas window (Muscio and Horsfield, 1996), which are not soluble in water.

4.5 Summary and Conclusion

We provide molecular insight into the composition of extracted DOM of six Posidonia shale samples as analyzed by ESI FT-ICR-MS in negative ion mode and highlight the compositional differences between the water extracts with respect to different shale organic

matter. The general composition of extracted DOM has been compared with the published data of solvent extracts from the same samples. Enormous differences have been observed between the organic compounds in water and solvent extracts. In extracted DOM, S_1O_x class was the dominant elemental class followed by O_x class and the relative intensities of the different elemental classes do not show obvious variation with increasing maturation of the original shales. However, in the solvent extracts the most prominent elemental classes are O_x , N_y and O_xN_y classes and the relative intensity variations of these elemental classes show close correlations to the thermal maturity of the original samples. This indicated that composition of extracted DOM is strongly determined by polarity and water solubility of the organic compounds. The relative intensity of O_4 class in the extracted DOM was the highest for the two immature samples. The highest intensity shifted to O_2 class for the extracted DOM from three oil window samples, which was attributed to the defunctionalization reactions during diagenesis. The extracted DOM of gas window sample showed the highest relative intensity of O_5 class. In contrast, the relative intensities of the S_1O_x classes exhibited almost the same normal Gaussian distribution with the exception of steep increase from S_1O_2 class to S_1O_3 class. This might be caused by the strong electrospray ionization of sulfonic acids, which was assumed to be the common functional group for most compounds in $S_1O_{\geq 3}$ classes. Possible molecular structures of extracted DOM in different O_x and S_1O_x classes have been speculated based on their DBE and carbon number distributions. It has been speculated that most compounds in extracted DOM of the mature samples contain an additional benzene ring compared to extracted DOM of the immature samples. The aromaticity of DOM increase from immature samples to mature samples and then decrease for the overmature sample. Thus, thermal maturation of the sedimentary organic matter also plays an important role in composition of both the O_x class and the S_1O_x class.

4.6 Acknowledgements

This work was carried out in the framework of Yaling Zhu's Ph.D. at the Technical University of Berlin, which is financially supported by the Chinese Scholarship Council. The authors thank Cornelia Karger and Kristin Günther in GFZ for their technical support in the laboratory work.

4.7 Supplementary material

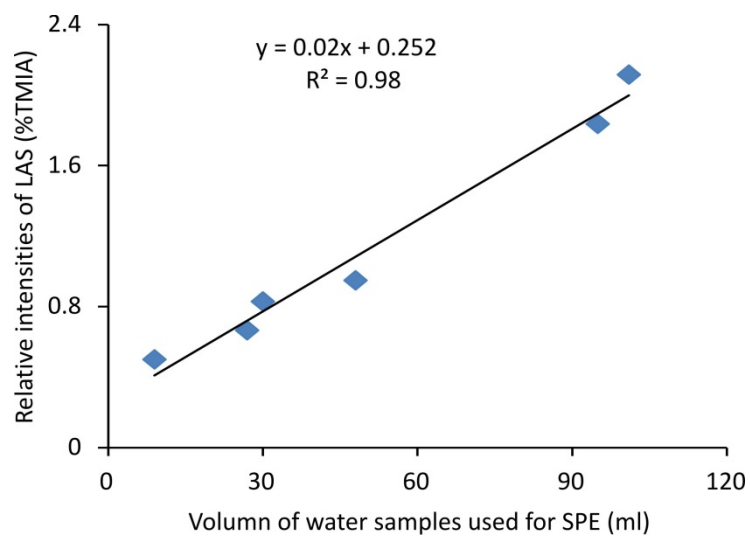


Figure S4.1. The linear correlation between the relative intensity of LAS and the volume of water extracts used for SPE.

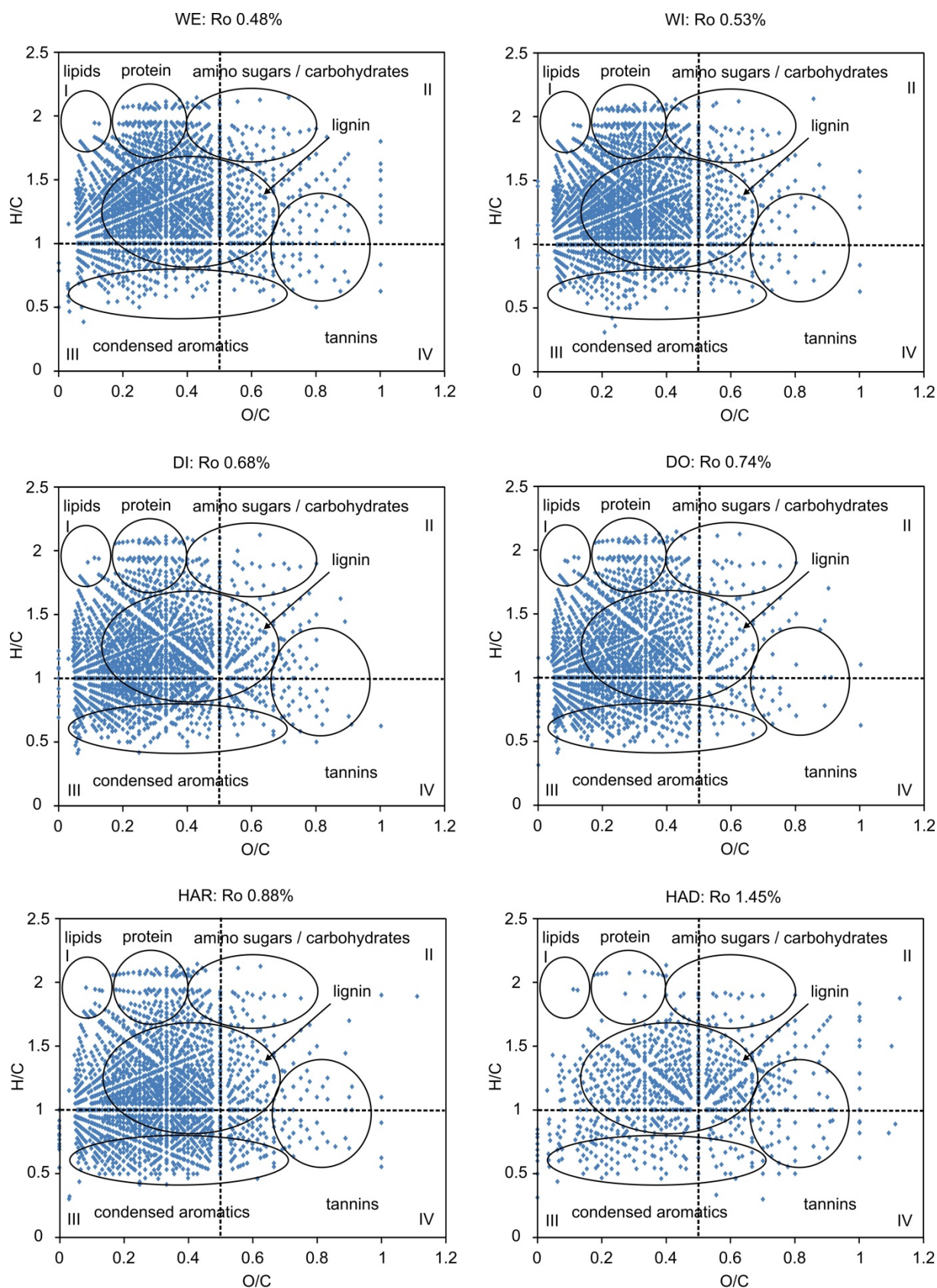


Figure S4.2. Van Krevelen diagrams based on extracted DOM of the *Posidonia* shales from negative ion mode ESI FT-ICR-MS analysis. Ellipses indicate elemental ratios consistent with compound classes listed (Sleighter and Hatcher, 2007; Hockaday et al., 2009). The compounds are

divided into four groups according to the O/C and H/C values (I: $H/C > 1$ and $O/C < 0.5$ including lipids, proteins and part of the lignins, II: $H/C > 1$ and $O/C > 0.5$ including amino sugars, carbohydrates and part of the tannins, III: $H/C < 1$ and $O/C < 0.5$ including condensed hydrocarbons and part of the lignins and IV: $H/C < 1$ and $O/C > 0.5$ including partly condensed hydrocarbons and tannins).

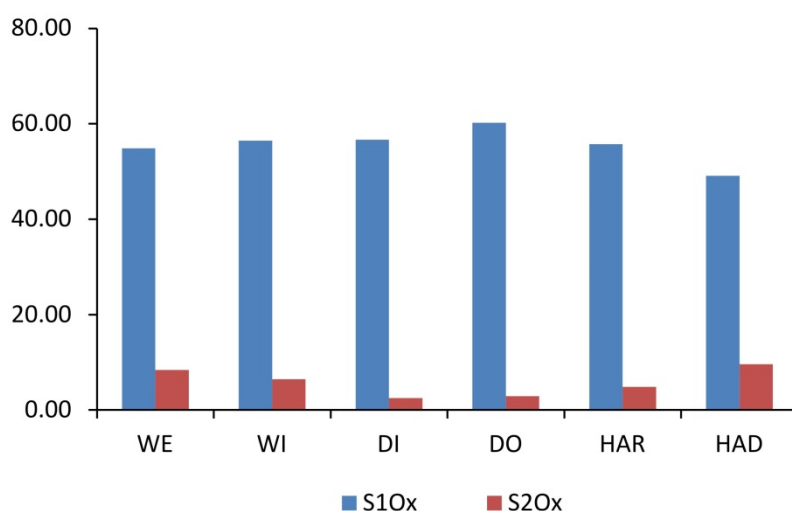


Figure S4.3. Compound class distribution of the O_xS₁ and O_xS₂ classes in the water extracts of the six Posidonia shale samples.

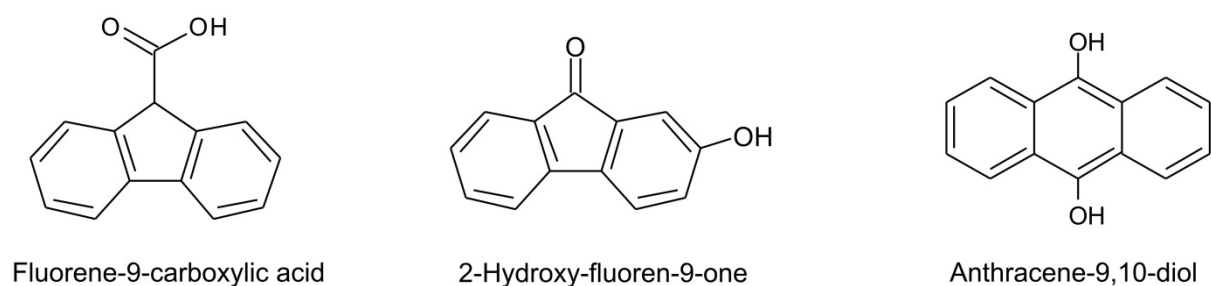


Figure S4.4. The possible core structures of compounds with 10 DBE in O₂ class.

5. SUMMARY AND OUTLOOK

5.1 Summary

The aim of this dissertation was to obtain quantitative and qualitative information about the extracted DOM of black shales and coals in laboratory experiments to better understand the water - rock interactions taking place in both geological and human timescales. The selected samples, 30 black shales from four different geological settings in Germany, the USA, Canada and Denmark as well as 5 New Zealand coal samples, representing different kerogen types, litho- and organofacies, and maturity range from $R_o = 0.3 - 2.6\%$. To be able to directly compare the composition of the extracted DOM, all samples were extracted with deionized water for 48 h under atmospheric pressure and a temperature around 100°C . The extracted DOM was analyzed by different chromatographic and mass spectrometric methods to cover a broad range from bulk to molecular level composition. The major findings are summarized below by answering the research questions presented before:

1) What is the composition of the extracted DOM of black shales and coals? Is the extracted DOM comparable to DOM in natural waters?

Although the samples were collected from five locations with different geological backgrounds, comparable concentrations of DOC can be observed for the samples with the same thermal maturation. The extracted DOM of black shales and coals consists of a continuum of organic compounds from HMW to LMW. Using SEC, DOM was divided into four different fractions according to their molecular size: Macro-2 fraction, Macro-3 fraction, LMW Acids and LMW Neutrals.

HMW organic compounds within the extracted DOM have been detected by FT-ICR-MS combined with ESI in negative ion mode. The DOM was grouped into different elemental classes according to the heteroatoms within the assigned molecular formulae. The extracted DOM of coals is characterized by high abundance of O_x class with relative abundance above 80% TMIA. In contrast, the extracted DOM of the shales is dominant with S1O_x class (around 60% TMIA) followed by O_x class (around 30% TMIA). The high abundance of sulfur containing compounds within the extracted DOM of the shales might due to the higher sulfur content in the shale samples compared to the coal samples. The mass spectra of the extracted DOM of the coals were characterized by several prominent peaks corresponding to

benzenepolycarboxylic acids and naphthalenepolycarboxylic acids with varying numbers of carboxyl and hydroxyl groups.

The concentrations of different LMWOAs in the extracted DOM have been analyzed by IC. Acetate and formate were the two main LMWOAs with concentrations ranging from 0.3 – 5.1 mg/g TOC and 0.2 – 2.4 mg/g TOC, respectively. Other acids like oxalate, propionate, butyrate and valerate were only present in some of the samples. For shale extracts, the acetate concentrations were twice as high as the concentrations of formate, independent of the shale origin, only few *Posidonia* samples were out of this correlation. It can be assumed that the *Posidonia* samples are outliers due to hydrothermal influence to the site. The hydrothermal activity could provide water and heat source to promote the generation of acetate. The coal samples are out of this correlation as they consist of a different kerogen type. As most published data about LMW acids in deep groundwater does not give information about formate, background about this compound is very scarce. Therefore, it is of great interest to check if this observed linear correlation between the concentrations of acetate and formate can be confirmed by extraction of additional shale as well as investigating natural samples.

The compositions of extracted DOM are not comparable with natural DOM with respect to concentrations depending on the fluid:solid ratio that is probably much lower in these experiments than in nature. Analytically speaking, having a low fluid:solid ratio helps to get detectable concentrations of the individually compounds and to avoid any additional sample preparation step for enrichment of compounds (and the additional sample preparation step also provides the risk of sample contamination and loss of compounds). For the extracted DOM of coals, it was shown that only a small proportion of the coal organic matter can be mobilized by water extraction in comparison to the yields of solvent extraction.

Significant compositional differences have been observed by comparing natural DOM with coal extracts using Van Krevelen plots. The extracted DOM of the coals only reflects the geogenic carbon, the mobile part of the sedimentary organic carbon from the geological carbon cycle, whereas natural DOM also contains biogenic carbon from the biological carbon cycle. The extracted DOM of the coals show much higher amount of condensed aromatics-like compounds and the lipid-, protein-, and amino sugar-like compounds are missing.

2) What differences can be observed in the extracted DOM related to kerogen type and organofacies of the sedimentary organic matter?

All experiments were run with water at the same conditions. Therefore, all DOM compounds have to be water soluble at these conditions irrespective of the overall composition of the sedimentary organic matter. One may hypothesize that only a small portion of the available organic compounds is water soluble and therefore the same baseload of water-soluble compounds may always become mobilized by water at these conditions, but this is not the case. Even at the bulk level, the extracted DOM of shale and coals is different and these differences are observable down to the molecular level. The extracted DOM of coals tends to have higher molecular weight in Macro-2 and Macro-3 fractions than the extracted DOM of shales. This was also observed for average M_n and M_w of coal and shale extracts, which indicates that the highly aromatic compounds of the coal organic matter are still water soluble at molecular weights where the aliphatic compounds of the shale organic matter already lost their ability to be part of the extracted DOM.

Aromaticity of compounds in water extracts, as indicated by UV-intensity in LC-OCD analysis is also strongly correlated to kerogen type. Type III kerogen results in highly aromatic extracted DOM as shown by strong UV intensities whereas type II kerogen results in extracted DOM with lower aromaticity. The aromaticity differences between the shale and coal extracts can also be observed in FT-ICR-MS data. The average DBE values of the extracted DOM of shales are much lower compared to that of the coals indicating the lower aromaticity of the extracted DOM of the shales compared to the coals. By comparing the Van Krevelen diagram of the DOM released from black shale and coal samples of comparable thermal maturity, there is a shift to lower H/C and higher O/C ratios from the shale extracts to the coal extracts. It indicates that extracted DOM composition is definitely dependent on kerogen type of the organic matter.

The coal samples can be divided into two different organofacies according to the chain length distributions of *n*-alkanes from the pyrolysates and their palynofloras differences. As the five coal samples cover a very narrow maturity range, the higher OI values of the two lignites compared to the three bituminous coals might also be correlated to their organofacies differences. Comparable IR and UV signals of the extracted DOM of the two lignites as well as the three bituminous coals can be observed from the measurements by LC-OCD. The influence of organofacies on the extracted DOM composition can also be indicated by the FT-ICR-MS results. The numbers of assigned monoisotopic signals, the mean values of DBE, carbon number and oxygen number as well as the M_n and M_w of the extracted DOM of the two lignites are much higher than for extracted DOM of the three bituminous coals. Also, the

oxygen class distributions and the DBE class distributions of the oxygen classes in DOM of the two lignite extracts are comparable and much different from the three bituminous coals.

3) Which effect does the thermal maturity of the sedimentary organic matter have on the molecular composition of the extracted DOM?

Thermal maturity of the original sedimentary organic matter can quantitatively influence the extracted DOM. In general, the amount of the extracted DOM tends to decrease with increasing maturity, as indicated by DOC concentrations over T_{\max} values for all extracts. But this trend is not an excellent linear correlation. The concentrations of extracted DOC decreased steeply with increasing diagenesis and remained low throughout catagenesis. The relative abundance of individual DOM fractions also changes with thermal maturity. Relatively higher amount of compounds with high molecular size (Macro-2 and Macro-3 fractions) could be detected in DOM of the immature samples and more Neutrals existed in the water extracts of the mature and overmature samples. The neutral fractions were likely to represent the final degradation products of organic matter during geological maturation. The concentrations of formate and acetate decrease with increasing maturity of the shale samples. The concentrations of acids correlate quite well with OI of the shales and coals, but there is no overall trend for all samples. In general, OI decreases with increasing maturation of the sedimentary organic matter and with this, concentrations of acids also decrease. This trend seems to depend on the organic matter type of the individual sample location as well as the organofacies. Different BPCAs have been detected in the water extracts of the coal samples. The water extracts of the two lignites are rich in B4CA and B5CA whereas the three bituminous coals show high abundance of in B2CA and B3C. With increase of coal rank more BCAs with small number of carboxyl groups have been mobilized, the variability in the relative abundance of the different BCAs in the coal extracts might be related to the coalification degree of the original coal samples.

The variation of extracted DOM with increasing maturation of the sedimentary organic matter can also be observed on a molecular level for both coals and shales. For coal extracts, it has been speculated that distribution of oxygen containing functional groups changes with number of oxygen atoms. When plotting the average DBE of each oxygen class over the number of the oxygen atoms, we have deduced that more hydroxyl and ether functional groups existed in O_{1-5} classes and more carboxyl and carbonyl functional groups existed in O_{9-16} classes. Within the oxygen class distributions, the relatively low abundance of O_{9-16} classes in the extracted DOM of the bituminous coals compared to the lignites has been

ascribed to the preferential elimination of carboxyl and carbonyl groups with increasing maturation. The modified aromaticity index AI_{coal} has been applied for the evaluation of aromaticity and unsaturation of the oxygen containing compounds. The extracted DOM of the bituminous coals is more aromatic than the extracted DOM of the lignites, which is consistent with the high aromaticity of the original organic matter of the bituminous coals. The molecular structures of compounds in O_x and S_1O_x classes of the shale extracts have been discussed based on their carbon number and DBE distributions. It has been speculated that most compounds in DOM of the mature samples contain an additional benzene ring compared to the DOM of the immature samples. Additionally, it can be assumed from the DBE distribution that the extracted DOM from the mature shale samples is more aromatic than the extracted DOM of the immature shale samples.

4) What are other controlling factors of the composition and amount of individual compounds in the extracted DOM?

As the compounds have been mobilized during water extraction, they need to have certain water solubility and their octanol-water partitioning should be favored to partitioning in water. Thus, the polarity of the organic compounds has been considered to be another factor that determines the composition of the extracted DOM.

The organic compounds in the water and solvent extracts of the same six Posidonia shale samples have been compared. One very obvious difference can be seen in the Van Krevelen diagram where the organic compounds in the water extracts show a broader range of O/C values compared to the solvent extracts. The high number of oxygen atoms in extracted DOM can definitely lead to increased water solubility. In the water extracts, S_zO_x class is the dominant elemental class followed by O_x class. The relative abundances of the elemental classes do not show obvious variation with increasing maturation. However, the solvent extracts showed high abundance of O_x , N_y and O_xN_y classes, and their relative abundances were controlled by the thermal maturation of the original shale samples. Thus, in addition to kerogen type, organofacies and thermal maturity, the water solubility of the organic matter also plays a significant role in controlling the composition of the extracted DOM.

5.2 Outlook

The present dissertation provided qualitative and quantitative information about the extracted DOM of black shales and coals. The extracted DOM compositions were constrained

by different factors: thermal maturity, kerogen type, organofacies and water solubility. However, the experiments were performed at fixed experimental conditions. The sediments were extracted with deionized water under atmosphere pressure at 100 °C for 48 hours in this study. In order to have a more comprehensive understanding of the interaction between rock and water at in-situ conditions, different experimental pressure and temperature as well as the extraction duration have to be considered in further investigations. But more important, other solvents (e.g. acidic and alkaline solutions, presence of different salts) have to be chosen to investigate the influence of pH and salt composition on the mobilization of organic compounds.

With the development of unconventional gas and oil exploitation, special attention has been paid to possible environmental impacts caused by flowback and produced water. The DOM released from black shales and water interaction can provide a baseline for investigating the influence of fracking fluid to the composition of flowback and produced water. Thus, simulated experiments using fracking fluids with different chemical additives and black shales can be performed and compared with the experimental results of the water extraction to evaluate the effect of chemicals on the release of organic compounds in the future.

Additionally, the water-soluble organic compounds derived from oil spills and natural seepages might threaten the global and local environments over both short and long time scales. In order to investigate the composition and potential toxicity of DOM of crude oil and refined petroleum products, extraction experiments of crude oil and water can be performed.

REFERENCES

Aiken, G.R., 1985. Humic substances in soil, sediment, and water: geochemistry, isolation, and characterization.

Akob, D.M., Cozzarelli, I.M., Dunlap, D.S., Rowan, E.L., Lorah, M.M., 2015. Organic and inorganic composition and microbiology of produced waters from Pennsylvania shale gas wells. *Applied Geochemistry* 60, 116-125.

al Sandouk-Lincke, N.A., Schwarzbauer, J., Volk, H., Hartkopf-Fröder, C., Fuentes, D., Young, M., Littke, R., 2013. Alteration of organic material during maturation: A pyrolytic and infrared spectroscopic study of isolated bisaccate pollen and total organic matter (Lower Jurassic, Hils Syncline, Germany). *Organic Geochemistry* 59, 22-36.

Allpike, B.P., Heitz, A., Joll, C.A., Kagi, R.I., 2007. A new organic carbon detector for size exclusion chromatography. *Journal of Chromatography A* 1157, 472-476.

Amrani, A., 2014. Organosulfur Compounds: Molecular and Isotopic Evolution from Biota to Oil and Gas. *Annual Review of Earth and Planetary Sciences* 42, 733-768.

Anderson, T.F., Pratt, L.M., 1995. Isotopic Evidence for the Origin of Organic Sulfur and Elemental Sulfur in Marine Sediments, *Geochemical Transformations of Sedimentary Sulfur*. American Chemical Society, pp. 378-396.

Artinger, R., Buckau, G., Geyer, S., Fritz, P., Wolf, M., Kim, J.I., 2000. Characterization of groundwater humic substances: influence of sedimentary organic carbon. *Applied Geochemistry* 15, 97-116.

Bae, E., Yeo, I.J., Jeong, B., Shin, Y., Shin, K.-H., Kim, S., 2011. Study of Double Bond Equivalents and the Numbers of Carbon and Oxygen Atom Distribution of Dissolved Organic Matter with Negative-Mode FT-ICR MS. *Analytical Chemistry* 83, 4193-4199.

Barbot, E., Vidic, N.S., Gregory, K.B., Vidic, R.D., 2013. Spatial and Temporal Correlation of Water Quality Parameters of Produced Waters from Devonian-Age Shale following Hydraulic Fracturing. *Environmental Science & Technology* 47, 2562-2569.

Barth, T., 1987. Multivariate analysis of aqueous organic acid concentrations and geological properties of north sea reservoirs. *Chemometrics and Intelligent Laboratory Systems* 2, 155-160.

Barth, T., Borgund, A.E., Hopland, A.L., Graue, A., 1988. Volatile organic acids produced during kerogen maturation— amounts, composition and role in migration of oil. *Organic Geochemistry* 13, 461-465.

Barth, T., 1991. Organic acids and inorganic ions in waters from petroleum reservoirs, Norwegian continental shelf: a multivariate statistical analysis and comparison with American reservoir formation waters. *Applied Geochemistry* 6, 1-15.

Barth, T., Bjørlykke, K., 1993. Organic acids from source rock maturation: generation potentials, transport mechanisms and relevance for mineral diagenesis. *Applied Geochemistry* 8, 325-337.

Barwise, A.J.G., Mann, A.L., Eglinton, G., Gowar, A.P., Wardroper, A.M.K., Gutteridge, C.S., 1984. Kerogen characterisation by ^{13}C NMR spectroscopy and pyrolysis-mass spectrometry. *Organic Geochemistry* 6, 343-349.

Beesley, L., Moreno-Jimenez, E., Gomez-Eyles, J.L., 2010. Effects of biochar and greenwaste compost amendments on mobility, bioavailability and toxicity of inorganic and organic contaminants in a multi-element polluted soil. *Environ Pollut* 158, 2282-2287.

Behar, F., Vandenbroucke, M., 1987. Chemical modelling of kerogens. *Organic Geochemistry* 11, 15-24.

Behar, F., Vandenbroucke, M., Teermann, S.C., Hatcher, P.G., Leblond, C., Lerat, O., 1995. Experimental simulation of gas generation from coals and a marine kerogen. *Chemical Geology* 126, 247-260.

Behar, F., Gillaizeau, B., Derenne, S., Largeau, C., 2000. Nitrogen Distribution in the Pyrolysis Products of a Type II Kerogen (Cenomanian, Italy). Timing of Molecular Nitrogen Production versus Other Gases. *Energy & Fuels* 14, 431-440.

Behar, F., Lorant, F., Lewan, M., 2008a. Role of NSO compounds during primary cracking of a Type II kerogen and a Type III lignite. *Organic Geochemistry* 39, 1-22.

Behar, F., Lorant, F., Mazeas, L., 2008b. Elaboration of a new compositional kinetic schema for oil cracking. *Organic Geochemistry* 39, 764-782.

Behar, F., Roy, S., Jarvie, D., 2010. Artificial maturation of a Type I kerogen in closed system: Mass balance and kinetic modelling. *Organic Geochemistry* 41, 1235-1247.

Benner, R., 2002. Chapter 3 - Chemical Composition and Reactivity A2 - Hansell, Dennis A, in: Carlson, C.A. (Ed.), *Biogeochemistry of Marine Dissolved Organic Matter*. Academic Press, San Diego, pp. 59-90.

Bernard, S., Horsfield, B., Schulz, H.-M., Schreiber, A., Wirth, R., Anh Vu, T.T., Perssen, F., Könitzer, S., Volk, H., Sherwood, N., Fuentes, D., 2010. Multi-scale detection of organic and inorganic signatures provides insights into gas shale properties and evolution. *Chemie der Erde - Geochemistry* 70, Supplement 3, 119-133.

Bernard, S., Horsfield, B., Schulz, H.-M., Wirth, R., Schreiber, A., Sherwood, N., 2012. Geochemical evolution of organic-rich shales with increasing maturity: A STXM and TEM study of the Posidonia Shale (Lower Toarcian, northern Germany). *Marine and Petroleum Geology* 31, 70-89.

Berner, R.A., 1984. Sedimentary pyrite formation: An update. *Geochimica et Cosmochimica Acta* 48, 605-615.

Berrueta, L.A., Fernández, L.A., Vicente, F., 1991. Fluorescence study of the solubilization of benzo[a]pyrene: application to its detection in coal washing waters. *Analytica Chimica Acta* 243, 115-119.

- Boreham, C.J., Powell, T.G., 1993. Petroleum source rock potential of coal and associated sediments: qualitative and quantitative aspects, *Hydrocarbons from Coal*. American Association of Petroleum Geologists, Tulsa, OK, pp. 133-158.
- Borgund, A.E., Barth, T., 1994. Generation of short-chain organic acids from crude oil by hydrous pyrolysis. *Organic Geochemistry* 21, 943-952.
- Bou-Raad, M., Hobday, M.D., Rix, C.J., 2000. Aqueous extraction of oxalate and other anions from coal. *Fuel* 79, 1185-1193.
- Bourbonniere, R.A., 1989. Distribution patterns of dissolved organic matter fractions in natural waters from eastern Canada. *Organic Geochemistry* 14, 97-107.
- Bray, E.E., Evans, E.D., 1961. Distribution of n-paraffins as a clue to recognition of source beds. *Geochimica et Cosmochimica Acta* 22, 2-15.
- Broholm, K., Hansen, A.B., Jørgensen, P.R., Arvin, E., Hansen, M., 1999. Transport and biodegradation of creosote compounds in a large, intact, fractured clayey till column. *Journal of Contaminant Hydrology* 39, 331-348.
- Bu, X., Wang, L., Ma, W., Yu, X., McDowell, W.H., Ruan, H., 2010. Spectroscopic characterization of hot-water extractable organic matter from soils under four different vegetation types along an elevation gradient in the Wuyi Mountains. *Geoderma* 159, 139-146.
- Buchardt, B., Clausen, J., Thomsen, E., 1986. Carbon isotope composition of lower palaeozoic kerogen: Effects of maturation. *Organic Geochemistry* 10, 127-134.
- Buchardt, B., Lewan, M.D., 1990. Reflectance of vitrinite-like macerals as a thermal maturity index for Cambrian-Ordovician Alum Shale, southern Scandinavia. *AAPG Bulletin* 74, 394-406.
- Bushaw, K.L., Zepp, R.G., Tarr, M.A., Schulz-Jander, D., Bourbonniere, R.A., Hodson, R.E., Miller, W.L., Bronk, D.A., Moran, M.A., 1996. Photochemical release of biologically available nitrogen from aquatic dissolved organic matter. *Nature* 381, 404.
- Butkovskyi, A., Bruning, H., Kools, S., Rijnaarts, H., P van Wezel, A., 2017. Organic Pollutants in Shale Gas Flowback and Produced Waters: Identification, Potential Ecological Impact, and Implications for Treatment Strategies.
- Carlson, C.A., Hansell, D.A., 2015. Chapter 3 - DOM Sources, Sinks, Reactivity, and Budgets, in: Hansell, D.A., Carlson, C.A. (Eds.), *Biogeochemistry of Marine Dissolved Organic Matter* (Second Edition). Academic Press, Boston, pp. 65-126.
- Carothers, W.W., Kharaka, Y.K., 1978. Aliphatic acid anions in oil-field waters; implications for origin of natural gas. *AAPG Bulletin* 62, 2441-2453.
- Chin, Y.P., Traina, S.J., Swank, C.R., Backhus, D., 1998. Abundance and properties of dissolved organic matter in pore waters of a freshwater wetland. *Limnology and Oceanography* 43, 1287-1296.
- Chow, N., Wendte, J., Stasiuk, L.D., 1995. Productivity versus preservation controls on two organic-rich carbonate facies in the Devonian of Alberta; sedimentological and organic petrological evidence. *Bulletin of Canadian Petroleum Geology* 43, 433-460.

Cluff, M.A., Hartsock, A., MacRae, J.D., Carter, K., Mouser, P.J., 2014. Temporal Changes in Microbial Ecology and Geochemistry in Produced Water from Hydraulically Fractured Marcellus Shale Gas Wells. *Environmental Science & Technology* 48, 6508-6517.

Cooles, G.P., Mackenzie, A.S., Parkes, R.J., 1987. Non-hydrocarbons of significance in petroleum exploration: volatile fatty acids and nonhydrocarbon gases. *Mineralogical Magazine* 51, 483-493.

Creaney, S., Allan, J., 1990. Hydrocarbon generation and migration in the Western Canada sedimentary basin. Geological Society, London, Special Publications 50, 189-202.

D'Andrilli, J., Dittmar, T., Koch, B.P., Purcell, J.M., Marshall, A.G., Cooper, W.T., 2010. Comprehensive characterization of marine dissolved organic matter by Fourier transform ion cyclotron resonance mass spectrometry with electrospray and atmospheric pressure photoionization. *Rapid Communications in Mass Spectrometry* 24, 643-650.

D'Hondt, S., Rutherford, S., Spivack, A.J., 2002. Metabolic Activity of Subsurface Life in Deep-Sea Sediments. *Science* 295, 2067-2070.

D'Andrilli, J., Chanton, J.P., Glaser, P.H., Cooper, W.T., 2010. Characterization of dissolved organic matter in northern peatland soil porewaters by ultra high resolution mass spectrometry. *Organic Geochemistry* 41, 791-799.

Dahm, K.G., Guerra, K.L., Xu, P., Drewes, J.E., 2011. Composite Geochemical Database for Coalbed Methane Produced Water Quality in the Rocky Mountain Region. *Environmental Science & Technology* 45, 7655-7663.

De Leeuw, J., Largeau, C., 1993. A review of macromolecular organic compounds that comprise living organisms and their role in kerogen, coal, and petroleum formation, *Organic Geochemistry*. Springer, pp. 23-72.

Dembicki, H., Pirkle, F.L., 1985. Regional source rock mapping using a source potential rating index. *AAPG Bulletin* 69, 567-581.

Derenne, S., Largeau, C., Casadevall, E., Sinninghe Damsté, J.S., Tegelaar, E.W., de Leeuw, J.W., 1990. Characterization of Estonian Kukersite by spectroscopy and pyrolysis: Evidence for abundant alkyl phenolic moieties in an Ordovician, marine, type II/I kerogen. *Organic Geochemistry* 16, 873-888.

Derenne, S., Nguyen Tu, T.T., 2014. Characterizing the molecular structure of organic matter from natural environments: An analytical challenge. *Comptes Rendus Geoscience* 346, 53-63.

Didyk, B.M., Simoneit, B.R.T., Brassell, S.C., Eglinton, G., 1978. Organic geochemical indicators of palaeoenvironmental conditions of sedimentation. *Nature* 272, 216-222.

Dieckmann, V., Schenk, H.J., Horsfield, B., Welte, D.H., 1998. Kinetics of petroleum generation and cracking by programmed-temperature closed-system pyrolysis of Toarcian Shales. *Fuel* 77, 23-31.

Dieckmann, V., 1999. The prediction of the oil and gas composition by the integration of laboratory experiments and case studie. RWTH Aachen University, PhD Thesis, p. 285.

- Dieckmann, V., Fowler, M., Horsfield, B., 2004. Predicting the composition of natural gas generated by the Duvernay Formation (Western Canada Sedimentary Basin) using a compositional kinetic approach. *Organic Geochemistry* 35, 845-862.
- Dittmar, T., 2008. The molecular level determination of black carbon in marine dissolved organic matter. *Organic Geochemistry* 39, 396-407.
- Dittmar, T., Koch, B., Hertkorn, N., Kattner, G., 2008. A simple and efficient method for the solid-phase extraction of dissolved organic matter (SPE-DOM) from seawater. *Limnology and Oceanography: Methods* 6, 230-235.
- Dittmar, T., Stubbins, A., 2014. Dissolved Organic Matter in Aquatic Systems, in: Holland, H.D., Turekian, K.K. (Eds.), *Treatise on Geochemistry (Second Edition)*. Elsevier, Oxford, pp. 125-156.
- Dittmar, T., Stubbins, A., Ito, T., Jones, D.C., 2017. Comment on “Dissolved organic sulfur in the ocean: Biogeochemistry of a petagram inventory”. *Science* 356, 813-813.
- Dobson, K.R., Stephenson, M., Greenfield, P.F., Bell, P.R.F., 1985. Identification and treatability of organics in oil shale retort water. *Water Res* 19, 849-856.
- Dórea, H.S., Bispo, J.R.L., Aragão, K.A.S., Cunha, B.B., Navickiene, S., Alves, J.P.H., Romão, L.P.C., Garcia, C.A.B., 2007. Analysis of BTEX, PAHs and metals in the oilfield produced water in the State of Sergipe, Brazil. *Microchemical Journal* 85, 234-238.
- Doskočil, L., Grasset, L., Enev, V., Kalina, L., Pekař, M., 2015. Study of water-extractable fractions from South Moravian lignite. *Environmental earth sciences* 73, 3873-3885.
- Dubinenkov, I., Flerus, R., Schmitt-Kopplin, P., Kattner, G., Koch, B.P., 2015. Origin-specific molecular signatures of dissolved organic matter in the Lena Delta. *Biogeochemistry* 123, 1-14.
- Dupont, C.L., Moffett, J.W., Bidigare, R.R., Ahner, B.A., 2006. Distributions of dissolved and particulate biogenic thiols in the subarctic Pacific Ocean. *Deep Sea Research Part I: Oceanographic Research Papers* 53, 1961-1974.
- Durand, B., Espitalié, J., 1973. Evolution de la matière organique au cours de l'enfouissement des sédiments. *Comptes Rendus Academie des Sciences (Paris)* 276, 2253-2256.
- Durand, B., 1980. *Kerogen : insoluble organic matter from sedimentary rocks*. Ed. Technip, Paris.
- Eglinton, T.I., Curtis, C.D., Rowland, S.J., 1987. Generation of water-soluble organic acids from kerogen during hydrous pyrolysis: implications for porosity development. *Mineralogical Magazine* 51, 495-503.
- Eglinton, T.I., Sinninghe Damsté, J.S., Pool, W., de Leeuw, J.W., Eijk, G., Boon, J.J., 1992. Organic sulphur in macromolecular sedimentary organic matter. II. Analysis of distributions of sulphur-containing pyrolysis products using multivariate techniques. *Geochimica et Cosmochimica Acta* 56, 1545-1560.

Eglinton, T.I., Irvine, J.E., Vairavamurthy, A., Zhou, W., Manowitz, B., 1994. Formation and diagenesis of macromolecular organic sulfur in Peru margin sediments. *Organic Geochemistry* 22, 781-799.

Engel, M.H., Macko, S.A., 2013. *Organic geochemistry: principles and applications*. Springer Science & Business Media.

Espitalie, J., Madec, M., Tissot, B., Mennig, J., Leplat, P., 1977. Source rock characterization method for petroleum exploration, Offshore Technology Conference. Offshore Technology Conference.

Fakhru'l-Razi, A., Pendashteh, A., Abdullah, L.C., Biak, D.R.A., Madaeni, S.S., Abidin, Z.Z., 2009. Review of technologies for oil and gas produced water treatment. *Journal of Hazardous Materials* 170, 530-551.

Falk, H., Lavergren, U., Bergbäck, B., 2006. Metal mobility in alum shale from Öland, Sweden. *Journal of Geochemical Exploration* 90, 157-165.

Ferrer, I., Thurman, E.M., 2015. Chemical constituents and analytical approaches for hydraulic fracturing waters. *Trends in Environmental Analytical Chemistry* 5, 18-25.

Fester, J.I., Robinson, W.E., 1966. Oxygen Functional Groups in Green River Oil-Shale Kerogen and Trona Acids, *Coal Science*. AMERICAN CHEMICAL SOCIETY, pp. 22-31.

Finke, N., Vandieken, V., Jørgensen, B.B., 2007. Acetate, lactate, propionate, and isobutyrate as electron donors for iron and sulfate reduction in Arctic marine sediments, Svalbard. *FEMS Microbiology Ecology* 59, 10-22.

Fisher, I.S.J., Hudson, J., 1987. Pyrite formation in Jurassic shales of contrasting biofacies. *Geological Society, London, Special Publications* 26, 69-78.

Fisher, J.B., 1987. Distribution and occurrence of aliphatic acid anions in deep subsurface waters. *Geochimica et Cosmochimica Acta* 51, 2459-2468.

Fisher, J.G., Santamaria, A., 2002. Dissolved organic constituents in coal-associated waters and implications for human and ecosystem health, 9th Annual International Petroleum Environmental Conference.

Forsman, J.P., Hunt, J.M., 1958. Insoluble organic matter (kerogen) in sedimentary rocks. *Geochimica et Cosmochimica Acta* 15, 170-182.

Ghani, A., Dexter, M., Perrott, K.W., 2003. Hot-water extractable carbon in soils: a sensitive measurement for determining impacts of fertilisation, grazing and cultivation. *Soil Biology and Biochemistry* 35, 1231-1243.

Given, P.H., Dickinson, C., 1975. *Biochemistry and microbiology of peats*. Soil biochemistry.

Glombitza, C., Mangelsdorf, K., Horsfield, B., 2009. A novel procedure to detect low molecular weight compounds released by alkaline ester cleavage from low maturity coals to assess its feedstock potential for deep microbial life. *Organic Geochemistry* 40, 175-183.

Glombitza, C., 2011. *New Zealand Coals - a Potential Feedstock for Deep Microbial Life*. Omniscryptum GmbH & Company Kg.

- Gomez-Saez, G.V., Niggemann, J., Dittmar, T., Pohlabein, A.M., Lang, S.Q., Noowong, A., Pichler, T., Wörmer, L., Bühring, S.I., 2016. Molecular evidence for abiotic sulfurization of dissolved organic matter in marine shallow hydrothermal systems. *Geochimica et Cosmochimica Acta* 190, 35-52.
- Gong, G.Z., Wei, X.Y., Wang, S.L., Liu, S.P., Yao, T., Zhou, J.S., Qie, L.M., Li, J.N., Lv, J., Zong, Z.M., 2011. Preparation of Benzene Polycarboxylic Acids by Oxidation of Coal with NaOCl, *Advanced Materials Research. Trans Tech Publ*, pp. 864-867.
- Gonsior, M., Valle, J., Schmitt-Kopplin, P., Hertkorn, N., Bastviken, D., Luek, J., Harir, M., Bastos, W., Enrich-Prast, A., 2016. Chemodiversity of dissolved organic matter in the Amazon Basin. *Biogeosciences* 13, 4279-4290.
- Gordalla, B., Ewers, U., Frimmel, F., 2013. Hydraulic fracturing: a toxicological threat for groundwater and drinking-water? *Environmental earth sciences* 70, 3875-3893.
- Gregorich, E.G., Beare, M.H., Stoklas, U., St-Georges, P., 2003. Biodegradability of soluble organic matter in maize-cropped soils. *Geoderma* 113, 237-252.
- Gregory, K.B., Vidic, R.D., Dzombak, D.A., 2011. Water Management Challenges Associated with the Production of Shale Gas by Hydraulic Fracturing. *Elements* 7, 181-186.
- Hansell, D.A., Carlson, C.A., Repeta, D.J., Schlitzer, R., 2009. Dissolved organic matter in the ocean: A controversy stimulates new insights. *Oceanography* 22, 202-211.
- Hartman, B.E., Chen, H., Hatcher, P.G., 2015. A non-thermogenic source of black carbon in peat and coal. *International Journal of Coal Geology* 144–145, 15-22.
- Hatcher, P.G., 1990. Chemical structural models for coalified wood (vitrinite) in low rank coal. *Organic Geochemistry* 16, 959-968.
- Hatcher, P.G., Clifford, D.J., 1997. The organic geochemistry of coal: from plant materials to coal. *Organic Geochemistry* 27, 251-274.
- Hatcher, P.G., Dria, K.J., Kim, S., Frazier, S.W., 2001. Modern analytical studies of humic substances. *Soil Science* 166, 770-794.
- Hayes, T., 2009. Sampling and Analysis of Water Streams Associated with the Development of Marcellus Shale Gas.
- Headley, J., Barrow, M., Peru, K., Fahlman, B., Frank, R., Bickerton, G., McMaster, M., Parrott, J., Hewitt, L., 2011. Preliminary fingerprinting of Athabasca oil sands polar organics in environmental samples using electrospray ionization Fourier transform ion cyclotron resonance mass spectrometry. *Rapid Communications in Mass Spectrometry* 25, 1899-1909.
- Helz, G.R., Miller, C.V., Charnock, J.M., Mosselmans, J.F.W., Patrick, R.A.D., Garner, C.D., Vaughan, D.J., 1996. Mechanism of molybdenum removal from the sea and its concentration in black shales: EXAFS evidence. *Geochimica et Cosmochimica Acta* 60, 3631-3642.
- Herbert, B.E., Bertsch, P.M., 1995. Characterization of dissolved and colloidal organic matter in soil solution: A review. In *Carbon forms and functions in forest soils*. J. M. Kelly and W. W. McFee (eds.). SSSA, Madison, WI, 63-88.

Hertkorn, N., Benner, R., Frommberger, M., Schmitt-Kopplin, P., Witt, M., Kaiser, K., Kettrup, A., Hedges, J.I., 2006. Characterization of a major refractory component of marine dissolved organic matter. *Geochimica et Cosmochimica Acta* 70, 2990-3010.

Hertkorn, N., Harir, M., Koch, B.P., Michalke, B., Schmitt-Kopplin, P., 2013. High-field NMR spectroscopy and FTICR mass spectrometry: powerful discovery tools for the molecular level characterization of marine dissolved organic matter. *Biogeosciences* 10, 1583-1624.

Hockaday, W.C., Grannas, A.M., Kim, S., Hatcher, P.G., 2006. Direct molecular evidence for the degradation and mobility of black carbon in soils from ultrahigh-resolution mass spectral analysis of dissolved organic matter from a fire-impacted forest soil. *Organic Geochemistry* 37, 501-510.

Hockaday, W.C., Purcell, J.M., Marshall, A.G., Baldock, J.A., Hatcher, P.G., 2009. Electrospray and photoionization mass spectrometry for the characterization of organic matter in natural waters: a qualitative assessment. *Limnology and Oceanography: Methods* 7, 81-95.

Holowenko, F.M., MacKinnon, M.D., Fedorak, P.M., 2002. Characterization of naphthenic acids in oil sands wastewaters by gas chromatography-mass spectrometry. *Water Res* 36, 2843-2855.

Horsfield, B., 1989. Practical criteria for classifying kerogens: Some observations from pyrolysis-gas chromatography. *Geochimica et Cosmochimica Acta* 53, 891-901.

Horsfield, B., Disko, U., Leistner, F., 1989. The micro-scale simulation of maturation: outline of a new technique and its potential applications. *Geologische Rundschau* 78, 361-373.

Horsfield, B., Dueppenbecker, S.J., 1991. The decomposition of posidonia shale and green river shale kerogens using microscale sealed vessel (MSSV) pyrolysis. *Journal of Analytical and Applied Pyrolysis* 20, 107-123.

Horsfield, B., Schenk, H.J., Mills, N., Welte, D.H., 1992. An investigation of the in-reservoir conversion of oil to gas: compositional and kinetic findings from closed-system programmed-temperature pyrolysis. *Organic Geochemistry* 19, 191-204.

Horsfield, B., Schenk, H.J., Zink, K., Ondrak, R., Dieckmann, V., Kallmeyer, J., Mangelsdorf, K., di Primio, R., Wilkes, H., Parkes, R.J., Fry, J., Cragg, B., 2006. Living microbial ecosystems within the active zone of catagenesis: Implications for feeding the deep biosphere. *Earth and Planetary Science Letters* 246, 55-69.

Horsfield, B., Leistner, F., Hall, K., 2015. CHAPTER 7 Microscale Sealed Vessel Pyrolysis, Principles and Practice of Analytical Techniques in Geosciences. *The Royal Society of Chemistry*, pp. 209-250.

Huber, S.A., Frimmel, F.H., 1996. Size-exclusion-chromatography with organic carbon detection (LC-OCD): A fast and reliable method for the characterization of hydrophilic organic matter in natural waters. *Vom Wasser* 86, 277-290.

Huber, S.A., Balz, A., Abert, M., Pronk, W., 2011. Characterisation of aquatic humic and non-humic matter with size-exclusion chromatography – organic carbon detection – organic nitrogen detection (LC-OCD-OND). *Water Res* 45, 879-885.

Hughey, C.A., Rodgers, R.P., Marshall, A.G., Walters, C.C., Qian, K., Mankiewicz, P., 2004. Acidic and neutral polar NSO compounds in Smackover oils of different thermal maturity revealed by electrospray high field Fourier transform ion cyclotron resonance mass spectrometry. *Organic Geochemistry* 35, 863-880.

Hughey, C.A., Galasso, S.A., Zumberge, J.E., 2007. Detailed compositional comparison of acidic NSO compounds in biodegraded reservoir and surface crude oils by negative ion electrospray Fourier transform ion cyclotron resonance mass spectrometry. *Fuel* 86, 758-768.

Hunt, J.M., 1991. Generation of gas and oil from coal and other terrestrial organic matter. *Organic Geochemistry* 17, 673-680.

Ibarra, J., Muñoz, E., Moliner, R., 1996. FTIR study of the evolution of coal structure during the coalification process. *Organic Geochemistry* 24, 725-735.

Isaksen, G., Curry, D., Yeakel, J., Jenssen, A., 1998. Controls on the oil and gas potential of humic coals. *Organic Geochemistry* 29, 23-44.

Islam, A., Ahmed, A., Hur, M., Thorn, K., Kim, S., 2016. Molecular-level evidence provided by ultrahigh resolution mass spectrometry for oil-derived doc in groundwater at Bemidji, Minnesota. *Journal of Hazardous Materials* 320, 123-132.

Jacquemet, V., Gaval, G., Rosenberger, S., Lesjean, B., Schrotter, J.C., 2005. Towards a better characterisation and understanding of membrane fouling in water treatment. *Desalination* 178, 13-20.

Jaffe, L.A., Peucker-Ehrenbrink, B., Petsch, S.T., 2002. Mobility of rhenium, platinum group elements and organic carbon during black shale weathering. *Earth and Planetary Science Letters* 198, 339-353.

Jarvie, D.M., Hill, R.J., Ruble, T.E., Pollastro, R.M., 2007. Unconventional shale-gas systems: The Mississippian Barnett Shale of north-central Texas as one model for thermogenic shale-gas assessment. *AAPG Bulletin* 91, 475-499.

Jenkyns, H.C., 1980. Cretaceous anoxic events: from continents to oceans. *Journal of the Geological Society* 137, 171-188.

Jenkyns, H.C., Clayton, C., 1997. Lower Jurassic epicontinental carbonates and mudstones from England and Wales: chemostratigraphic signals and the early Toarcian anoxic event. *Sedimentology* 44, 687-706.

Jiang, C., Li, M., Osadetz, K.G., Snowdon, L.R., Obermajer, M., Fowler, M.G., 2001. Bakken/Madison petroleum systems in the Canadian Williston Basin. Part 2: molecular markers diagnostic of Bakken and Lodgepole source rocks. *Organic Geochemistry* 32, 1037-1054.

Jiang, C., Li, M., 2002. Bakken/Madison petroleum systems in the Canadian Williston Basin. Part 3: geochemical evidence for significant Bakken-derived oils in Madison Group reservoirs. *Organic Geochemistry* 33, 761-787.

Jin, L., Mathur, R., Rother, G., Cole, D., Bazilevskaya, E., Williams, J., Carone, A., Brantley, S., 2013. Evolution of porosity and geochemistry in Marcellus Formation black shale during weathering. *Chemical Geology* 356, 50-63.

Kallmeyer, J., Mangelsdorf, K., Cragg, B., Horsfield, B., 2006. Techniques for Contamination Assessment During Drilling for Terrestrial Subsurface Sediments. *Geomicrobiology Journal* 23, 227-239.

Kawamura, K., Tannenbaum, E., Huizinga, B.J., Kaplan, I.R., 1986. Volatile organic acids generated from kerogen during laboratory heating. *Geochemical journal* 20, 51-59.

Kawamura, K., Kaplan, I.R., 1987. Dicarboxylic acids generated by thermal alteration of kerogen and humic acids. *Geochimica et Cosmochimica Acta* 51, 3201-3207.

Kelemen, S.R., Afeworki, M., Gorbaty, M.L., Cohen, A.D., 2002. Characterization of Organically Bound Oxygen Forms in Lignites, Peats, and Pyrolyzed Peats by X-ray Photoelectron Spectroscopy (XPS) and Solid-State ¹³C NMR Methods. *Energy & Fuels* 16, 1450-1462.

Kelemen, S.R., Afeworki, M., Gorbaty, M.L., Sansone, M., Kwiatek, P.J., Walters, C.C., Freund, H., Siskin, M., Bence, A.E., Curry, D.J., Solum, M., Pugmire, R.J., Vandenbroucke, M., Leblond, M., Behar, F., 2007. Direct Characterization of Kerogen by X-ray and Solid-State ¹³C Nuclear Magnetic Resonance Methods. *Energy & Fuels* 21, 1548-1561.

Kellerman, A.M., Kothawala, D.N., Dittmar, T., Tranvik, L.J., 2015. Persistence of dissolved organic matter in lakes related to its molecular characteristics. *Nature Geoscience* 8, 454.

Kennedy, M.D., Chun, H.K., Quintanilla Yangali, V.A., Heijman, B.G.J., Schippers, J.C., 2005. Natural organic matter (NOM) fouling of ultrafiltration membranes: fractionation of NOM in surface water and characterisation by LC-OCD. *Desalination* 178, 73-83.

Khan, N.A., Engle, M., Dungan, B., Holguin, F.O., Xu, P., Carroll, K.C., 2016. Volatile-organic molecular characterization of shale-oil produced water from the Permian Basin. *Chemosphere* 148, 126-136.

Kharaka, Y.K., Carothers, W.W., Rosenbauer, R.J., 1983. Thermal decarboxylation of acetic acid: Implications for origin of natural gas. *Geochimica et Cosmochimica Acta* 47, 397-402.

Killops, S., Funnell, R., Suggate, R., Sykes, R., Peters, K., Walters, C., Woolhouse, A., Weston, R., Boudou, J.-P., 1998. Predicting generation and expulsion of paraffinic oil from vitrinite-rich coals. *Organic Geochemistry* 29, 1-21.

Killops, S.D., Killops, V.J., 2013. *Introduction to organic geochemistry*. John Wiley & Sons.

Kim, S., Kramer, R.W., Hatcher, P.G., 2003a. Graphical Method for Analysis of Ultrahigh-Resolution Broadband Mass Spectra of Natural Organic Matter, the Van Krevelen Diagram. *Analytical Chemistry* 75, 5336-5344.

Kim, S., Simpson, A.J., Kujawinski, E.B., Freitas, M.A., Hatcher, P.G., 2003e. High resolution electrospray ionization mass spectrometry and 2D solution NMR for the analysis of DOM extracted by C18 solid phase disk. *Organic Geochemistry* 34, 1325-1335.

Kim, S., Kaplan, L.A., Benner, R., Hatcher, P.G., 2004. Hydrogen-deficient molecules in natural riverine water samples—evidence for the existence of black carbon in DOM. *Marine Chemistry* 92, 225-234.

King, R., Bonfiglio, R., Fernandez-Metzler, C., Miller-Stein, C., Olah, T., 2000. Mechanistic investigation of ionization suppression in electrospray ionization. *Journal of the American Society for Mass Spectrometry* 11, 942-950.

Kleerebezem, R., W. Hulshoff Pol, L., Lettinga, G., 1999. Anaerobic biodegradability of phthalic acid isomers and related compounds.

Klemme, H., Ulmishek, G.F., 1991. Effective petroleum source rocks of the world: stratigraphic distribution and controlling depositional factors (1). *AAPG Bulletin* 75, 1809-1851.

Koch, B.P., Witt, M., Engbrodt, R., Dittmar, T., Kattner, G., 2005. Molecular formulae of marine and terrigenous dissolved organic matter detected by electrospray ionization Fourier transform ion cyclotron resonance mass spectrometry. *Geochimica et Cosmochimica Acta* 69, 3299-3308.

Koch, B.P., Dittmar, T., 2006. From mass to structure: an aromaticity index for high-resolution mass data of natural organic matter. *Rapid Communications in Mass Spectrometry* 20, 926-932.

Koch, B.P., Ludwiczowski, K.-U., Kattner, G., Dittmar, T., Witt, M., 2008. Advanced characterization of marine dissolved organic matter by combining reversed-phase liquid chromatography and FT-ICR-MS. *Marine Chemistry* 111, 233-241.

Kong, J., Wei, X.-Y., Li, Z.-K., Yan, H.-L., Zhao, M.-X., Zong, Z.-M., 2016. Identification of organonitrogen and organooxygen compounds in the extraction residue from Buliangou subbituminous coal by FTICRMS. *Fuel* 171, 151-158.

Kosateva, A., Stefanova, M., Marinov, S., Czech, J., Carleer, R., Yperman, J., 2017. Characterization of organic components in leachables from Bulgarian lignites by spectroscopy, chromatography and reductive pyrolysis. *International Journal of Coal Geology* 183, 100-109.

Ksionzek, K.B., Lechtenfeld, O.J., McCallister, S.L., Schmitt-Kopplin, P., Geuer, J.K., Geibert, W., Koch, B.P., 2016. Dissolved organic sulfur in the ocean: Biogeochemistry of a petagram inventory. *Science* 354, 456-459.

Kuhn, P., Primio, R.D., Horsfield, B., 2010. Bulk composition and phase behaviour of petroleum sourced by the Bakken Formation of the Williston Basin. *Geological Society, London, Petroleum Geology Conference* 7, 1065-1077.

Kuhn, P.P., di Primio, R., Hill, R., Lawrence, J.R., Horsfield, B., 2012. Three-dimensional modeling study of the low-permeability petroleum system of the Bakken Formation. *AAPG Bulletin* 96, 1867-1897.

Kujawinski, E.B., Del Vecchio, R., Blough, N.V., Klein, G.C., Marshall, A.G., 2004. Probing molecular-level transformations of dissolved organic matter: insights on photochemical degradation and protozoan modification of DOM from electrospray ionization Fourier transform ion cyclotron resonance mass spectrometry. *Marine Chemistry* 92, 23-37.

Lankes, U., Müller, M.B., Weber, M., Frimmel, F.H., 2009. Reconsidering the quantitative analysis of organic carbon concentrations in size exclusion chromatography. *Water Res* 43, 915-924.

- Lara-Martín, P.A., Gómez-Parra, A., Sanz, J.L., González-Mazo, E., 2010. Anaerobic Degradation Pathway of Linear Alkylbenzene Sulfonates (LAS) in Sulfate-Reducing Marine Sediments. *Environmental Science & Technology* 44, 1670-1676.
- Lavergren, U., Astrom, M.E., Bergback, B., Holmstrom, H., 2009. Mobility of trace elements in black shale assessed by leaching tests and sequential chemical extraction. *Geochemistry: Exploration, Environment, Analysis* 9, 71-79.
- Leenheer, J.A., Noyes, T.I., Stuber, H.A., 1982. Determination of polar organic solutes in oil-shale retort water. *Environmental Science & Technology* 16, 714-723.
- Leenheer, J.A., Croué, J.-P., 2003. Peer Reviewed: Characterizing Aquatic Dissolved Organic Matter. *Environmental Science & Technology* 37, 18A-26A.
- Leenheer, M.J., 1984. Mississippian Bakken and equivalent formations as source rocks in the Western Canadian Basin. *Organic Geochemistry* 6, 521-532.
- Lepane, V., Leeben, A., Malashenko, O., 2004. Characterization of sediment pore-water dissolved organic matter of lakes by high-performance size exclusion chromatography. *Aquatic Sciences* 66, 185-194.
- Lester, Y., Ferrer, I., Thurman, E.M., Sitterley, K.A., Korak, J.A., Aiken, G., Linden, K.G., 2015. Characterization of hydraulic fracturing flowback water in Colorado: Implications for water treatment. *Science of The Total Environment* 512–513, 637-644.
- Levine, N.M., 2016. Putting the spotlight on organic sulfur. *Science* 354, 418-419.
- Lewan, M., Fisher, J., 1994. Organic acids from petroleum source rocks, Organic acids in geological processes. Springer, pp. 70-114.
- Lewan, M.D., Spiro, B., Illich, H., Raiswell, R., Mackenzie, A.S., Durand, B., Manning, D.A.C., Comet, P.A., Berner, R.A., Leeuw, J.W.D., 1985. Evaluation of Petroleum Generation by Hydrous Pyrolysis Experimentation [and Discussion].
- Lewan, M.D., 1997. Experiments on the role of water in petroleum formation. *Geochimica et Cosmochimica Acta* 61, 3691-3723.
- Li, M., Yao, H., Stasiuk, L.D., Fowler, M.G., Larter, S.R., 1997. Effect of maturity and petroleum expulsion on pyrrolic nitrogen compound yields and distributions in Duvernay Formation petroleum source rocks in central Alberta, Canada. *Organic Geochemistry* 26, 731-744.
- Liao, Y., Shi, Q., Hsu, C.S., Pan, Y., Zhang, Y., 2012. Distribution of acids and nitrogen-containing compounds in biodegraded oils of the Liaohe Basin by negative ion ESI FT-ICR MS. *Organic Geochemistry* 47, 51-65.
- Lis, G.P., Mastalerz, M., Schimmelmann, A., Lewan, M.D., Stankiewicz, B.A., 2005. FTIR absorption indices for thermal maturity in comparison with vitrinite reflectance R₀ in type-II kerogens from Devonian black shales. *Organic Geochemistry* 36, 1533-1552.
- Littke, R., Baker, D.R., Leythaeuser, D., 1988. Microscopic and sedimentologic evidence for the generation and migration of hydrocarbons in Toarcian source rocks of different maturities. *Organic Geochemistry* 13, 549-559.

- Littke, R., Leythaeuser, D., Rullkötter, J., Baker, D.R., 1991. Keys to the depositional history of the Posidonia Shale (Toarcian) in the Hils Syncline, northern Germany. Geological Society, London, Special Publications 58, 311-333.
- Liu, P., Li, M., Jiang, Q., Cao, T., Sun, Y., 2015. Effect of secondary oil migration distance on composition of acidic NSO compounds in crude oils determined by negative-ion electrospray Fourier transform ion cyclotron resonance mass spectrometry. *Organic Geochemistry* 78, 23-31.
- Liu, Y., Kujawinski, E.B., 2015. Chemical Composition and Potential Environmental Impacts of Water-Soluble Polar Crude Oil Components Inferred from ESI FT-ICR MS. *Plos One* 10, e0136376.
- Longnecker, K., Kujawinski, E.B., 2011. Composition of dissolved organic matter in groundwater. *Geochimica et Cosmochimica Acta* 75, 2752-2761.
- Loucks, R.G., Reed, R.M., Ruppel, S.C., Jarvie, D.M., 2009. Morphology, Genesis, and Distribution of Nanometer-Scale Pores in Siliceous Mudstones of the Mississippian Barnett Shale. *J Sed Res* 79, 848-861.
- Luek, J.L., Gonsior, M., 2017. Organic compounds in hydraulic fracturing fluids and wastewaters: A review. *Water Res* 123, 536-548.
- Lundegard, P.D., Senftle, J.T., 1987. Hydrous pyrolysis: a tool for the study of organic acid synthesis. *Applied Geochemistry* 2, 605-612.
- Mackenzie, A.S., Brassell, S.C., Eglinton, G., Maxwell, J.R., 1982. Chemical Fossils: The Geological Fate of Steroids. *Science* 217, 491-504.
- Maguire-Boyle, S.J., Barron, A.R., 2014. Organic compounds in produced waters from shale gas wells. *Environmental Science-Processes & Impacts* 16, 2237-2248.
- Maharaj, S.V.M., Orem, W.H., Tatu, C.A., Lerch, H.E., III, Szilagyi, D.N., 2014. Organic compounds in water extracts of coal: links to Balkan endemic nephropathy. *Environmental Geochemistry and Health* 36, 1-17.
- Mahlstedt, N., Horsfield, B., Wilkes, H., Poetz, S., 2016. Tracing the Impact of Fluid Retention on Bulk Petroleum Properties Using Nitrogen-Containing Compounds. *Energy & Fuels* 30, 6290-6305.
- Mann, U., Müller, P.J., 1988. Source rock evaluation by well log analysis (Lower Toarcian, Hils syncline). *Organic Geochemistry* 13, 109-119.
- Marmonier, P., Fontvieille, D., Gibert, J., Vanek, V., 1995. Distribution of dissolved organic carbon and bacteria at the interface between the Rhône River and its alluvial aquifer. *Journal of the North American Benthological Society* 14, 382-392.
- Mathia, E., Rexer, T., Bowen, L., Aplin, A., 2013. Evolution of porosity and pore systems in organic-rich Posidonia and Wealden Shales, 75th EAGE Conference & Exhibition incorporating SPE EUROPEC 2013.

- Matilainen, A., Gjessing, E.T., Lahtinen, T., Hed, L., Bhatnagar, A., Sillanpää, M., 2011. An overview of the methods used in the characterisation of natural organic matter (NOM) in relation to drinking water treatment. *Chemosphere* 83, 1431-1442.
- Means, J.L., Hubbard, N., 1987. Short-chain aliphatic acid anions in deep subsurface brines: A review of their origin, occurrence, properties, and importance and new data on their distribution and geochemical implications in the Palo Duro Basin, Texas. *Organic Geochemistry* 11, 177-191.
- Melendez-Perez, J.J., Martínez-Mejía, M.J., Awan, A.T., Fadini, P.S., Mozeto, A.A., Eberlin, M.N., 2016. Characterization and comparison of riverine, lacustrine, marine and estuarine dissolved organic matter by ultra-high resolution and accuracy Fourier transform mass spectrometry. *Organic Geochemistry* 101, 99-107.
- Meylan, W.M., Howard, P.H., Boethling, R.S., 1996. Improved method for estimating water solubility from octanol/water partition coefficient. *Environmental Toxicology and Chemistry* 15, 100-106.
- Michels, R., Langlois, E., Ruau, O., Mansuy, L., Elie, M., Landais, P., 1996. Evolution of Asphaltenes during Artificial Maturation: A Record of the Chemical Processes. *Energy & Fuels* 10, 39-48.
- Minor, E.C., Steinbring, C.J., Longnecker, K., Kujawinski, E.B., 2012. Characterization of dissolved organic matter in Lake Superior and its watershed using ultrahigh resolution mass spectrometry. *Organic Geochemistry* 43, 1-11.
- Minor, E.C., Swenson, M.M., Mattson, B.M., Oyler, A.R., 2014. Structural characterization of dissolved organic matter: a review of current techniques for isolation and analysis. *Environmental Science: Processes & Impacts* 16, 2064-2079.
- Mopper, K., Kieber, D.J., 2002. Photochemistry and the cycling of carbon, sulfur, nitrogen and phosphorus, *Biogeochemistry of marine dissolved organic matter*. Academic Press San Diego, CA.
- Mopper, K., Stubbins, A., Ritchie, J.D., Bialk, H.M., Hatcher, P.G., 2007. Advanced Instrumental Approaches for Characterization of Marine Dissolved Organic Matter: Extraction Techniques, Mass Spectrometry, and Nuclear Magnetic Resonance Spectroscopy. *Chemical Reviews* 107, 419-442.
- Mukhopadhyay, P.K., Hatcher, P.G., Calder, J.H., 1991. Hydrocarbon generation from deltaic and intermontane fluviodeltaic coal and coaly shale from the Tertiary of Texas and Carboniferous of Nova Scotia. *Organic Geochemistry* 17, 765-783.
- Murata, S., Tani, Y., Hiro, M., Kidena, K., Artok, L., Nomura, M., Miyake, M., 2001. Structural analysis of coal through RICO reaction: detailed analysis of heavy fractions. *Fuel* 80, 2099-2109.
- Murphy, K.R., Stedmon, C.A., Waite, T.D., Ruiz, G.M., 2008. Distinguishing between terrestrial and autochthonous organic matter sources in marine environments using fluorescence spectroscopy. *Marine Chemistry* 108, 40-58.

- Muscio, G.P.A., Horsfield, B., Welte, D.H., 1994. Occurrence of thermogenic gas in the immature zone—implications from the Bakken in-source reservoir system. *Organic Geochemistry* 22, 461-476.
- Muscio, G.P.A., Horsfield, B., 1996. Neoformation of Inert Carbon during the Natural Maturation of a Marine Source Rock: Bakken Shale, Williston Basin. *Energy & Fuels* 10, 10-18.
- Nakajima, T., Kanda, T., Fukuda, T., Takanashi, H., Ohki, A., 2005. Characterization of eluent by hot water extraction of coals in terms of total organic carbon and environmental impacts. *Fuel* 84, 783-789.
- Navi, M., Skelly, C., Taulis, M., Nasiri, S., 2015. Coal seam gas water: potential hazards and exposure pathways in Queensland. *International Journal of Environmental Health Research* 25, 162-183.
- Nebbioso, A., Piccolo, A., 2013. Molecular characterization of dissolved organic matter (DOM): a critical review. *Analytical and Bioanalytical Chemistry* 405, 109-124.
- Nelson, C.S., Mildenhall, D.C., Todd, A.J., Pocknall, D.T., 1988. Subsurface stratigraphy, paleoenvironments, palynology, and depositional history of the late Neogene Tauranga Group at Ohinewai, Lower Waikato Lowland, South Auckland, New Zealand. *New Zealand Journal of Geology and Geophysics* 31, 21-40.
- Ohno, T., Ohno, P.E., 2013. Influence of heteroatom pre-selection on the molecular formula assignment of soil organic matter components determined by ultrahigh resolution mass spectrometry. *Analytical and Bioanalytical Chemistry* 405, 3299-3306.
- Oldenburg, T.B.P., Brown, M., Bennett, B., Larter, S.R., 2014. The impact of thermal maturity level on the composition of crude oils, assessed using ultra-high resolution mass spectrometry. *Organic Geochemistry* 75, 151-168.
- Olivella, M.A., Palacios, J.M., Vairavamurthy, A., del Río, J.C., de las Heras, F.X.C., 2002. A study of sulfur functionalities in fossil fuels using destructive- (ASTM and Py-GC-MS) and non-destructive- (SEM-EDX, XANES and XPS) techniques. *Fuel* 81, 405-411.
- Olsson, O., Weichgrebe, D., Rosenwinkel, K.-H., 2013. Hydraulic fracturing wastewater in Germany: composition, treatment, concerns. *Environmental earth sciences* 70, 3895-3906.
- Oni, O.E., Schmidt, F., Miyatake, T., Kasten, S., Witt, M., Hinrichs, K.-U., Friedrich, M.W., 2015. Microbial communities and organic matter composition in surface and subsurface sediments of the Helgoland mud area, North Sea. *Frontiers in Microbiology* 6.
- Orem, W., Feder, G.L., Finkelman, R.B., 1999. A possible link between Balkan endemic nephropathy and the leaching of toxic organic compounds from Pliocene lignite by groundwater: preliminary investigation. *International Journal of Coal Geology* 40, 237-252.
- Orem, W., Tatu, C., Lerch, H.E., Rice, C.A., Bartos, T.T., Bates, A.L., Tewalt, S., Corum, M.D., 2007a. Organic compounds in produced waters from coalbed natural gas wells in the Powder River Basin, Wyoming, USA. *Applied Geochemistry* 22, 2240-2256.

Orem, W., Tatu, C., Pavlovic, N., Bunnell, J., Lerch, H., Paunescu, V., Ordodi, V., Flores, D., Corum, M., Bates, A., 2007c. Health effects of toxic organic substances from coal: Toward “panendemic” nephropathy. *AMBIO: A Journal of the Human Environment* 36, 98-102.

Orem, W., Tatu, C., Varonka, M., Lerch, H., Bates, A., Engle, M., Crosby, L., McIntosh, J., 2014. Organic substances in produced and formation water from unconventional natural gas extraction in coal and shale. *International Journal of Coal Geology* 126, 20-31.

Orr, W.L., 1986. Kerogen/asphaltene/sulfur relationships in sulfur-rich Monterey oils. *Organic Geochemistry* 10, 499-516.

Pan, Y., Liao, Y., Shi, Q., Hsu, C.S., 2013. Acidic and Neutral Polar NSO Compounds in Heavily Biodegraded Oils Characterized by Negative-Ion ESI FT-ICR MS. *Energy & Fuels* 27, 2960-2973.

Parkes, R.J., Cragg, B.A., Wellsbury, P., 2000. Recent studies on bacterial populations and processes in subseafloor sediments: A review. *Hydrogeology Journal* 8, 11-28.

Patience, R.L., Mann, A.L., Poplett, I.J.F., 1992. Determination of molecular structure of kerogens using ¹³C NMR spectroscopy: II. The effects of thermal maturation on kerogens from marine sediments. *Geochimica et Cosmochimica Acta* 56, 2725-2742.

Pelekani, C., Newcombe, G., Snoeyink, V.L., Hepplewhite, C., Assemi, S., Beckett, R., 1999. Characterization of Natural Organic Matter Using High Performance Size Exclusion Chromatography. *Environmental Science & Technology* 33, 2807-2813.

Penru, Y., Simon, F.X., Guastalli, A., Esplugas, S., Llorens, J., 2013. Characterization of natural organic matter from Mediterranean coastal seawater. *Aqua* 62, 42-51.

Perdue, E., Ritchie, J., 2003. Dissolved organic matter in freshwaters. *Treatise on geochemistry* 5, 605.

Peters, K., Walters, C., Moldowan, J., 2007. The biomarker guide: Volume 2, Biomarkers and isotopes in petroleum systems and earth history. Cambridge University Press.

Petersen, H.I., Rosenberg, P., Nytoft, H.P., 2008. Oxygen groups in coals and alginite-rich kerogen revisited. *International Journal of Coal Geology* 74, 93-113.

Petmecky, S., Meier, L., Reiser, H., Littke, R., 1999. High thermal maturity in the Lower Saxony Basin: intrusion or deep burial? *Tectonophysics* 304, 317-344.

Peuravuori, J., Žbáňková, P., Pihlaja, K., 2006. Aspects of structural features in lignite and lignite humic acids. *Fuel Processing Technology* 87, 829-839.

Phan, T.T., Paukert Vankeuren, A.N., Hakala, J.A., 2018. Role of water–rock interaction in the geochemical evolution of Marcellus Shale produced waters. *International Journal of Coal Geology* 191, 95-111.

Piszczyk, K., Luczak, J., Hupka, J., 2014. Mobility of shale drill cuttings constituents. *Physicochemical Problems of Mineral Processing* 50, 795--810.

Pittman, E.D., Lewan, M.D., 1994. Organic Acids in Geological Processes. Springer-Verlag Berlin Heidelberg.

- Pocknall, D.T., 1991. Palynostratigraphy of the Te Kuiti Group (late Eocene - Oligocene), Waikato Basin, New Zealand. *New Zealand Journal of Geology and Geophysics* 34, 407-417.
- Poetz, S., Horsfield, B., Wilkes, H., 2014. Maturity-Driven Generation and Transformation of Acidic Compounds in the Organic-Rich Posidonia Shale as Revealed by Electrospray Ionization Fourier Transform Ion Cyclotron Resonance Mass Spectrometry. *Energy & Fuels* 28, 4877-4888.
- Pohlabein, A.M., Dittmar, T., 2015. Novel insights into the molecular structure of non-volatile marine dissolved organic sulfur. *Marine Chemistry* 168, 86-94.
- Pohlabein, A.M., Gomez-Saez, G.V., Noriega-Ortega, B.E., Dittmar, T., 2017. Experimental Evidence for Abiotic Sulfurization of Marine Dissolved Organic Matter. *Frontiers in Marine Science* 4.
- Putschew, A., Schaeffer-Reiss, C., Schaeffer, P., Koopmans, M.P., de Leeuw, J.W., Lewan, M.D., Sinninghe Damsté, J.S., Maxwell, J.R., 1998. Release of sulfur- and oxygen-bound components from a sulfur-rich kerogen during simulated maturation by hydrous pyrolysis. *Organic Geochemistry* 29, 1875-1890.
- Radke, M., Willsch, H., Welte, D.H., 1980. Preparative hydrocarbon group type determination by automated medium pressure liquid chromatography. *Analytical Chemistry* 52, 406-411.
- Raine, J.I., 1984. Outline of a palynological zonation of Cretaceous to Paleogene terrestrial sediments in West Coast region South Island, New Zealand. Dept. of Scientific and Industrial Research New Zealand.
- Ray, P.Z., Chen, H., Podgorski, D.C., McKenna, A.M., Tarr, M.A., 2014. Sunlight creates oxygenated species in water-soluble fractions of Deepwater horizon oil. *Journal of Hazardous Materials* 280, 636-643.
- Reemtsma, T., 2001. The use of liquid chromatography-atmospheric pressure ionization-mass spectrometry in water analysis – Part II: Obstacles. *TrAC Trends in Analytical Chemistry* 20, 533-542.
- Reid, M.C., Davis, J.W., Minear, R.A., Sayler, G.S., 1988. Fulvic acid constituents of coal slurry transport wastewater. *Water Res* 22, 127-131.
- Requejo, A.G., Allan, J., Creaney, S., Gray, N.R., Cole, K.S., 1992. Aryl isoprenoids and diaromatic carotenoids in Paleozoic source rocks and oils from the Western Canada and Williston Basins. *Organic Geochemistry* 19, 245-264.
- Robin, P.L., Rouxhet, P.G., 1978. Characterization of kerogens and study of their evolution by infrared spectroscopy: carbonyl and carboxyl groups. *Geochimica et Cosmochimica Acta* 42, 1341-1349.
- Röhl, H.-J., Schmid-Röhl, A., Oschmann, W., Frimmel, A., Schwark, L., 2001. The Posidonia Shale (Lower Toarcian) of SW-Germany: an oxygen-depleted ecosystem controlled by sea level and palaeoclimate. *Palaeogeography, Palaeoclimatology, Palaeoecology* 165, 27-52.

Rossel, P.E., Bienhold, C., Boetius, A., Dittmar, T., 2016. Dissolved organic matter in pore water of Arctic Ocean sediments: Environmental influence on molecular composition. *Organic Geochemistry* 97, 41-52.

Rullkötter, J., Leythaeuser, D., Horsfield, B., Littke, R., Mann, U., Müller, P.J., Radke, M., Schaefer, R.G., Schenk, H.J., Schwochau, K., Witte, E.G., Welte, D.H., 1988. Organic matter maturation under the influence of a deep intrusive heat source: A natural experiment for quantitation of hydrocarbon generation and expulsion from a petroleum source rock (Toarcian shale, northern Germany). *Organic Geochemistry* 13, 847-856.

Rullkötter, J., Marzi, R., Meyers, P.A., 1992. Biological markers in Paleozoic sedimentary rocks and crude oils from the Michigan Basin: Reassessment of sources and thermal history of organic matter, *Early Organic Evolution*. Springer, pp. 324-335.

Salmon, E., Behar, F., Lorant, F., Hatcher, P.G., Marquaire, P.-M., 2009. Early maturation processes in coal. Part 1: Pyrolysis mass balance and structural evolution of coalified wood from the Morwell Brown Coal seam. *Organic Geochemistry* 40, 500-509.

Šantl-Temkiv, T., Finster, K., Dittmar, T., Hansen, B.M., Thyraug, R., Nielsen, N.W., Karlson, U.G., 2013. Hailstones: A Window into the Microbial and Chemical Inventory of a Storm Cloud. *Plos One* 8, e53550.

Sarkhot, D.V., Grunwald, S., Ge, Y., Morgan, C.L.S., 2011. Comparison and detection of total and available soil carbon fractions using visible/near infrared diffuse reflectance spectroscopy. *Geoderma* 164, 22-32.

Saxby, J.D., Shibaoka, M., 1986. Coal and coal macerals as source rocks for oil and gas. *Applied Geochemistry* 1, 25-36.

Schenk, H.J., Witte, E.G., Müller, P.J., Schwochau, K., 1986. Infrared estimates of aliphatic kerogen carbon in sedimentary rocks. *Organic Geochemistry* 10, 1099-1104.

Schenk, H.J., Horsfield, B., 1998. Using natural maturation series to evaluate the utility of parallel reaction kinetics models: an investigation of Toarcian shales and Carboniferous coals, Germany. *Organic Geochemistry* 29, 137-154.

Schiff, J.A., Fankhauser, H., 1981. *Assimilatory Sulfate Reduction*. Springer Berlin Heidelberg, Berlin, Heidelberg, pp. 153-168.

Schmidt, F., Elvert, M., Koch, B.P., Witt, M., Hinrichs, K.-U., 2009. Molecular characterization of dissolved organic matter in pore water of continental shelf sediments. *Geochimica et Cosmochimica Acta* 73, 3337-3358.

Schmidt, F., Koch, B.P., Elvert, M., Schmidt, G., Witt, M., Hinrichs, K.-U., 2011. Diagenetic Transformation of Dissolved Organic Nitrogen Compounds under Contrasting Sedimentary Redox Conditions in the Black Sea. *Environmental Science & Technology* 45, 5223-5229.

Schmidt, F., Koch, B.P., Witt, M., Hinrichs, K.-U., 2014. Extending the analytical window for water-soluble organic matter in sediments by aqueous Soxhlet extraction. *Geochimica et Cosmochimica Acta* 141, 83-96.

Schmidt, F., Koch, B.P., Goldhammer, T., Elvert, M., Witt, M., Lin, Y.-S., Wendt, J., Zabel, M., Heuer, V.B., Hinrichs, K.-U., 2017. Unraveling signatures of biogeochemical processes

and the depositional setting in the molecular composition of pore water DOM across different marine environments. *Geochimica et Cosmochimica Acta* 207, 57-80.

Schneckenburger, P., Adam, P., Albrecht, P., 1998. Thioketones as key intermediates in the reduction of ketones to thiols by HS⁻ in natural environments. *Tetrahedron Letters* 39, 447-450.

Schnitzer, M., 1985. Aromaticity of soil fulvic acid. *Nature* 316, 658.

Schopf, J.M., 1956. A definition of coal. *Economic Geology* 51, 521-527.

Schovsbo, N.H., Nielsen, A.T., Klitten, K., Mathiesen, A., Rasmussen, P., 2011. Shale gas investigations in Denmark: Lower Palaeozoic shales on Bornholm. *Geological Survey of Denmark and Greenland Bulletin*, 9-12.

Seewald, J.S., 2001a. Model for the origin of carboxylic acids in basinal brines. *Geochimica et Cosmochimica Acta* 65, 3779-3789.

Seewald, J.S., 2001c. Aqueous geochemistry of low molecular weight hydrocarbons at elevated temperatures and pressures: constraints from mineral buffered laboratory experiments. *Geochimica et Cosmochimica Acta* 65, 1641-1664.

Seidel, M., Beck, M., Riedel, T., Waska, H., Suryaputra, I.G.N.A., Schnetger, B., Niggemann, J., Simon, M., Dittmar, T., 2014. Biogeochemistry of dissolved organic matter in an anoxic intertidal creek bank. *Geochimica et Cosmochimica Acta* 140, 418-434.

Seidel, M., Yager, P.L., Ward, N.D., Carpenter, E.J., Gomes, H.R., Krusche, A.V., Richey, J.E., Dittmar, T., Medeiros, P.M., 2015. Molecular-level changes of dissolved organic matter along the Amazon River-to-ocean continuum. *Marine Chemistry* 177, Part 2, 218-231.

Shi, Q., Hou, D., Chung, K.H., Xu, C., Zhao, S., Zhang, Y., 2010a. Characterization of Heteroatom Compounds in a Crude Oil and Its Saturates, Aromatics, Resins, and Asphaltenes (SARA) and Non-basic Nitrogen Fractions Analyzed by Negative-Ion Electrospray Ionization Fourier Transform Ion Cyclotron Resonance Mass Spectrometry. *Energy & Fuels* 24, 2545-2553.

Shi, Q., Zhao, S., Xu, Z., Chung, K.H., Zhang, Y., Xu, C., 2010b. Distribution of Acids and Neutral Nitrogen Compounds in a Chinese Crude Oil and Its Fractions: Characterized by Negative-Ion Electrospray Ionization Fourier Transform Ion Cyclotron Resonance Mass Spectrometry. *Energy & Fuels* 24, 4005-4011.

Shipkova, P.A., Heimark, L., Bartner, P.L., Chen, G., Pramanik, B.N., Ganguly, A.K., Cody, R.B., Kusai, A., 2000. High-resolution LC/MS for analysis of minor components in complex mixtures: negative ion ESI for identification of impurities and degradation products of a novel oligosaccharide antibiotic. *Journal of Mass Spectrometry* 35, 1252-1258.

Simjouw, J.-P., Minor, E.C., Mopper, K., 2005. Isolation and characterization of estuarine dissolved organic matter: Comparison of ultrafiltration and C18 solid-phase extraction techniques. *Marine Chemistry* 96, 219-235.

Sinninghe Damste, J.S., De Leeuw, J.W., 1990. Analysis, structure and geochemical significance of organically-bound sulphur in the geosphere: State of the art and future research. *Organic Geochemistry* 16, 1077-1101.

Sinninghe Damsté, J.S., Rijpstra, W.I.C., Kock-van Dalen, A.C., De Leeuw, J.W., Schenck, P.A., 1989. Quenching of labile functionalised lipids by inorganic sulphur species: Evidence for the formation of sedimentary organic sulphur compounds at the early stages of diagenesis. *Geochimica et Cosmochimica Acta* 53, 1343-1355.

Sleighter, R.L., Hatcher, P.G., 2007. The application of electrospray ionization coupled to ultrahigh resolution mass spectrometry for the molecular characterization of natural organic matter. *Journal of Mass Spectrometry* 42, 559-574.

Sleighter, R.L., Hatcher, P.G., 2008. Molecular characterization of dissolved organic matter (DOM) along a river to ocean transect of the lower Chesapeake Bay by ultrahigh resolution electrospray ionization Fourier transform ion cyclotron resonance mass spectrometry. *Marine Chemistry* 110, 140-152.

Sleighter, R.L., Chin, Y.-P., Arnold, W.A., Hatcher, P.G., McCabe, A.J., McAdams, B.C., Wallace, G.C., 2014. Evidence of Incorporation of Abiotic S and N into Prairie Wetland Dissolved Organic Matter. *Environmental Science & Technology Letters* 1, 345-350.

Smernik, R.J., Schwark, L., Schmidt, M.W.I., 2006. Assessing the quantitative reliability of solid-state ¹³C NMR spectra of kerogens across a gradient of thermal maturity. *Solid State Nuclear Magnetic Resonance* 29, 312-321.

Smith, M.G., Bustin, R.M., 1998. Production and preservation of organic matter during deposition of the Bakken Formation (Late Devonian and Early Mississippian), Williston Basin. *Palaeogeography, Palaeoclimatology, Palaeoecology* 142, 185-200.

Sørensen, J., Christensen, D., Jørgensen, B.B., 1981. Volatile Fatty Acids and Hydrogen as Substrates for Sulfate-Reducing Bacteria in Anaerobic Marine Sediment. *Applied and Environmental Microbiology* 42, 5-11.

Spencer, R.G.M., Aiken, G.R., Butler, K.D., Dornblaser, M.M., Striegl, R.G., Hernes, P.J., 2009. Utilizing chromophoric dissolved organic matter measurements to derive export and reactivity of dissolved organic carbon exported to the Arctic Ocean: A case study of the Yukon River, Alaska. *Geophysical Research Letters* 36.

Stach, E., Mackowsky, M.-T., Teichmüller, M., Taylor G. H., Chandra, D., Teichmüller, R., 1982. *Stach's textbook of coal petrology*.

Stanford, L.A., Kim, S., Klein, G.C., Smith, D.F., Rodgers, R.P., Marshall, A.G., 2007. Identification of Water-Soluble Heavy Crude Oil Organic-Acids, Bases, and Neutrals by Electrospray Ionization and Field Desorption Ionization Fourier Transform Ion Cyclotron Resonance Mass Spectrometry. *Environmental Science & Technology* 41, 2696-2702.

Stearman, W., Taulis, M., Smith, J., Corkeron, M., 2014. Assessment of Geogenic Contaminants in Water Co-Produced with Coal Seam Gas Extraction in Queensland, Australia: Implications for Human Health Risk. *Geosciences* 4, 219-239.

Stenson, A.C., Landing, W.M., Marshall, A.G., Cooper, W.T., 2002. Ionization and Fragmentation of Humic Substances in Electrospray Ionization Fourier Transform-Ion Cyclotron Resonance Mass Spectrometry. *Analytical Chemistry* 74, 4397-4409.

Stenson, A.C., Marshall, A.G., Cooper, W.T., 2003. Exact masses and chemical formulas of individual Suwannee River fulvic acids from ultrahigh resolution electrospray ionization Fourier transform ion cyclotron resonance mass spectra. *Analytical Chemistry* 75, 1275-1284.

Stevenson, F.J., 1994. *Humus chemistry: genesis, composition, reactions*. John Wiley and Sons, New York.

Strong, L., Gould, T., Kasinkas, L., Sadowsky, M., Aksan, A., Wackett, L., 2013. Biodegradation in Waters from Hydraulic Fracturing: Chemistry, Microbiology, and Engineering. *Journal of Environmental Engineering* 140, B4013001.

Summons, R.E., 2013. Biogeochemical Cycles: A Review of Fundamental Aspects of Organic Matter. *Organic geochemistry: principles and applications* 11, 3-21.

Surdam, R., Crossey, L.J., 1985. Organic-inorganic reactions during progressive burial: key to porosity and permeability enhancement and preservation. *Phil. Trans. R. Soc. Lond. A* 315, 135-156.

Surdam, R.C., Boese, S.W., Crossey, L.J., 1984. The Chemistry of Secondary Porosity: Part 2. Aspects of Porosity Modification. In: McDonald, D.A. and Surdam, R.C. (eds.), *Clastic Diagenesis*. AAPG Memoir 37, 127-149.

Surdam, R.C., Jiao, Z.S., MacGowan, D.B., 1993. Redox reactions involving hydrocarbons and mineral oxidants; a mechanism for significant porosity enhancement in sandstones. *AAPG Bulletin* 77, 1509-1518.

Swanson, V.E., Swanson, V.E., 1961. *Geology and geochemistry of uranium in marine black shales: a review*. US Government Printing Office Washington, DC.

Tang, J.Y., Taulis, M., Edebeli, J., Leusch, F.D., Jagals, P., Jackson, G.P., Escher, B.I., 2014. Chemical and bioanalytical assessment of coal seam gas associated water. *Environmental Chemistry* 12, 267-285.

Taylor, G., Teichmüller, M., Davis, A., Diessel, C., Littke, R., Robert, P., 1998. *Organic petrology*: Berlin. Gebrüder Borntraeger.

Tellez, G.T., Nirmalakhandan, N., Gardea-Torresdey, J.L., 2005. Comparison of purge and trap GC/MS and spectrophotometry for monitoring petroleum hydrocarbon degradation in oilfield produced waters. *Microchemical Journal* 81, 12-18.

Tfaily, M.M., Hamdan, R., Corbett, J.E., Chanton, J.P., Glaser, P.H., Cooper, W.T., 2013. Investigating dissolved organic matter decomposition in northern peatlands using complimentary analytical techniques. *Geochimica et Cosmochimica Acta* 112, 116-129.

Thacker, J., Carlton, D., Hildenbrand, Z., Kadjo, A., Schug, K., 2015. Chemical Analysis of Wastewater from Unconventional Drilling Operations. *Water* 7, 1568.

Thurman, E., 1985. Amount of organic carbon in natural waters, *Organic geochemistry of natural waters*. Springer, pp. 7-65.

Thurman, E.M., Ferrer, I., Barceló, D., 2001. Choosing between Atmospheric Pressure Chemical Ionization and Electrospray Ionization Interfaces for the HPLC/MS Analysis of Pesticides. *Analytical Chemistry* 73, 5441-5449.

Tissot, B.P., Welte, D.H., 1984. *Petroleum Formation and Occurrence*. Springer-Verlag, Berlin.

Tourtelot, H.A., 1979. Black shale; its deposition and diagenesis. *Clays and Clay Minerals* 27, 313-321.

Tremblay, L.B., Dittmar, T., Marshall, A.G., Cooper, W.J., Cooper, W.T., 2007. Molecular characterization of dissolved organic matter in a North Brazilian mangrove porewater and mangrove-fringed estuaries by ultrahigh resolution Fourier Transform-Ion Cyclotron Resonance mass spectrometry and excitation/emission spectroscopy. *Marine Chemistry* 105, 15-29.

Tuttle, M.L.W., Breit, G.N., 2009. Weathering of the New Albany Shale, Kentucky, USA: I. Weathering zones defined by mineralogy and major-element composition. *Applied Geochemistry* 24, 1549-1564.

Vairavamurthy, A., Zhou, W., Eglinton, T., Manowitz, B., 1994. Sulfonates: A novel class of organic sulfur compounds in marine sediments. *Geochimica et Cosmochimica Acta* 58, 4681-4687.

Vairavamurthy, M.A., Schoonen, M.A.A., Eglinton, T.I., Luther, G.W., Manowitz, B., 1995. *Geochemical Transformations of Sedimentary Sulfur*. American Chemical Society.

Valle, J., Gonsior, M., Harir, M., Enrich-Prast, A., Schmitt-Kopplin, P., Bastviken, D., Conrad, R., Hertkorn, N., 2018. Extensive processing of sediment pore water dissolved organic matter during anoxic incubation as observed by high-field mass spectrometry (FTICR-MS). *Water Res* 129, 252-263.

Van Krevelen, D., 1950. Graphical-statistical method for the study of structure and reaction processes of coal. *Fuel* 29, 269-284.

Vandenbroucke, M., Largeau, C., 2007. Kerogen origin, evolution and structure. *Organic Geochemistry* 38, 719-833.

Vieth, A., Mangelsdorf, K., Sykes, R., Horsfield, B., 2008. Water extraction of coals – potential for estimating low molecular weight organic acids as carbon feedstock for the deep terrestrial biosphere. *Organic Geochemistry* 39, 985-991.

Vine, J.D., Tourtelot, E.B., 1970. Geochemistry of black shale deposits; a summary report. *Economic Geology* 65, 253-272.

Volk, H., Pinetown, K., Johnston, C., McLean, W., 2011. A desktop study of the occurrence of Total Petroleum Hydrocarbon (TPH) and partially water-soluble organic compounds in Permian coals and associated coal seam groundwater. CSIRO Petroleum and Geothermal Research Portfolio Report EP-13-09-11.

Vu, T.A.T., Horsfield, B., Sykes, R., 2008. Influence of in-situ bitumen on the generation of gas and oil in New Zealand coals. *Organic Geochemistry* 39, 1606-1619.

Vu, T.T.A., Zink, K.G., Mangelsdorf, K., Sykes, R., Wilkes, H., Horsfield, B., 2009. Changes in bulk properties and molecular compositions within New Zealand Coal Band solvent extracts from early diagenetic to catagenetic maturity levels. *Organic Geochemistry* 40, 963-977.

- Vu, T.T.A., Horsfield, B., Mahlstedt, N., Schenk, H.J., Kelemen, S.R., Walters, C.C., Kwiatek, P.J., Sykes, R., 2013. The structural evolution of organic matter during maturation of coals and its impact on petroleum potential and feedstock for the deep biosphere. *Organic Geochemistry* 62, 17-27.
- Wang, W., Hou, Y., Niu, M., Wu, T., Wu, W., 2013. Production of benzene polycarboxylic acids from bituminous coal by alkali-oxygen oxidation at high temperatures. *Fuel Processing Technology* 110, 184-189.
- Wassenaar, L., Aravena, R., Fritz, P., Barker, J., 1990. Isotopic composition (^{13}C , ^{14}C , ^2H) and geochemistry of aquatic humic substances from groundwater. *Organic Geochemistry* 15, 383-396.
- Watson, D.F., Farrimond, P., 2000. Novel polyfunctionalised geohopanoids in a recent lacustrine sediment (Priest Pot, UK). *Organic Geochemistry* 31, 1247-1252.
- Webster, R.L., 1984. Petroleum source rocks and stratigraphy of Bakken formation in North Dakota.
- Weiss, H.M., Wilhelms, A., Mills, N., Scotchmer, J., Hall, P.B., Lind, K., Brekke, T., 2000. NIGOGA - The Norwegian Industry Guide to Organic Geochemical Analyses. Edition 4.0. Available: <http://www.npd.no/engelsk/nigoga/default.htm>.
- Werner-Zwanziger, U., Lis, G., Mastalerz, M., Schimmelmanna, A., 2005. Thermal maturity of type II kerogen from the New Albany Shale assessed by ^{13}C CP/MAS NMR. *Solid State Nuclear Magnetic Resonance* 27, 140-148.
- Wilkes, H., Clegg, H., Disko, U., Willsch, H., Horsfield, B., 1998. Fluoren-9-ones and carbazoles in the Posidonia Shale, Hils Syncline, northwest Germany. *Fuel* 77, 657-668.
- Wilkes, H., Schwarzbauer, J., 2010. Hydrocarbons: an introduction to structure, physico-chemical properties and natural occurrence, *Handbook of hydrocarbon and lipid microbiology*. Springer, pp. 1-48.
- Wolford, R., 2011. Characterization of organics in the Marcellus shale flowback and produced waters, Department of Civil and Environmental Engineering. Pennsylvania State University, MS Thesis, p. 87.
- Yang, F., Hou, Y., Wu, W., Wang, Q., Niu, M., Ren, S., 2017. The relationship between benzene carboxylic acids from coal via selective oxidation and coal rank. *Fuel Processing Technology* 160, 207-215.
- Zhang, Y., Shi, Q., Li, A., Chung, K.H., Zhao, S., Xu, C., 2011. Partitioning of Crude Oil Acidic Compounds into Subfractions by Extrography and Identification of Isoprenoidyl Phenols and Tocopherols. *Energy & Fuels* 25, 5083-5089.
- Zhou, Q., Cabaniss, S.E., Maurice, P.A., 2000. Considerations in the use of high-pressure size exclusion chromatography (HPSEC) for determining molecular weights of aquatic humic substances. *Water Res* 34, 3505-3514.
- Zhou, X., Zhang, D., 1994. Structural investigation of fulvic acid from weathered coal by using capillary GC-MS. *Fuel Science & Technology International* 12, 1169-1182.

Zhu, M.-X., Chen, L.-J., Yang, G.-P., Huang, X.-L., Ma, C.-Y., 2014. Humic sulfur in eutrophic bay sediments: Characterization by sulfur stable isotopes and K-edge XANES spectroscopy. *Estuarine, Coastal and Shelf Science* 138, 121-129.

Zhu, Y., Vieth-Hillebrand, A., Wilke, F.D.H., Horsfield, B., 2015. Characterization of water-soluble organic compounds released from black shales and coals. *International Journal of Coal Geology* 150–151, 265-275.

Ziemkiewicz, P.F., Thomas He, Y., 2015. Evolution of water chemistry during Marcellus Shale gas development: A case study in West Virginia. *Chemosphere* 134, 224-231.

Zinger, A.S., Kravchik, T.E., 1973. Simpler organic acids in groundwater in the Lower Volga Region (genesis and possible use for prospecting for oil). *Doklady Akademii Nauk (Academy of Sciences Reports) S.S.S.R.* 202, 218-221.